DISSERTATION

REGULATION OF TRANSCRIPTION BY UBIQUITIN AND THE INO80 CHROMATIN REMODELING COMPLEX

Submitted by

Ada Ndoja

Department of Biochemistry and Molecular Biology

In partial fulfillment of the requirements

For the Degree of Doctor of Philosophy

Colorado State University

Fort Collins, Colorado

Summer 2015

Doctoral Committee:

Advisor: Tingting Yao
Co-advisor: Robert Cohen

Laurie Stargell
Jeffrey Hansen
Carol Wilusz

ABSTRACT

REGULATION OF TRANSCRIPTION BY UBIQUITIN AND THE INO80 CHROMATIN REMODELING COMPLEX

Transcription in eukaryotes is a crucial process that is tightly regulated in order to maintain cellular homeostasis and offer optimal responses to environmental changes. Transcriptional activators (TAs) regulate this process by orchestrating time and locus-specific assembly of complex transcription machinery. Thus, the abundance, localization and activity of TAs are all subject to tight control. One way in which TAs are controlled is by the covalent attachment of the conserved protein ubiquitin. Ubiquitination of TAs has been reported to affect transcription via proteolytic and non-proteolytic routes, yet the function of the ubiquitin signal in the non-proteolytic process is poorly understood. Through studies of a series of synthetic and natural activators in yeast and mammalian cells, we found that mono-ubiquitinated TAs cannot stably interact with DNA to promote transcription. We have identified the AAA+ ATPase Cdc48 and its cofactors as the Ub receptor responsible for extracting mono-ubiquitinated activators from chromatin, independently of proteolysis. These findings describe a novel mechanism by which gene repression can be maintained without destroying the activator. Upon appropriate stimulus, deubiquitinating enzymes can readily reverse mono- or oligo-ubiquitination of the activator and transcription can initiate without the requirement for new protein synthesis. This mechanism may facilitate rapid switching between “on” and “off” states of transcription and may serve as a general strategy to prevent spurious transcription in the “off” state.

Compaction of DNA into chromatin imparts further layers of complexity to the control of eukaryotic gene expression. Cooperation between chromatin remodelers, histone variants, and histone post-translational modifications (PTMs) offers diverse regulatory options in DNA metabolic processes, including transcription and DNA repair. The human INO80 chromatin-remodeling complex (hINO80) has been shown to facilitate transcription by promoting an open chromatin environment at promoter regions. How and whether hINO80 directly promotes an open chromatin environment is not yet understood. In an effort to elucidate how hINO80 regulates transcription, we have characterized the nucleosome sliding activity of hINO80 and examined how histone variant H2A.Z and histone PTMs modulate its activity *in vitro*. Our results suggest that nucleosomes containing H2A.Z or the H3 acetylation mimic, K56Q, are mobilized by hINO80 with faster kinetics compared to canonical unmodified nucleosomes, and their effects are additive. In contrast, ubiquitination of H2A or H2B does not affect the sliding activity of hINO80. Nucleosomes containing both H2A.Z and H3-K56Ac are enriched at promoter regions and DNA damage sites in mammalian cells. These nucleosomes have been shown to exhibit rapid turnover kinetics *in vivo*. Our studies provide biochemical evidence that hINO80 participates in transcription and DNA repair processes by ATP-dependent mobilization of H2A.Z/H3-K56Ac-containing nucleosomes. Future studies will be required to elucidate how nucleosome mobilization *in vitro* relates to chromatin dynamics *in vivo.*

AKNOWLEDGEMENTS

When I started my graduate student career I knew to expect hard working days in the lab, exams and homeworks. These past six years have been so much more. They have tremendously contributed to my personal growth and especially have allowed me to get to know and be surrounded by amazing people. This section of my thesis is dedicated to those incredible individuals without whom this experience would not have been the same.

My mentor Tingting Yao has been the foundation of my scientific growth during these years. Her attitude toward scientific problems and her mentoring style have shaped my way of thinking and being a scientist. I will forever be grateful to her for all she has given me consciously and unconsciously.

The long days in the lab would not have been the same without current and previous lab members. Lindsey Long has been a great ally with whom to navigate the uncharted waters of life as a graduate student. Sharing my bench with Melonnie Furgason was the best decision that I made because I found a friend. I want to thank Aixin Song, Nouf Omar, Yun-Seok Choi, Ben Schmitt, Sarah Bollinger and Joe Thelen for their camaraderie and for sharing their scientific expertise whenever needed.

Special thanks to my co-advisor, Robert Cohen, for his scientific assistance and fitting advice whenever necessary. I want to thank my committee members, Laurie Stargell, Carol Wilusz and Jeff Hansen, for their invaluable advice and support during these years.

Last, I would like to thank my parents for always believing in me and helping me see the big picture of life without losing focus of my goals. A big “thank you” to Francesco Scavone, who has been by my side during these years, even when the miles to go ahead of us were overwhelming.

TABLE OF CONTENTS

CHAPTER 1: INTRODUCTION

[1]Transcription is the foremost regulatory point during the process of producing a functional protein. Not only do specific genes need to be turned on and off according to growth and environmental conditions, the amounts and quality of transcripts produced are fine-tuned to offer optimal responses. As a result, numerous regulatory mechanisms converge to provide temporal and spatial specificity for this process.

For a gene to be transcribed, an army of general transcription factors (GTFs) is necessary to recruit RNA Polymerase II (RNAPII) and assemble the pre-initiation complex at the promoter. This initiation phase is followed by the elongation phase, during which RNAPII engages the DNA and synthesizes a complementary strand of RNA that serves as a template for protein synthesis. Productive elongation is followed by termination, when transcribed RNA is processed and released for exporting into the cytoplasm and RNAPII is released from DNA. Repetition of these three phases in a cyclical manner over a gene determines its expression levels. There are numerous obstacles that must be overcome during each phase of the transcription cycle. These obstacles in turn provide many critical regulatory opportunities.

Because eukaryotic DNA is packaged into chromatin, the transcription machinery must also deal with the nucleosome barrier in order to access DNA (Li et al., 2007). Nucleosomes positioned at the promoter regions prevent binding of transcription factors and block RNAPII loading and formation of the pre-initiation complex (Lorch et al., 1987; Teves et al., 2014). *In vitro,* a nucleosome positioned downstream of the elongating RNAPII

[1] This chapter is related to Yao T. and Ndoja A. (2012) Semin. Cell. Dev. Biol. *23(5)*, 523-529. Published figures include 1.1, 1.2A and 1.2B.

is sufficient to inhibit elongation (Izban and Luse, 1992; Shaw et al., 1978). However, *in vivo* transcription of nucleosome associated DNA occurs at speeds comparable to those seen on naked DNA templates (Singh and Padgett, 2009). This implies that histones must be either locally remodeled during the passage of RNAPII or evicted from DNA ahead of the elongating RNAPII complex (Park and Luger, 2008). Conversely, because nucleosomes also act to conceal cryptic promoter elements throughout the genome, histones must be re-deposited appropriately in the wake of RNAPII to prevent transcription of spurious RNAs (Carrozza et al., 2005; Kaplan et al., 2003). The ability of nucleosomes to control DNA accessibility affords tremendous regulatory potential. Numerous chromatin modifying and remodeling factors, as well as different histone variants, have evolved not only to control transcriptional processes but also to signal the cell the transcriptional state of a given gene.

In the past decade, the ubiquitin-proteasome system (UPS), which is best known as a pathway for intracellular proteolysis, has emerged as a pivotal player in the control of gene expression. There is increasing evidence that the UPS has both proteolytic and non-proteolytic functions in multiple aspects of the transcription process. In this chapter, I will focus on the roles of UPS in the regulation of transcriptional activators and chromatin dynamics.

1.1 Regulation of transcriptional activators by the ubiquitin proteasome system

Typically, transcriptional activators (TAs) possess a sequence-specific DNA-binding domain and an activation domain that, directly or via co-activators, interacts with GTFs or RNAPII (Baumann et al., 2010; Geng et al., 2012; Li et al., 2007). TAs have important roles in coordinating the assembly of complex protein machineries –RNAPII, GTFs, and various

co-activators with chromatin modifying and remodeling activities – with the goal to activate gene expression in a time and locus specific manner. Research from multiple laboratories has revealed that the UPS regulates TAs by limiting their abundance and also by assisting productive transcription in a variety of ways.

1.1.1 The ubiquitin proteasome system

In eukaryotes, the covalent attachment of the small protein ubiquitin (Ub) to other proteins regulates multiple and diverse aspects of cell physiology, including endocytosis, cell cycle, DNA repair, transcriptional regulation, and chromatin dynamics (Pickart, 2001). In many respects, ubiquitination is analogous to phosphorylation and its function is analogous to signaling by protein kinases. However, the Ub signal is structurally more versatile (Figure 1.1A). Because Ub can be attached to other Ub molecules to form polyUb chains, the type of Ub modification can differ in the number of Ub molecules attached to the substrate and the linkage between the Ubs in a polyUb chain (Hershko and Ciechanover, 1998; Ikeda and Dikic, 2008; Varshavsky, 2005). Ub has seven lysines and an N-terminal amine, each of which can engage in polyUb chain formation *in vivo* (Peng et al., 2003). Classically, modification by a K48-linked polyUb chain targets a protein substrate to the 26S proteasome for subsequent degradation. More recent studies have shown that the functions of mono-ubiquitination and other types of polyUb linkages are much more diverse (Hicke, 2001; Pickart and Fushman, 2004; Sun and Chen, 2004). In particular, mono-ubiquitination of TAs and histone proteins does not lead to protein degradation (Kodadek et al., 2006; Osley et al., 2006; Weake and Workman, 2008).

1.1.2 Proteasome assemblies

The proteasome is the central machinery that handles regulated proteolysis in cells. The 20S core particle (CP) is a cylinder-shaped particle composed of four 7-subunit rings (Figure 1.1B) (Groll et al., 1997). The rings are stacked to form a self-compartmentalized protease complex with a C2 symmetry. The two inner rings contain seven distinct β-type subunits, of which three have proteolytic activities, whereas the two outer rings contain α-type subunits that control access to the proteolytic sites sequestered within the cylinder's interior. By itself, the 20S CP can only degrade unfolded polypeptides. It is the 19S Regulatory Particle (RP) that ties the 20S CP to the Ub system. Consisting of at least 18 different subunits, the 19S RP orchestrates all the steps that lead to degradation of ubiquitinated proteins (Pickart and Cohen, 2004); these include recognition of polyUb, substrate unfolding, substrate deubiquitination, and substrate translocation into the 20S catalytic core (Finley, 2009). The 26S proteasome is formed upon binding of a 19S RP to one or both ends of the 20S CP.

Although the distribution and dynamics of 19S, 20S, and 26S particles in cells are not well understood and may vary with cell type and growth conditions, it is generally believed that the 19S RP exists both as an independent complex and as part of the 26S proteasome (Peters et al., 1994). By itself, the 19S RP has non-proteolytic functions through interactions with ubiquitinated proteins (Braun et al., 1999; Liu et al., 2002). There is also evidence that it directly interacts with some TAs and co-activators (Bhat et al., 2008; Ferdous et al., 2007; Gonzalez et al., 2002; Lee et al., 2005). The 19S RP can be further divided into two subassemblies: the Base and the Lid (Glickman et al., 1998). The Base, also known as APIS (ATPase Independent of 20S), is comprised of six ATPases (Rpt1-6), Rpn1,

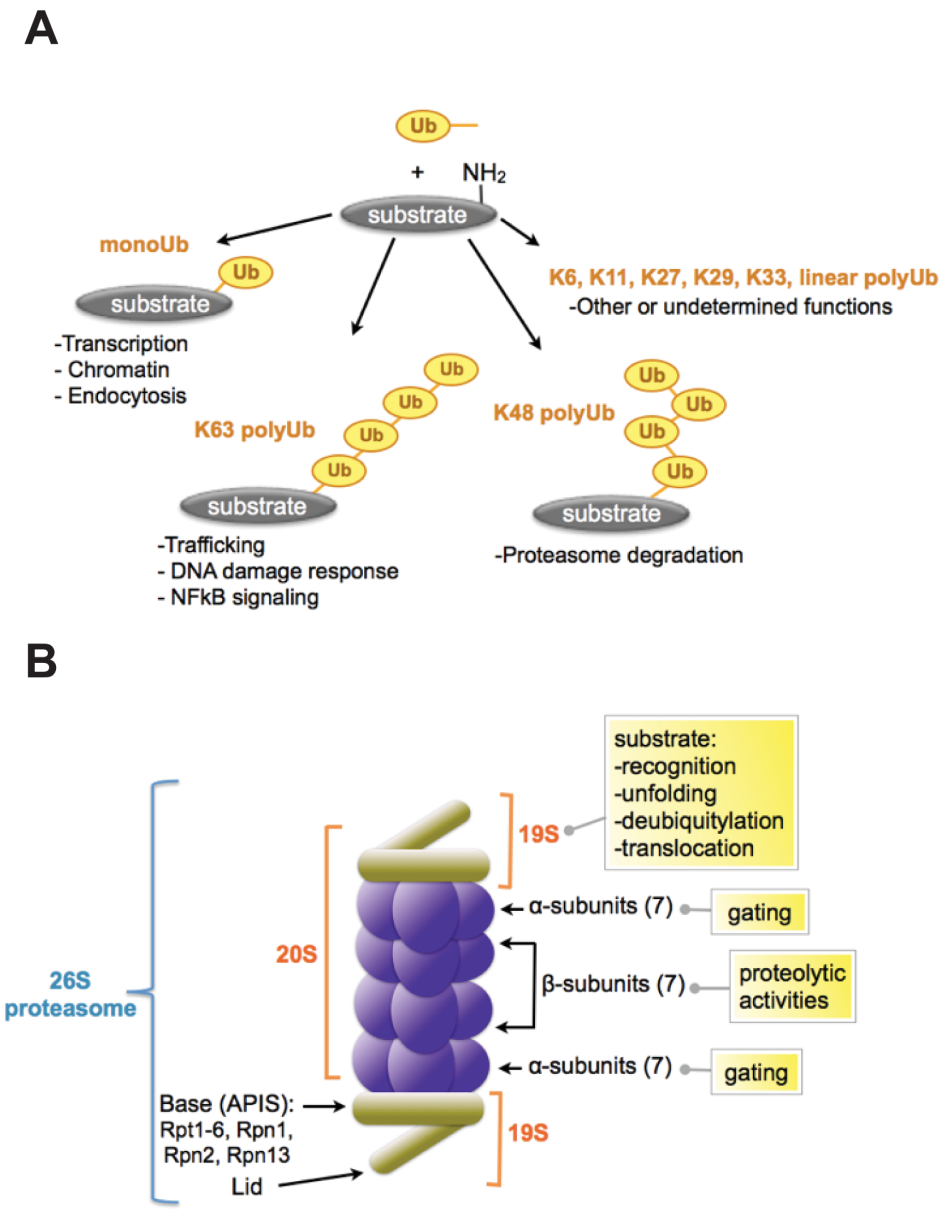

Figure 1.1. Ubiquitin modifications and the 26S proteasome.
(A) Ubiquitin has seven lysines and an N-terminal amine, each of which can engage in polyUb chain formation. These diverse modifications are associated with a large variety of biological functions, some of which are still poorly understood. **(B)** A schematic of the 26S proteasome and its subcomplexes.

Rpn2, and Rpn13. It contains polyUb recognition and protein unfolding activities and has been implicated in transcription activation (Braun et al., 1999; Gonzalez et al., 2002; Husnjak et al., 2008; Metivier et al., 2003; Schreiner et al., 2008). However, it has not been demonstrated that the Base exists as an independent complex *in vivo.*

1.1.3 Proteolytic control of transcriptional activators

At first glance, it seems that the classical Ub-proteasome pathway is perfectly suited for regulating the amounts of specific TAs in the cell. For a subset of activators that include HIF-1α, ubiquitination induces degradation by the proteasome; this leads to reduced levels of the activator and lower transcription of its target gene(s) (Kamura et al., 2000). However, for another subset of activators, their turnover is coupled to their transcriptional activities. In 1999 Molinari et al. reported that activators with high transcription potency are often short-lived proteins (Molinari et al., 1999). Subsequent work from multiple laboratories showed that there is interdependence between transcription activation and degradation of the activator protein (Muratani and Tansey, 2003).

First, there is an inverse relationship between transcription potency and activator half-life. Salghetti et al. constructed a series of synthetic activators consisting of the yeast Gal4 DNA binding domain (DBD) fused to tandem copies of a short acidic fragment (VN8) derived from Herpes Simplex virus protein VP16 (Salghetti et al., 2000). With more copies of VN8, higher transcription was observed together with shorter half-lives of the activator. Conversely, mutations in VN8 that attenuated its transcription potency increased its half-life. Second, inhibition of UPS-mediated degradation not only stabilized the activator but also inhibited transcription activation. In budding yeast, transcription activation by Gcn4

and Gal4 is inhibited by the proteasome inhibitor MG132 (Lipford et al., 2005; Muratani et al., 2005). In mammalian cells, Myc and estrogen receptor alpha (ERα) are two of the best-studied cases where transcription activation is inhibited either by proteasome inhibition or by inactivation of the ubiquitination machinery (Kim et al., 2003; Reid et al., 2003; von der Lehr et al., 2003). More recently, Wang et al. constructed a series of non-classical synthetic activators consisting of the bacterial LexA DBD fused to the C-terminus of each of 17 Mediator subunits (Wang et al., 2010). Mediator is a large protein complex that interacts with RNAPII and plays essential roles in activator-dependent transcription. A Med–LexA fusion is predicted to recruit the Mediator to LexA-binding sites and activate transcription from a reporter gene. Among the 17 subunits only 3 that reside in the tail module of the Mediator activated transcription when fused to LexA, which may be a result of structural constraints that are imposed by the artificial fusion. However, all 3 fusions that are capable of activating transcription were short-lived proteins. Proteasome mutations that stabilize these fusions also inhibited transcription of the reporter gene. This observation lends further support to the hypothesis that activator degradation is an intrinsic requirement for certain types of transcription, such as those that require direct interactions between the activator and the Mediator.

Interestingly, for many natural activators, their transcription activation domains (ADs) overlap with the sequences that are responsible for Ub-dependent degradation (degrons). Examples include ATF6, E2F-1, ERα, Fos, Gcn4, IRF-1, Jun, Myc, and p53 (Muratani and Tansey, 2003; Salghetti et al., 2000). The co-localization of ADs and degrons suggests coupling between transcription activation and degradation. However, it is generally unclear if degradation is merely a consequence of transcription or whether it also

plays a positive role in transcription activation. Studies of ERα suggest that in this case activator degradation is required to promote multiple rounds of transcription. By following synchronized induction of estrogen-response genes, Metivier et al. showed that ERα and transcription machinery are recruited to a promoter in a cyclic manner, each cycle corresponding to one round of transcription (Metivier et al., 2003; Reid et al., 2003). At a late point of each cycle, E3 Ub ligases and components of the proteasome are recruited, followed by disappearance of the activator from the promoter. Inhibition of the proteasome prolonged the presence of the activator at the promoter and prevented additional transcription cycles. These observations led to a model in which, after each round of transcription, the activator and other components of the transcription machinery must be cleared from the promoter through proteasome-dependent degradation of the activator (Figure 1.2A).

Another study suggests that activator ubiquitination and degradation may also play an important role in mRNA processing. The F-box is a protein motif that can associate with other proteins to form a SCF-type of E3 Ub ligase (Deshaies, 1999). Yeast strains that lack the F-box protein Dsg1 (also known as Mdm30) cannot use galactose as carbon source. Muratani et al. found that Dsg1 is involved in ubiquitination and degradation of a specific population of Gal4 that is engaged in transcription (Muratani et al., 2005). These Gal4 molecules are marked by S699 and S837 phosphorylation, mediated by components of the transcription pre-initiation complex. Phosphorylated Gal4 is ubiquitinated by SCF^{Dsg1} and subsequently degraded by the proteasome. In the absence of Dsg1, there is a defect in phosphorylation of RNAPII at Ser5 and Ser2 positions within the C-terminal domain (CTD).

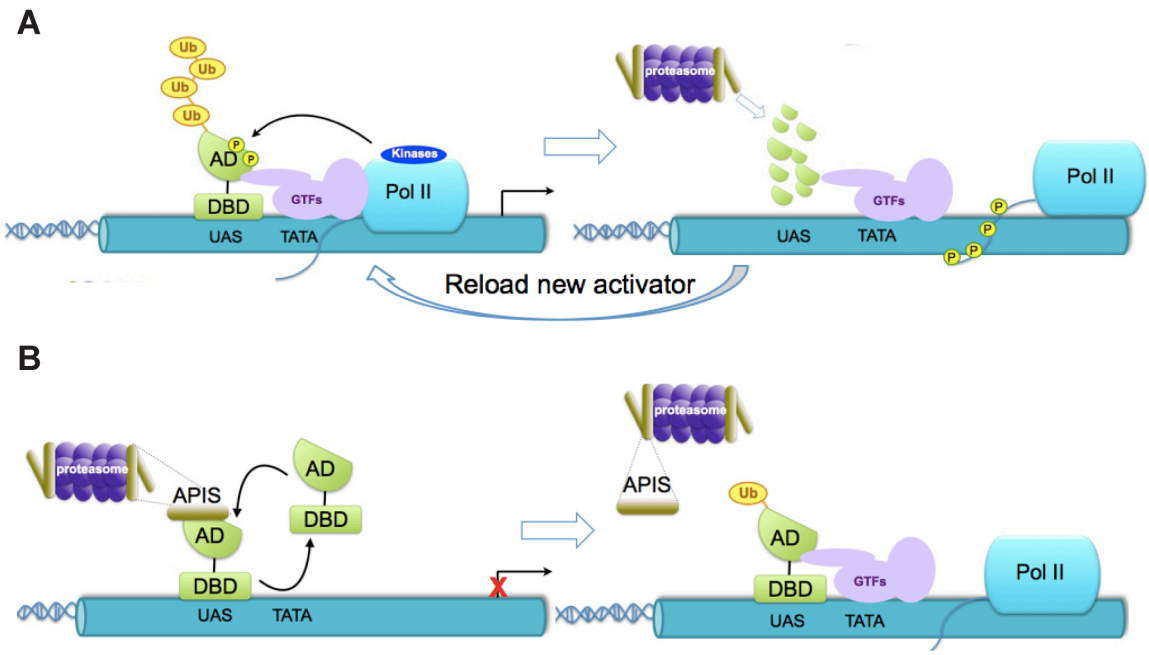

Figure 1.2.The UPS regulates transcription via both proteolytic and non-proteolytic approaches.
(A) Ubiquitination and degradation of the activator facilitates promoter escape of RNA polymerase II in each round of transcription. AD, activation domain; DBD, DNA binding domain; UAS, upstream activating sequences; GTF, general transcription factor. **(B)** Mono-ubiquitination of the activator facilitates transcription by preventing APIS from stripping the activator off DNA.

This defect did not affect the amounts of the transcripts produced or mRNA export, yet the transcripts were poorly translated, indicating a defect in the quality of the transcripts. Although the detailed mechanisms remain unclear, it is possible that failure to degrade Gal4 leads to inefficient disassembly of the initiation complex, and/or recruitment of mRNA processing factors.

It is important to keep in mind that there may be more than one E3 Ub ligases for a given TA, and each may play a different role in regulating activator function. In the case of Gal4, whereas Dsg1 regulates the pool engaged in transcription, another F-box protein, Grr1, regulates the overall abundance of the protein (Muratani et al., 2005). When yeast cells are grown in raffinose, Grr1 helps to keep the *GAL* genes repressed by limiting total amounts of Gal4 in the cell. Deletion of *GRR1* leads to derepression. When the carbon source is switched to galactose, Dsg1-dependent degradation of Gal4 plays a positive role in transcription, opposite to Grr1. A similar case in mammals is seen with the oncoprotein Myc. Whereas the overall abundance of Myc is regulated by the F-box protein Fbw7 (Welcker et al., 2004; Yada et al., 2004), transcription activation by Myc requires a different F-box protein, Skp2 (Kim et al., 2003; von der Lehr et al., 2003). As the ability to identify E3 ligase substrates improves, we are likely to see more cases like those of Gal4 and Myc. Transcription-coupled phosphorylation is likely a general strategy to mark the subset of an activator that is engaged in transcription (Chi et al., 2001). By using multiple E3 Ub ligases that recognize different populations of the activator, the cell can fine-tune its response to changing environments. Thus, it may be no coincidence that activators known to be regulated by the UPS are involved in inducible rather than constitutive transcription.

1.1.4 Non-proteolytic roles of ubiquitin in controlling transcriptional activators

Transcription-coupled degradation typically involves poly-ubiquitination of the activator. Interestingly, there are a few cases where mono-ubiquitination of the activator plays a non-proteolytic role in transcription (Archer et al., 2008a; Bhat et al., 2008; Bres et al., 2003; Ferdous et al., 2007; Zou et al., 2011). In a pioneering study, Salghetti et al. demonstrated that a Ub-activator fusion protein can bypass the need for the ubiquitination machinery and activate transcription directly (Salghetti et al., 2001). They constructed a heterologous activator consisting of LexA DBD and VP16 AD. When introduced into yeast, LexA–VP16 is a potent activator with a half-life of ~3 min. Transcription activation and degradation of LexA–VP16 both depend on the yeast F-box protein Met30 – in the absence of Met30, LexA–VP16 no longer activates transcription. However, transcription is restored if monoUb is fused to the N-terminus of LexA–VP16. Surprisingly, the fused Ub does not lead to turnover of the activator, which suggests that the monoUb signal can activate transcription independent of proteolysis.

Another example comes from a series of studies from the Kodadek and Johnston laboratories on Gal4 (Archer et al., 2008a; Archer et al., 2008b; Archer and Kodadek, 2010; Collins et al., 2009; Ferdous et al., 2007; Nalley et al., 2006). Using an *in vitro* system containing HeLa nuclear extract, they found that Gal4–VP16 is rapidly displaced from DNA in an ATP-dependent manner by the 19S RP (Ferdous et al., 2007). Interestingly, a small fraction of Gal4–VP16 is mono-ubiquitinated by the extract and able to bind to DNA stably. Similarly, a Ub–Gal4–VP16 genetic fusion also can stably bind to DNA (Figure 1.2B). Such behavior is mirrored by a Gal4 mutant named Gap71, which contains three point mutations in the DBD of native Gal4. In the absence of nuclear extract, Gap71 has an affinity for DNA

similar to native Gal4. However, *in vivo*, Gap71 does not activate *GAL* genes efficiently and is not detected at the promoters upon galactose induction. A mutation in the proteasome ATPase Rpt6 (*sug1-20*) can partially rescue the transcriptional defects of Gap71. Both genetic and biochemical evidence suggest that Gal4 directly interacts with two ATPases of the 19S RP, Rpt4 and Rpt6 (also known as Sug2 and Sug1, respectively) (Archer et al., 2008a; Gonzalez et al., 2002). It was proposed that these interactions remove Gal4 from DNA through the unfoldase activities of the 19S RP. Mono-ubiquitination of Gal4 may protect against this removal from the DNA, thereby promoting transcription. The failure of the Gap71 mutant to activate transcription may be due to defective ubiquitination (Archer et al., 2008a; Archer et al., 2008b; Archer and Kodadek, 2010; Ferdous et al., 2008; Ferdous et al., 2007).

Although the generality of activator mono-ubiquitination is unclear, the studies cited above demonstrate that the UPS can regulate activator proteins via multiple mechanisms. Because transcription is a complex process involving initiation, elongation, termination and re-initiation, it has been proposed that monoUb and polyUb signals are used at different stages of this process (Bhat and Greer, 2011; Kodadek et al., 2006); yet convincing evidence for this model is still lacking. Genome-wide studies showed that both 19S and 20S components are recruited to transcriptionally active chromatin, in a virtually indistinguishable manner, suggesting prevalent involvement of the proteasome in transcription regulation (Auld et al., 2006; Geng and Tansey, 2012; Gillette et al., 2004; Sikder et al., 2006). What their functions are at different gene loci are among the major questions for future studies in this field.

Finally, the UPS also has been implicated in transcription repression through both proteolytic and non-proteolytic mechanisms. The transcription factor Met4 regulates a subset of genes referred to as *MET* genes in yeast. These genes encode proteins required for the biosynthesis of sulfur containing metabolites such as methionine, cysteine, glutathione and S-adenosylmethionine (Lee et al., 2010). When yeast is grown under limiting intracellular methionine levels as well as heavy metal stress (cadmium or arsenic), Met4 activates transcription of the *MET* genes. This pathway directly connects sulfur-containing metabolite balance to cell cycle regulation, because full activation of Met4 induces a cell cycle arrest to maintain cellular and genetic integrity during nutrient limitation or heavy metal stress (Flick et al., 2004). The products of *MET* genes are utilized to induce metabolic pathways to restore intracellular levels of sulfur metabolites. Once this is achieved, Met4 is ubiquitinated by the SCF^{Met30} E3 ligase, which rapidly turns off gene expression. While Met4 poly-ubiquitination can lead to its rapid degradation by the proteasome (Kuras et al., 2002; Rouillon et al., 2000), this is not necessarily the case. Indeed, Met4 modified by a canonical K48-linked Ub chain generally remains stable (Flick et al., 2006; Kaiser et al., 2000). The Kaiser group identified two internal Ub-binding domains in Met4 that sequester the Ub chain in cis and prevent Met4 from being targeted to the proteasome (Tyrrell et al., 2010). Ubiquitination of Met4 is sufficient to turn off gene expression without invoking proteolysis. Met4 ubiquitination has been correlated with loss of promoter recruitment, but the molecular determinants of this regulation remain to be identified. This pathway is crucial for cell survival and tightly controlled ubiquitination of Met4 is necessary to fine-tune activation and repression cycles.

Although many studies have revealed multiple modes of regulation of transcription by the UPS, each study typically focuses on only one mode and many controversies remain. Is there a unified mechanism that underlies the coupling of transcription and degradation of the activator? Why is degradation of the activator necessary in some cases and not in others? Answers to these questions are needed to resolve controversies and to bring the big picture into focus.

1.1.5 The AAA-ATPase Cdc48 and its cofactors Ufd1 and Npl4

Cdc48 (in budding yeast), p97 or VCP (in mammals) is well conserved among all eukaryotes and has been found to be essential in *Saccharomyces cerevisiae* (Frohlich et al., 1991), *Drosophila melanogaster* (Leon and McKearin, 1999), *Caenorhabditis elegans* (Yamanaka et al., 2004) and mice (Muller et al., 2007). As the name indicates, the *CDC48* gene was first identified in a screen for conditional mutations that affect the cell division cycle in budding yeast (Frohlich et al., 1991). Subsequent studies have provided details on the biochemical and structural properties of Cdc48 and revealed its central function in Ub-dependent degradation (Baek et al., 2013).

Cdc48 belongs to the family of AAA (ATPases associated with various cellular activities) ATPases and forms a homo-hexameric, double-ring shaped structure (Figure 1.3). Each monomer contains a substrate and cofactor binding N-terminal domain, followed by two consecutive AAA ATPase domains, termed D1 and D2, and a C-terminal tail (Figure 1.3) (DeLaBarre and Brunger, 2003; Rouiller et al., 2002). Cdc48 converts the energy from ATP hydrolysis into mechanical forces to induce conformational changes of substrate proteins, leading to unfolding or disassembly of protein complexes (Wolf and Stolz, 2012; Ye, 2006). Despite the fact that Cdc48 is linked to a large variety of biological functions,

evidence from the past decade indicates that its primary biochemical function is to segregate ubiquitinated substrates from unmodified partners and target them for degradation by the proteasome (Buchberger, 2013; Wolf and Stolz, 2012; Ye, 2006).

How Cdc48 selects its substrate and determines its downstream fate is an area of active research. In a few cases, substrates have been reported to directly interact with Cdc48 (Dai and Li, 2001; Rape et al., 2001); however, by and large, ubiquitinated substrates are targeted through a plethora of cofactors, that are characterized by Ub-binding domains, and usually interact with the N-terminal domain of Cdc48 via conserved structural features (Figure 1.3) (Hartmann-Petersen et al., 2004; Meyer et al., 2002; Rape et al., 2001; Richly et al., 2005; Ye, 2006). The prevailing substrate-recruiting cofactors are the Ufd1-Npl4 heterodimer and Ubx1 (also called p47 in mammals). Each forms an exclusive complex with Cdc48 (Buchberger et al., 2001; Meyer et al., 2002). Ufd1 and Npl4 each possess a Ub-interacting domain and the heterodimer binds to the hexameric Cdc48 in 1:1 stoichiometry (Figure 1.3). The Ubx family of proteins is characterized by the presence of the UBX domain, which has a three-dimensional structure resembling that of Ub, although there is no primary sequence similarity (Buchberger et al., 2001; McNeill et al., 2004). Many of these cofactors are not essential for cell growth and viability, suggesting possible functional redundancy among them. There are seven UBX-containing genes identified in *S. cerevisiae* (Buchberger, 2013). Yeast cells lacking any one of these Ubx factors are viable, but deletion of multiple *UBX* genes leads to severe phenotypes, including cell death. This suggests they have critical, overlapping functions. Not all substrate-recruiting cofactors associate with Cdc48 in a mutually exclusive manner; for example, Cdc48 can bind to Ufd1-Npl4 and Ubx2 simultaneously (Schuberth and Buchberger, 2005). Association of Cdc48 with different

combinations of substrate-recruiting cofactors affords an incredible functional diversity, allowing Cdc48 to play critical roles in a broad range of diverse cellular processes, including Ub-proteasome degradation, membrane reassembly, ER associated degradation (ERAD), cell cycle regulation, autophagy, lipid droplets biogenesis, transcription and DNA repair (Baek et al., 2013; Jentsch and Rumpf, 2007; Olzmann et al., 2013).

Aside from substrate-recruiting cofactors, Cdc48 also associates with substrate-processing cofactors, mainly through its C-terminal tail (Rumpf and Jentsch, 2006). These proteins directly influence the degree of ubiquitination of the bound substrate by either promoting poly-ubiquitination, inhibiting poly-ubiquitination or even deubiquitinating the bound ubiquitinated substrate. For example, by forming a complex with Ufd1-Npl4 and the E4 enzyme Ufd2, Cdc48 mediates elongation of the Ub chain from mono- or oligo-ubiquitinated substrates (Koegl et al., 1999; Saeki et al., 2004). Ubiquitination is antagonized by association of Cdc48 with the deubiquitinating enzyme Otu1 (Rumpf and Jentsch, 2006). Apart from cofactors that alter the ubiquitination state of the bound substrate, there are also processing factors that modify the substrates in different ways: the peptide N-glycanase (PNGase) removes oligosaccharides from ERAD substrates before proteasomal degradation, whereas HDAC6, a deacetylating enzyme related to histone deacetylases, associates with ubiquitin–protein conjugates (Allen et al., 2006; Boyault et al., 2006). The balance between the distinct substrate-processing cofactors may determine whether a substrate is poly-ubiquitinated and routed to the proteasome for degradation or deubiquitinated and/or released for other purposes.

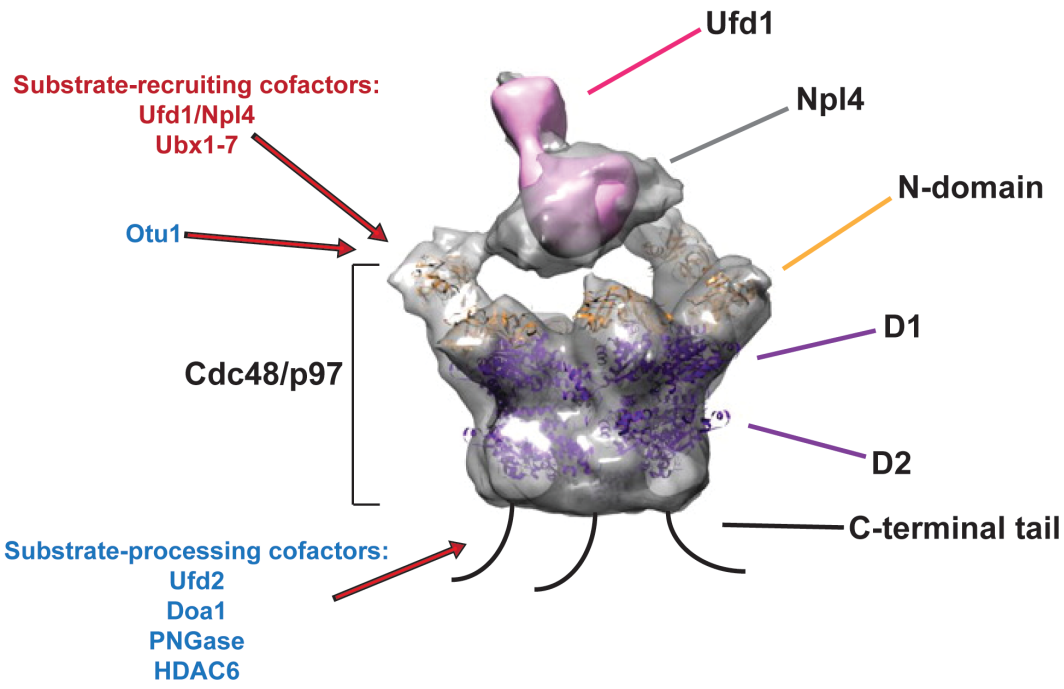

Figure 1.3. p97 and its cofactors.
Shown is the 3D reconstruction from cryo-electron microscopy images of mouse p97 in complex with Ufd1-Npl4 heterodimer (Bebeacua et al., 2012). Each subunit of p97 contains an N-terminal domain, two AAA ATPase domains D1 and D2, and a C-terminal tail. The N-terminal domain serves as a docking site for substrate recruiting cofactors such as Ufd1, Npl4, Ubx, etc. Substrate-processing cofactors such as Ufd2, Doa1, PNGase and HDAC6 typically interact with the C-terminal tail.

In the context of transcription, Cdc48 has been reported to remove poly-ubiquitinated yeast transcription repressor α2 from chromatin, which facilitates subsequent degradation by the proteasome (Wilcox and Laney, 2009). This was the first evidence that Cdc48 regulates chromatin-bound proteins. Subsequently, multiple groups have shown that proteasomal degradation of different chromatin-bound proteins often requires extraction by Cdc48. For example, the Cdc48-Ufd1-Npl4 complex and its adaptors Ubx4 or Ubx5 are required for proteasomal degradation of stalled RNAPII, which can occur during normal transcription or upon DNA damage (Verma et al., 2011). Similar requirements for Cdc48 have been shown for proteins involved in DNA repair (Acs et al., 2011; Meerang et al., 2011), as well as the replication-licensing factor Cdt1 (Raman et al., 2011). Additionally, Cdc48 has been shown to remove Aurora B kinase from chromatin independently of proteolysis (Ramadan et al., 2007). In all of these cases, poly-ubiquitination of the substrate appears to be a prerequisite for Cdc48 action.

1.2 Dynamic regulation of chromatin

The nucleosome represents the basic functional unit of chromatin. It contains 146 bp of DNA, wrapped around an octameric histone core, which consists of two copies of each of the canonical histones H2A, H2B, H3 and H4 (Luger et al., 1997). These four histone proteins interact in an ordered manner during nucleosome assembly, giving rise to the modular nature of the nucleosome. Each nucleosome core particle is joined by ~20-90 base pairs of linker DNA, giving the appearance of "beads on a string" when analyzed by electron microscopy (Bei et al., 1983). Histones and chromatin components have key roles in the decision making process of activating or repressing genes in a spatial and temporal fashion.

If as few as three inappropriate genes are turned off, a normal cell can be converted into a cancer cell. Therefore, understanding how chromatin is remodeled and regulates transcription is an important step towards fighting diseases like cancer.

1.2.1 Transcription in the context of chromatin

During transcription, nucleosomes act as barriers, hindering the accessibility to DNA and progress of RNAPII. Different mechanisms have evolved to overcome these barriers, and fine-tune the transcriptional response both temporally and spatially. These mechanisms fall into three broad categories: mechanisms that alter nucleosomes (mediated by chromatin modifiers), mechanisms that mobilize nucleosomes (mediated by chromatin remodelers), and mechanisms that facilitate RNAPII activity (mediated by elongation factors) (Venkatesh and Workman, 2015). Furthermore, coordination between histone post-translational modifications (PTMs) and chromatin remodelers represents an additional layer of regulation.

Different chromatin transactions have been reported to occur during the three main phases of transcription (Figure 1.4). Transcription initiation requires promoters to be kept devoid of nucleosomes. Genome-wide analysis of nucleosome positions in several organisms has shown that gene promoters have low nucleosome occupancy and often contain a nucleosome free region (NFR) (Schones et al., 2008; Yuan et al., 2005). NFRs are genomic regions that display increased micrococcal nuclease digestion and DNAseI hypersensitivity, and are usually found upstream of transcription start sites (TSSs). NFRs are flanked by two well-positioned nucleosomes. Depending on whether these nucleosomes are located upstream or downstream of the TSS, they are referred to as -1 and

+1 nucleosome, respectively. In budding yeast, the +1 nucleosome is positioned over the TSS, leading to its occlusion (Mavrich et al., 2008). In human cells, the +1 nucleosome is typically positioned 10 to 40 bp downstream of the TSS (Schones et al., 2008). Promoter regions upstream of the +1 nucleosome can be kept devoid of nucleosomes through the action of chromatin remodelers, which slide nucleosomes away from this region (Ganguli et al., 2014; Hartley and Madhani, 2009). In addition, other mechanisms contribute to the destabilization of nucleosomes flanking the promoter to ensure robust transcription initiation. One such mechanism is incorporation of the histone variant H2A.Z (Albert et al., 2007; Raisner et al., 2005). In *Drosophila melanogaster*, H2A.Z incorporation at +1 nucleosomes has been shown to lower the barrier for RNAPII elongation and decrease RNAPII stalling (Kwak et al., 2013; Weber et al., 2014). Exactly how H2A.Z facilitates the progression through the nucleosome remains unclear.

Passage of the elongating RNAPII within gene coding regions is aided by the histone chaperone complex FACT, which facilitates removal of H2A-H2B dimers from nucleosomes (Pavri et al., 2006). In metazoans, transcription elongation is additionally associated with the replacement of canonical H3 with the variant H3.3 by the HIRA chaperone (Pchelintsev et al., 2013).

The passage of RNAPII over the coding regions of the genes is accompanied by a disruption of the nucleosome structure. Resetting of chromatin to its original state occurs co-transcriptionally, immediately following the passage of RNAPII. The timing of resetting is highly regulated, as an improperly spaced chromatin structure exposes cryptic promoters, which can result in their use for transcription initiation events within the gene body (Carrozza et al., 2005; Kaplan et al., 2003). Work from multiple groups has identified

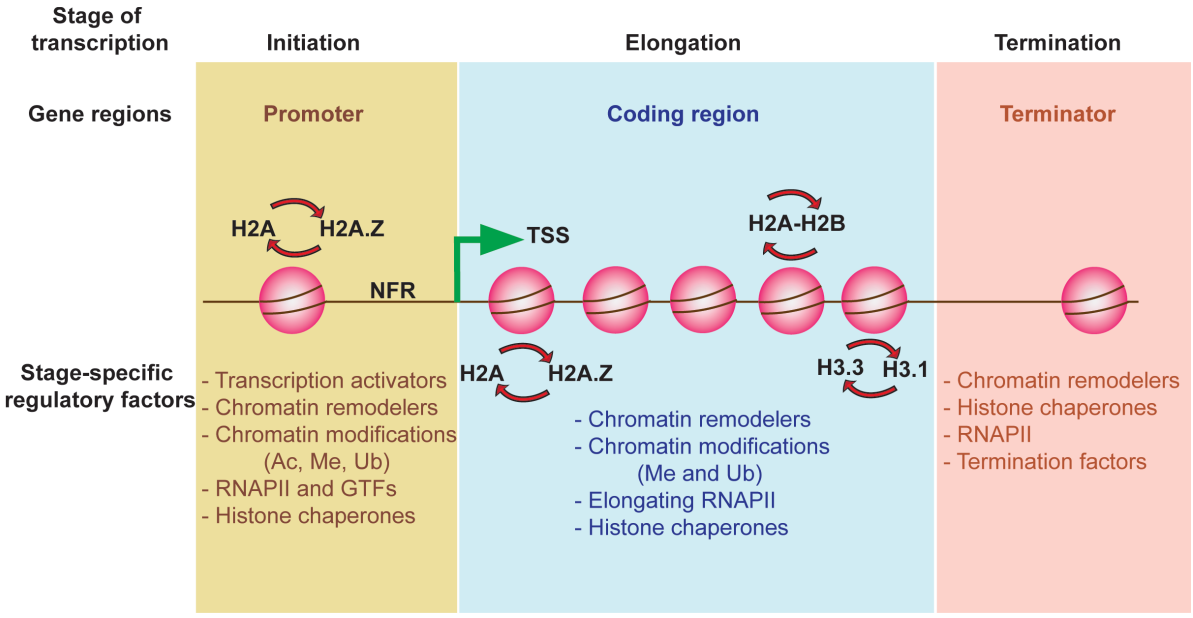

Figure 1.4. Factors involved in different stages of transcription.
Different factors are recruited over specific regions of the gene at different stages of transcription. Transcription activators orchestrate recruitment of GTFs and RNAPII at the promoter region. Chromatin remodelers slide nucleosomes away from this region to keep it free of nucleosomes. Flanking nucleosomes are enriched in H2A.Z and several PTMs, such as acetylation (Ac), methylation (Me) and ubiquitination (Ub). In the coding region chromatin remodelers facilitate nucleosome dynamics and the histone variant H3.3 is deposited into these nucleosomes. NFR: Nucleosome free region.

different signals that trigger the re-establishment of chromatin after the passage of the elongating RNAPII (Smolle et al., 2013). ATP-dependent chromatin remodelers, Chd1 and ISWI1b, are recruited in the coding regions to ensure proper nucleosome spacing (Smolle et al., 2012). In addition, chromatin modifiers mediate removal of acetylation marks from chromatin over coding regions (Joshi and Struhl, 2005).

1.2.2 The histone variant H2A.Z

Histone variants are non-allelic isoforms of canonical histones that differ in their primary sequences and their expression timing (Marzluff et al., 2002). Whereas expression of canonical histones is almost completely limited to S-phase, most histone variants are expressed throughout the cell cycle. This is mainly caused by their different mRNA structure. Canonical histones generally lack introns, and their mRNAs are stabilized by a unique 3' stem loop instead of being polyadenylated (Marzluff et al., 2008). In contrast, most variant histone mRNAs are polyadenylated and their pre-mRNAs contain introns (Marzluff et al., 2008).

The histone variant H2A.Z diverged from canonical H2A early in eukaryotic evolution, and it is highly conserved across eukaryotes (Thatcher and Gorovsky, 1994). In metazoans, H2A.Z is essential for viability, suggesting that H2A.Z fulfils specific and unique functions that cannot be carried out by other H2A variants (Faast et al., 2001; Iouzalen et al., 1996; van Daal and Elgin, 1992). Despite that H2A.Z has only ~60% amino acid sequence similarity with H2A, H2A.Z-containing nucleosomes have a structure that is almost identical to that of canonical nucleosomes (Figure 1.5A and 1.5B) (Luger et al., 1997; Suto et al., 2000). Two regions in the C-terminal tail of H2A.Z, designated as M6 (G92-

A102) and M7 (A105-G119), have been shown to be essential for H2A.Z function in *Drosophila melanogaster* (Figure 1.5A and 1.5B) (Clarkson et al., 1999). In line with this finding, the M6 region is required for its interaction with SWR-C chromatin-remodeling complex in yeast as well as the H2A.Z-specific chaperone ANP32E in mammals (Obri et al., 2014; Wu et al., 2005).

Whether the differences in primary sequence between H2A.Z and H2A significantly alter the stability of the H2A.Z-containing nucleosomes, has been controversial. Some studies have found that H2A.Z incorporation leads to stabilization of nucleosomes, whereas other studies have reported the opposite (reviewed in (Bonisch and Hake, 2012)). The reported differences can be attributed to the use of H2A.Z from different organisms (~20% divergence), different experimental setups or different sources of chromatin. This is further complicated by the fact that additional PTMs or incorporation of other histone variants have been reported to alter the stability of H2A.Z-containing nucleosomes and chromatin (Henikoff, 2009; Ishibashi et al., 2009; Jin and Felsenfeld, 2007). More recently, FRET measurements *in vitro* as well as FRAP analysis of H2A.Z mobility *in vivo*, have shown that there are only subtle effects on nucleosome stability as a consequence of H2A.Z incorporation (Higashi et al., 2007; Hoch et al., 2007).

H2A.Z is not uniformly distributed within the genome. Genome-wide studies have shown that H2A.Z is highly enriched within the few nucleosomes that flank the promoter NFR regions of RNAPII-transcribed-genes (Barski et al., 2007; Guillemette et al., 2005; Raisner et al., 2005; Zhang et al., 2005; Zilberman et al., 2008). Intriguingly, H2A.Z is enriched at both active and silent genes, yet how H2A.Z influences gene expression in a context-dependent manner has remained elusive. These contrasting transcriptional

outcomes are likely influenced by other factors including PTMs on other histones. For example, in mouse ESCs, H2A.Z is present at a large set of genes marked by H3 lysine 4 tri-methylation nucleosomes that include both active genes and silent developmental genes (Hu et al., 2013).

How is H2A.Z localized to specific positions throughout the genome? In *Saccharomyces cerevisiae*, the ATP-dependent chromatin remodeler SWR-C deposits H2A.Z by exchanging nucleosomal H2A-H2B dimers with free H2A.Z-H2B dimers, one copy at a time in a stepwise manner (Luk et al., 2010). yINO80 catalyzes the opposite reaction *in vitro* (Figure 1.5C) (Papamichos-Chronakis et al., 2011). Metazoans contain two SWR-C orthologs, SRCAP and p400/TIP60, both of which catalyze H2A.Z deposition by dimer exchange (Billon and Cote, 2013). Recently, a mammalian histone chaperone ANP32E has been shown to facilitate H2A.Z removal from nucleosomes *in vitro* and *in vivo* (Figure 1.5C) (Obri et al., 2014). ANP32E was co-purified with the p400/TIP60 complex. Whether H2A.Z incorporation at specific sites is regulated by targeting of the appropriate chromatin remodeler, or H2A.Z is randomly deposited and afterwards actively removed from non-specific sites, is still an open question.

Acetylation of H3 at K56 has a major impact on the H2A.Z exchange reaction *in vitro*. This specific modification abrogates the specificity of SWR-C, leading to promiscuous H2A.Z H2A exchange (Figure 1.5C) (Watanabe et al., 2013). In the case of yINO80, acetylation of H3 at K56 stimulates its dimer exchange activity. Consistent with these *in vitro* findings, H2A.Z or H3K56 acetylation has been shown to enhance rapid turnover of promoter nucleosomes in yeast (Dion et al., 2007; Rufiange et al., 2007). Mammalian gene promoters are enriched in nucleosomes harboring both H2A.Z and H3 acetylated at K56, suggesting a

A

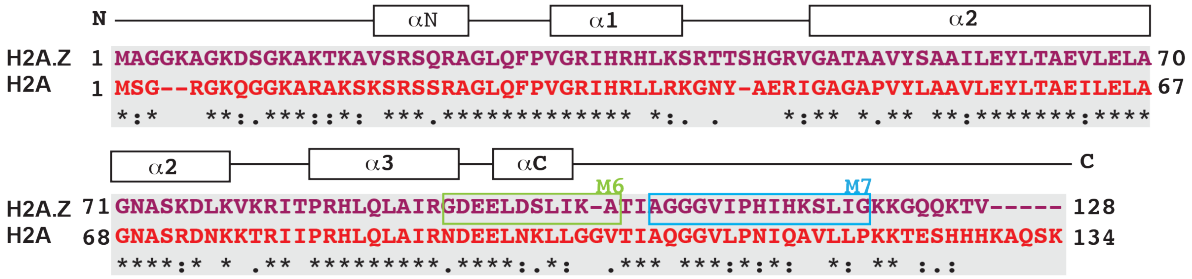
N
αN
α1
α2
H2A.Z 1 MAGGKAGKDSGKAKTKAVSRSQRAGLQFPVGRIHRHLKSRTTSHGRVGATAAVYSAAILEYLTAEVLELA 70
H2A 1 MSG--RGKQGGKARAKSKSRSSRAGLQFPVGRIHRLLRKGNY-AERIGAGAPVYLAAVLEYLTAEILELA 67
α2
α3
αC
C
M6
M7
H2A.Z 71 GNASKDLKVKRITPRHLQLAIRGDEELDSLIK-ATIAGGGVIPHIHKSLIGKKGQQKTV----- 128
H2A 68 GNASRDNKKTRIIPRHLQLAIRNDEELNKLLGGVTIAQGGVLPNIQAVLLPKKTESHHHKAQSK 134

B

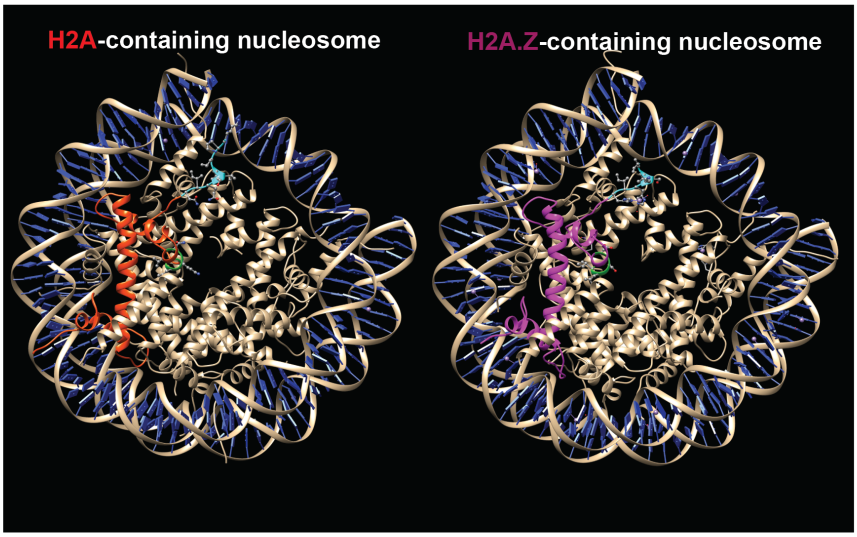
H2A-containing nucleosome
H2A.Z-containing nucleosome

C

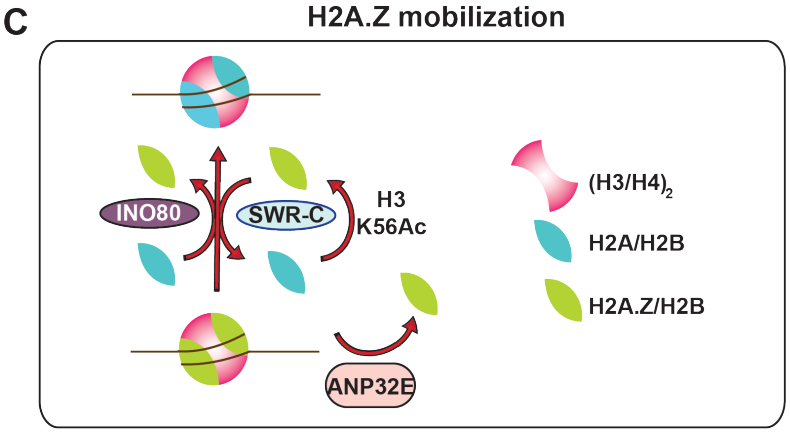
H2A.Z mobilization
INO80
SWR-C
H3
K56Ac
ANP32E
(H3/H4)2
H2A/H2B
H2A.Z/H2B

Figure 1.5. The histone variant H2A.Z.(A) Alignment of amino acid sequences of the human histone variant H2A.Z (NP_002097.1) and human histone H2A (NP_003501). Secondary structures are indicated above. The M6 and M7 regions of H2A.Z are highlighted with green and cyan boxes, respectively. **(B)** Crystal structures of the nucleosome harboring H2A (PDB ID: 1AOI) or H2A.Z (PDB ID: 1F66). One copy of H2A is shown in red, and one copy of H2A.Z is shown in magenta. All other histones are shown in tan and DNA is shown in tan and blue. The M6 and M7 regions of H2A.Z and their corresponding regions of H2A are highlighted in green and cyan respectively. Images were generated using the UCSF Chimera program. **(C)** H2A.Z dynamics is facilitated by SWR-C, INO80 and ANP32E.

conserved regulatory relationship between these marks (Barski et al., 2007; Xie et al., 2009).

Accurate levels of H2A.Z expression are required for the integrity and stability of the human genome. In human cells, altered expression levels of H2A.Z have recently been linked with specific types of cancer (Rangasamy, 2010). Gene expression analysis shows that H2A.Z is over-expressed in primary breast tumors and colorectal cancer (Hua et al., 2008). The elevated levels of H2A.Z expression are associated with the spread of the cancer to lymph nodes, metastasis and decreased patient survival. On the other hand, H2A.Z is significantly depleted in cancer cells that have chromosomal instability (Dunican et al., 2002). Therefore, H2A.Z expression levels and localization on chromatin needs to be tightly regulated to prevent cancer formation and progression.

1.2.3 Histone ubiquitination and its function in transcription

Histones contain many amino acids that are post-translationally modified. The most characterized modifications include phosphorylation on serines or threonines, methylation on lysines or arginines, acetylation, ubiquitination, and sumoylation on lysine residues and ADP-ribosylation on glutamic acids (Figure 1.6A) (Arnaudo and Garcia, 2013). Depending on the nature of the PTM, some can directly affect nucleosome stability by altering the chemical interactions within the nucleosome or among neighboring nucleosomes. For example, acetylation of lysine residues on histone tails can neutralize their positive charge, thus weakening the interactions between histone octamer and DNA (Hong et al., 1993). In another case, conjugation of Ub to H2B has been reported to antagonize chromatin compaction of nucleosomal arrays *in vitro* (Fierz et al., 2011). More recent evidence

suggests that the H3 tail interacts with linker DNA between two neighboring nucleosomes and aids chromatin compaction (Rhee et al., 2014). As a result, tri-methylation of the H3 tail at lysine 36 alters the potential of the H3 tail to interact with linker DNA, leading to a more open chromatin structure (Rhee et al., 2014).

Additionally histone PTMs can act as signaling platforms to recruit specific effector proteins, thus modulate the protein repertoire that interacts with chromatin (Bottomley, 2004). Several proteins involved in transcription contain domains that are tailored to specifically recognize PTMs on histone proteins. For example, bromodomain containing proteins are recruited through interactions with acetylated lysines on histones, whereas proteins harboring a chromodomain are recruited through methylated lysines (Dhalluin et al., 1999; Jacobs and Khorasanizadeh, 2002; Kanno et al., 2004; Nielsen et al., 2002). Conceptually, histone ubiquitination can also recruit or exclude interacting proteins by masking important histone association surfaces (Long et al., 2014b).

Ubiquitination of H2A—Ubiquitinated H2A was the first ubiquitinated protein identified (Goldknopf et al., 1975). Whereas monoubiquitinated H2A has not been identified in budding yeast, 10-15% of total metazoan H2A is monoubiquitinated at lysine 119, making UbH2A one of the most abundant ubiquitinated proteins in the nucleus (Hatch et al., 1983; Wu et al., 1981; Wunsch et al., 1987). UbH2A has been associated with gene silencing, an important mechanism utilized to achieve differential gene expression during cell differentiation and development (Fang et al., 2004). The main E3 ligase for H2A at lysine 119 is Ring1B, a subunit of the Polycomb Repressive Complex 1 (PRC1) (Cao et al., 2005). Both UbH2A and PRC1 have been found to localize to many silenced domains of the genome as well as some promoter regions where transcription is turned off (Cao et al.,

2005; Wang et al., 2004). Additionally, the X chromosome in mammals is coated with the UbH2A mark consistent with its silencing function (Fang et al., 2004). Despite strong evidence that links UbH2A to gene silencing, how UbH2A facilitates this process remains unclear. One possibility is that H2A ubiquitination facilitates higher order chromatin structure by increasing association of the histone linker H1 (Jason et al., 2005; Zhu et al., 2007).

Ubiquitination of H2B—In all eukaryotes, H2B is monoubiquitinated in its C-terminal tail (lysine 120 in humans and lysine 123 in yeast), a process carried out by the Rad6 family of Ub-conjugating enzymes and the Ub-ligase Rnf20/Rnf40 in humans (Kao et al., 2004; Kim et al., 2005; Robzyk et al., 2000). Although both H2A and H2B ubiquitination occurs in their C-terminal tails, when mapped onto the nucleosome structure, the Ub moiety is positioned at opposite ends of the nucleosome (Figures 1.6B and 1.6C).

Inherently, ubiquitination of H2B does not interfere with mono-nucleosome assembly (Davies and Lindsey, 1994). However, it impairs chromatin fiber formation and can act with other PTMs to relax higher-order chromatin structures (Fierz et al., 2011). This phenomenon is consistent with the bulky nature of this modification, which prevents tight compaction of chromatinized DNA strands and influences the ability of RNAPII to access its DNA template. However, *in vivo* this is unlikely to be the sole mechanism through which H2B ubiquitination works. *In vitro* chromatin compaction experiments have shown that replacement of Ub with another bulky Ub-like modification, such as SUMO or Hub1, cannot recapitulate the effects of H2B ubiquitination (Chandrasekharan et al., 2009; Fierz et al., 2011). Therefore, it has been suggested that components of the transcription machinery specifically recognize the Ub mark on H2B to elicit a biological response.

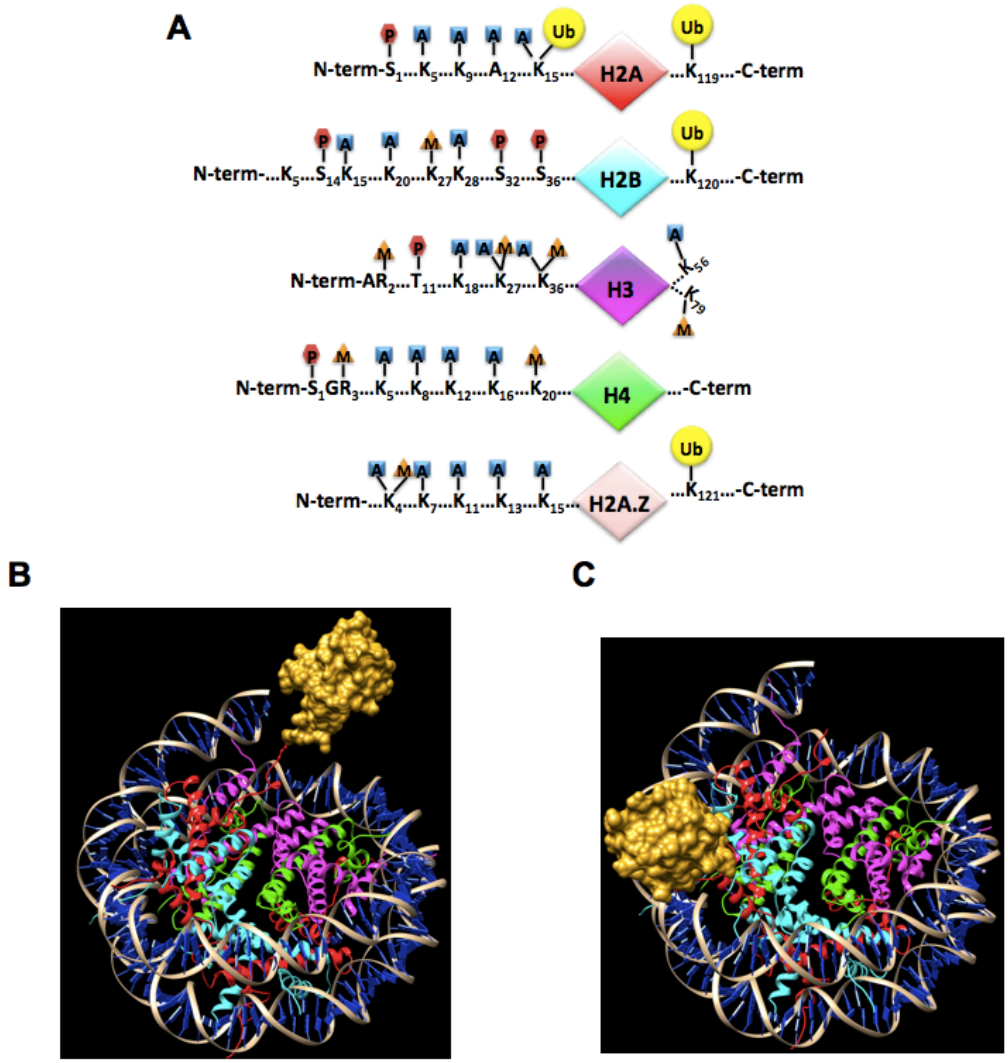

Figure 1.6. Post-translational modifications of the canonical human histones (H2A, H2B, H3, H4) and the histone variant H2A.Z.
(A) Illustration of some well characterized PTMs, such as acetylation (A), methylation (M), phosphorylation (P) and ubiquitination (Ub). Most of the known histone modifications occur on the N-terminal tails of histones, with some exceptions such as ubiquitination of H2A, H2B and H2A.Z in the C-terminal tail region and acetylation and methylation in the globular domain of H3 at K56 and K79, respectively. The globular domains of each histone are depicted as a colored diamond. **(B)** The structure of ubiquitin (PDB ID: 1UBQ) was placed at H2A K119 in the context of a nucleosome structure (PDB ID: 1AOI) (Luger et al., 1997). The figure was generated using the Chimera software to illustrate spatial and size relationships. No modeling was performed. The color-coding scheme is: H2A (red), H2B (cyan), H3 (magenta), H4 (green), ubiquitin (yellow), DNA phosphobackbone (tan) and DNA bases (blue). **(C)** Ubiquitin was placed at H2B K120 as described in B.

Ubiquitination of H2B is tightly coupled to active transcription and is a prerequisite for two other types of PTMs associated with active transcription: H3K4 di- and tri-methylation as well as H3K79 di- and tri-methylation (Nakanishi et al., 2009; Sun and Allis, 2002). In addition, UbH2B has been connected to the function of the histone chaperone FACT. The prevailing model is that during transcription elongation FACT displaces H2A-H2B dimers ahead of RNAPII and subsequently promotes nucleosome reassembly behind RNAPII. H2B ubiquitination promotes FACT recruitment to chromatin and stimulates its function; conversely, FACT promotes H2B ubiquitination both *in vivo* and *in vitro* (Fleming et al., 2008; Pavri et al., 2006). Despite their functional connections, it is not known whether UbH2B and FACT interact biochemically or how UbH2B affects FACT function as a chaperone.

Ubiquitination of H2B has also been reported to have negative effects on transcription elongation (Shema et al., 2011; Wyce et al., 2007). In human cells, UbH2B represses transcription of a set of pro-oncogenic genes by inhibiting recruitment of the elongation factor TFIIS (Shema et al., 2011). Given that H2B ubiquitination has both positive and negative roles in transcription, the timing and the dynamics of this modification may determine the biological consequences. As a result, timely deubiquitination of H2B is also important for optimal levels of transcription. UbH2B removal is mediated by the deubiquitinating enzyme USP22 in humans, which is an integral part of the SAGA co-activator complex (Kohler et al., 2008; Zhang et al., 2008; Zhao et al., 2008).

1.2.4 The INO80 family of chromatin remodeling complexes

ATP-dependent chromatin remodelers use the energy from ATP hydrolysis to directly alter the chromatin structure, catalyzing the assembly of nucleosomes, sliding of histone octamers along the DNA, eviction of histone H2A-H2B dimers or ejection of an entire histone octamer (reviewed in (Gerhold and Gasser, 2014)). All remodelers act through a Snf2 (sucrose non-fermenting)-type ATPase domain, which serves as a motor that functionally alters DNA-protein interactions (Flaus et al., 2006). Accessory modules regulate the functional consequence of the ATPase domain. Most nucleosome remodelers function as large, multi-subunit molecular machines, whose subunit complexity allows them to deliver a broad range of remodeling activities. There are four main families of remodelers classified based on their conserved ATPase domain: SWI/SNF (mating type switching/sucrose non-fermenting), ISWI (imitation switch), INO80 (inositol) and CHD (chromodomain helicase DNA-binding) (Figure 1.7) (Flaus et al., 2006).

The INO80 chromatin-remodeling complex is one of the two members of the INO80 family. The budding yeast INO80 complex (yINO80) was the first INO80 complex to be purified and characterized (Ebbert et al., 1999; Shen et al., 2000; Shen et al., 2003). Subsequently, the Conaway group purified and defined the subunit composition of the human INO80 complex (hINO80) (Cai et al., 2007; Jin et al., 2005). Aside from sharing a set of core subunits with the yeast counterpart, hINO80 contains several metazoan-specific subunits, including Gli-Kruppel zinc finger transcription factor YY1, deubiquitinating enzyme Uch37, and other proteins of little known function: NFRKB, Amida, Ino80D and CCDC95 (Figure 1.8A).

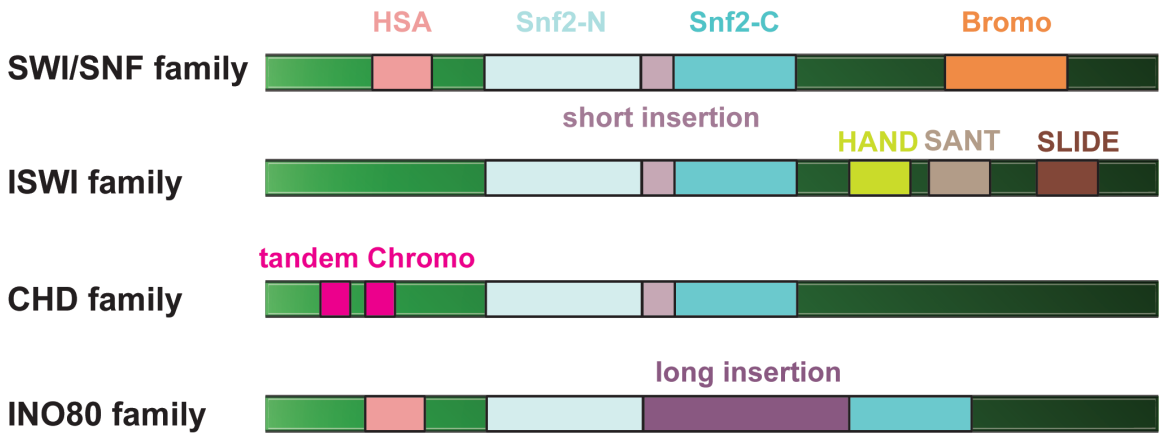

Figure 1.7. ATP-dependent chromatin remodeler families.
All families of chromatin remodelers contain a Snf2-ATPase subunit characterized by an ATPase domain that is split into two parts: Snf2-N (light blue) and Snf2-C (cyan). What distinguish each family are the unique domains residing within, or adjacent to, the ATPase domains. Remodelers of the SWI/SNF, ISWI and CHD families each have a distinctive short insertion (light purple) within the ATPase domain, whereas remodelers of the INO80 family contain a long insertion (dark purple). Each family is further characterized by distinct combinations of flanking domains: bromodomain (orange) and HSA (helicase-SANT) domain (pink) for the SWI/SNF family, SANT-SLIDE module (yellow and brown) for the ISWI family, tandem chromodomains (magenta) for the CHD family, and HSA domain (pink) for the INO80 family. Figure adapted from (Clapier et al., 2009).

The deubiquitinating enzyme Uch37 is recruited to hINO80 via interactions with the hINO80 subunit NFRKB, where it is held in an inactive state (Yao et al., 2008). Recent determination of the crystal structure of Uch37 in complex with $NFRKB^{NTD}$ revealed the structural basis for the inhibition of Uch37 (Sahtoe et al., 2015; VanderLinden et al., 2015). It was shown that $NFRKB^{NTD}$ interacts with the C-terminal tail of Uch37 and its catalytic UCH domain. These contacts block the Ub-binding site and induce a conformational change that distorts the active site of Uch37. Such stringent regulation of Uch37 activity begs the questions: What is the function of Uch37 within the hINO80 complex, and what are its physiological substrates? Since hINO80 is implicated in various DNA transactions, including transcription and DNA repair, ubiquitinated histones represent good candidates for potential physiological substrates of Uch37.

INO80 can regulate chromatin structure in at least two different ways (Figure 1.8B). First, it catalyzes nucleosome sliding along the DNA in an ATP-dependent manner (Jin et al., 2005; Shen et al., 2000). Detailed biochemical characterization of yINO80 showed that yINO80 binds to nucleosomes with >20 bp of extranucleosomal DNA with a dissociation constant of 10 nM (Udugama et al., 2011). However, 70 bp of extranucleosomal DNA is required for optimal mobilization of nucleosomes to the center of a DNA fragment *in vitro*. Second, yINO80 catalyzes the replacement of nucleosomal H2A.Z/H2B with free H2A/H2B dimer. This activity has been shown to contribute to genome-wide H2A.Z localization in yeast (Papamichos-Chronakis et al., 2011).

Ino80 and Swr1 represent the current classes of the INO80 family of chromatin remodelers. Every characterized eukaryote to date contains one member of the Ino80 class of enzymes, whereas mammals appear to have at least two distinct Swr1 class members,

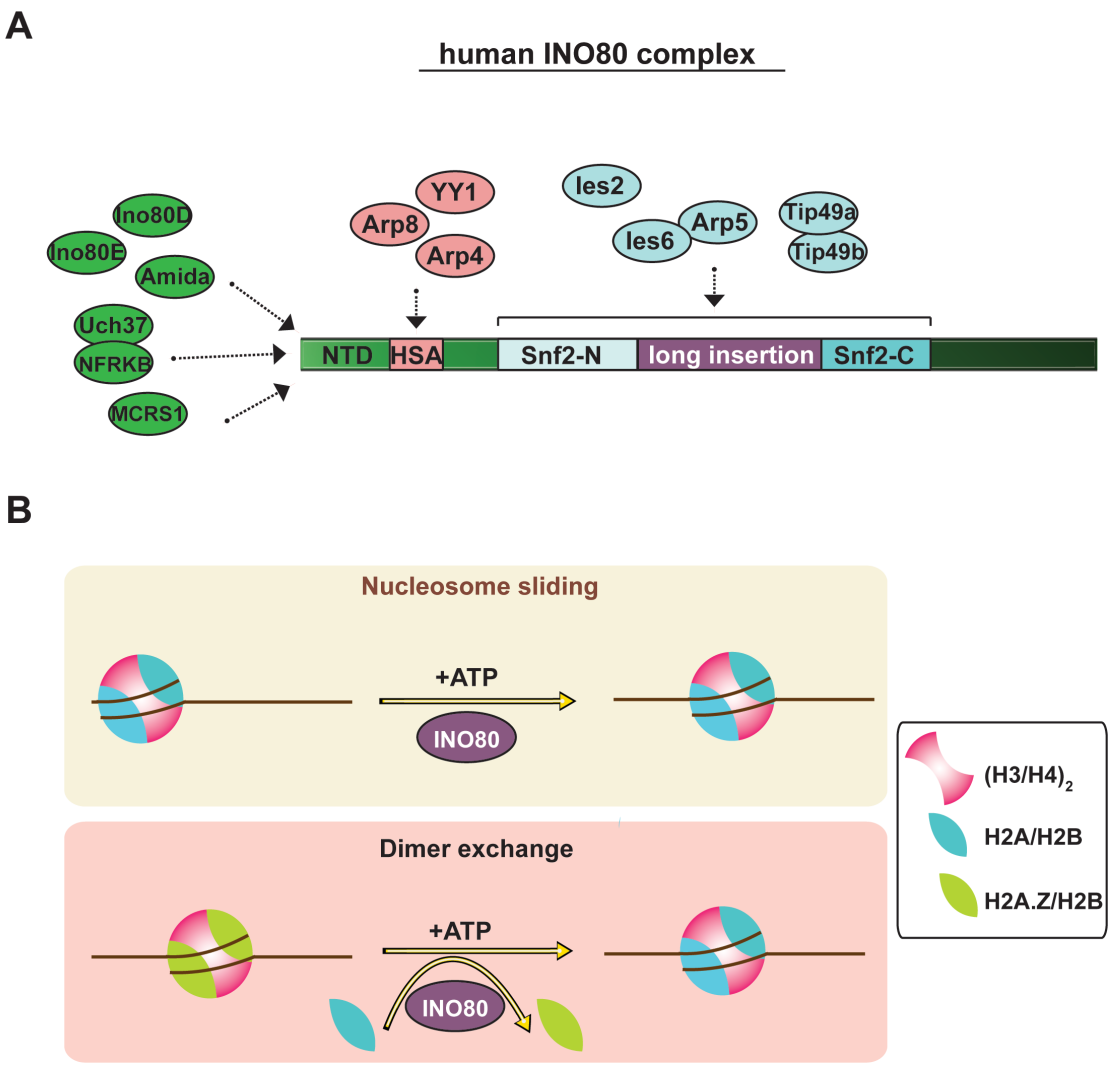

Figure 1.8. INO80 chromatin-remodeling complex: composition and biochemical activities.
(A) The Ino80 subunit contains regions that function as modular scaffolds on which other subunits assemble. Subunits shown in green associate with the NTD (N-terminal domain); subunits shown in pink associate with the HSA domain; subunits shown in light blue associate with the Snf2 ATPase domain. Figure adapted from (Chen et al., 2013).
(B) INO80 slides nucleosomes to the center of a DNA fragment in an ATP-dependent manner. Yeast INO80 has also been shown to exchange nucleosomal H2A.Z-H2B dimers with free H2A-H2B dimers.

SRCAP and p400/TIP60. The catalytic subunit of each INO80 family member is characterized by a large insertion between the helicase/ATPase motifs III and IV, which splits the conserved Snf2-like ATPase domain (Figure 1.7). These extra amino acids influence the outcome of the remodeling reaction and are required for unique subunit-subunit interactions that likely provide unique activities to this group of enzymes (Chen et al., 2011).

The structure and subunit topology of yINO80 has been recently revealed through an integrative approach of cryo-electron microscopy, crosslinking and mass spectrometry (Tosi et al., 2013). yINO80 consists of 25 subunits, which are organized in four modules in an elongated structure (Figure 1.9A). Modules containing Arp8 and Arp5 were found to participate in the nucleosome remodeling reaction, whereas the Nhp10 module was shown to have a role in DNA or nucleosome recognition. A model for the yINO80-nucleosome complex was developed on the basis of crosslinks and cryo-electron microscopy (Figure 1.9B) (Tosi et al., 2013). In this model, the nucleosome is placed in a central position within yINO80, and the H2A-H2B dimer is positioned near the domain containing the Ino80 ATPase. Therefore, it has been proposed that the force generated by Ino80 mediated ATP-hydrolysis is utilized to loosen the contacts between DNA and histones and facilitate dimer exchange.

hINO80 can be separated into three main modules that assemble onto the scaffold and catalytic subunit, Ino80 (Figure 1.8A) (Chen et al., 2011). Previously, it has been demonstrated that the hINO80 core complex, composed of both the HSA and the Snf2 modules, but lacking the N-terminal domain and associated metazoan-specific subunits, is sufficient to catalyze ATP-dependent nucleosome sliding *in vitro*. Among the core subunits,

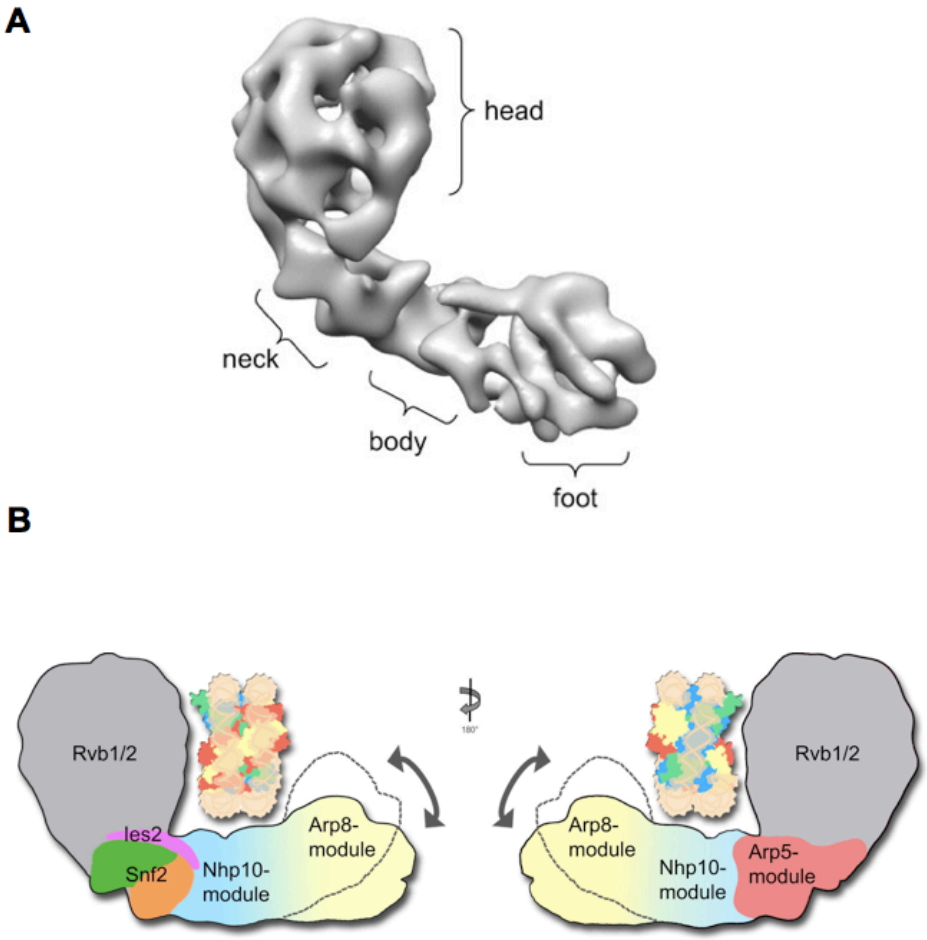

Figure 1.9. 3D structure of the yeast INO80 complex.
(A) Shown is the 3D reconstruction from cryo-electron microscopy images of the yeast INO80 complex (Tosi et al., 2013). yINO80 has an elongated shape with four modules: a globular head connected via a neck to the body and foot. **(B)** Shown is a model of yINO80 bound to the nucleosome. Figure adapted from (Tosi et al., 2013).

Ies2 stimulates the Ino80 DNA-dependent ATPase activity, whereas Arp5 and Ies6 are instead needed for nucleosome recognition and binding (Chen et al., 2013). These findings are in line with previous evidence that Ies2, Arp5 and Ies6 contribute to various INO80-dependent nuclear transactions in fungi and higher eukaryotes (Cai et al., 2007; Chambers et al., 2012; Hogan et al., 2010; Jiang et al., 2010; van Attikum et al., 2004; Yen et al., 2012).

INO80 in transcription regulation—Genome-wide transcriptional profiles have revealed that INO80 contributes to the regulation of 20% of genes in *Saccharomyces cerevisiae* and *Arabidopsis thaliana* (Fritsch et al., 2004; Jonsson et al., 2004; Mizuguchi et al., 2004; van Attikum et al., 2004) . The *PHO5* gene is among the best-studied genes in yeast regulated by yINO80. In yeast cells grown in rich media, *PHO5* is silenced with well-positioned nucleosomes covering the transcription-start site and the promoter region (Boeger et al., 2008; Svaren and Horz, 1997). Upon phosphate starvation, the activator Pho4 binds to the *PHO5* promoter and mediates recruitment of yINO80 and SWI/SNF chromatin remodeling complexes, which leads to sliding and/or removal of nucleosomes from the promoter (Barbaric et al., 2007; Boeger et al., 2008; Boeger et al., 2004). Although these chromatin regulators are not absolutely essential for *PHO5* gene expression, they affect the kinetics of induction (Barbaric et al., 2007). Recently, the only essential chromatin remodeler in yeast, RSC, has been also found to play a role in *PHO5* activation (Lorch et al., 2011). These findings suggest that there is substantial remodeler redundancy at the initial stages of transcription. Another example of yINO80-regulated gene is yeast *KAR4* (Papamichos-Chronakis et al., 2011). *In vivo* analysis revealed elevated H2A.Z levels at the *KAR4* promoter region in the *Δino80* strain. Biochemical and genetic evidence suggest that yINO80 drives eviction of H2A.Z at the *KAR4* promoter to facilitate

transcription activation. In addition, yINO80 has also been reported to regulate the transcription of *INO1* and *GAL1* genes (Ebbert et al., 1999; Ford et al., 2007).

How yINO80 is recruited at gene promoters in yeast is not fully understood, although there has been biochemical and genetic evidence favoring the idea that the yeast sequence-specific DNA-binding protein Nhp10 recruits INO80 to targeted histones (Morrison et al., 2004). *In vivo* analysis by the Pugh group has recently revealed that yINO80 is recruited to the NFR of genes, near the +1 nucleosome (Yen et al., 2013). Ultra-high resolution analysis of protein-DNA interactions revealed that yINO80 subunits cover 70 bp of NFR upstream of the +1 nucleosome, whereas the catalytic subunit Ino80 occupies much of the +1 nucleosome. yINO80 occupancy at the NFR correlates with that of the related chromatin remodeler SWR-C (Yen et al., 2013). SWR-C deposits H2A.Z at the +1 nucleosome, by exchanging nucleosomal H2A-H2B dimers with free H2A.Z-H2B dimers (Luk et al., 2010). Interestingly, the +1 nucleosome exhibits a higher turnover rate relative to all other nucleosomes across the genome (Dion et al., 2007; Yen at al., 2013). Therefore it has been suggested that, by localizing at the NFR, yINO80 and SWR-C enhance nucleosome turnover via the dynamic cycling of H2A.Z (Dion et al., 2007; Yen et al., 2013).

In human cells, the hINO80 subunit YY1 has been shown to recruit the complex to some target promoters, such as *CDC6* and *GRP78* (Cai et al., 2007). The requirement of hINO80 to YY1 localization at these promoters suggests that hINO80 may facilitate access of transcription factor to its target DNA sequences. In addition, hINO80 has been reported to be required for ESC self-renewal, as well as for reprogramming and embryonic development, by selectively occupying promoters of core pluripotency genes bound by the

master ESC transcription factors and promoting their expression (Wang et al., 2014). How hINO80 contributes to the transcriptional activation of these genes is not yet understood.

Erroneous expression of key genes leads to conversion of a normal cell into a cancer cell. The state of histone PTMs and ATP-driven chromatin remodeling can determine the accessibility and transcriptional competence of a gene. Much of the pathological gene silencing that occurs in cancer is a consequence of mistargeting of chromatin remodeling enzymes. Furthermore, mutations in the subunits hSNF5/INI1 and BRG1 of the human SWI/SNF homolog have emerged as molecular markers of various cancers, such as leukemia, malignant rhabdoid tumors, rhabdomyosarcomas, choroid plexus carcinomas and a subset of medulloblastomas and central primitive neuroectodermal tumors (Biegel et al., 2000; Sevenet et al., 1999). Therefore, in order to begin fighting cancer it is imperative to understand the precise mechanism by which these ATP-dependent complexes remodel chromatin, how they are recruited to particular target genes, and how these complexes work together with other histone PTMs or histone variants to activate and/or repress gene expression.

CHAPTER 2: UBIQUITIN SIGNALS PROTEOLYSIS-INDEPENDENT STRIPPING OF TRANSCRIPTION FACTORS

[2]Ubiquitination of transcription activators (TAs) has been reported to regulate transcription via both proteolytic and non-proteolytic routes, yet the function of the ubiquitin (Ub) signal in the non-proteolytic process is poorly understood. By use of the heterologous TA LexA-VP16 in *Saccharomyces cerevisiae*, we show that mono-ubiquitin fusion of the activator prevents stable interactions between the activator and DNA, leading to transcription inhibition without activator degradation. We identify the AAA^+ ATPase Cdc48 and its cofactors as the Ub receptor responsible for extracting the mono-ubiquitinated activator from DNA. Our results suggest that deubiquitination of the activator is critical for transcription activation. These findings with LexA-VP16 extend in both yeast and mammalian cells to native transcription activators Met4 and R-Smads, respectively, that are known to be oligo-ubiquitinated. The results reveal a previously unidentified mode of transcription regulation and illustrate a role for Ub and Cdc48 in gene expression that is independent of proteolysis.

2.1 Introduction

Eukaryotic gene expression is a crucial process that must be controlled in a time and locus-specific manner during cell growth and development. TAs play a key role in gene expression by coordinating the assembly of complex machineries including RNA polymerase II (RNAPII), general transcription factors, and various co-activators that

[2] This chapter is related to Ndoja, A. et al. (2014) Molecular Cell *53(6)*, 893-903.

modify or remodel chromatin. Not surprisingly, the abundance, localization, and activity of TAs all are subject to tight control. This is achieved in part through the action of the ubiquitin-proteasome system (UPS) (Geng et al., 2012; Yao and Ndoja, 2012; and references therein). One way in which the UPS regulates TAs is by controlling their abundance. A large number of activators contain transcription activation domains that overlap with degrons, which signal poly-ubiquitination and subsequent degradation of the activator. This and other observations suggest that destruction of the activator is linked to its ability to activate transcription. Another way the UPS regulates transcription activators is by controling their cellular localization. Depending on the activator, mono or oligo-ubiquitination can promote either nuclear localization (van der Horst et al., 2006) or nuclear export (Li et al., 2003). There also is evidence that mono or oligo-ubiquitination and the 19S RP of the proteasome have direct roles in transcription that are independent of proteolysis. In one case, mono-Ub was reported to stabilize transcription factor–DNA interactions (Archer et al., 2008; Ferdous et al., 2007). A consensus has yet to emerge on how mono-ubiquitination of TAs affects their activities.

For the yeast transcription repressor α2, poly-ubiquitination leads to removal of α2 from chromatin with subsequent degradation by the proteasome (Wilcox and Laney, 2009). Removal of α2 is mediated by the AAA^+ ATPase Cdc48 (known as p97 or valosin-containing protein (VCP) in mammals). Although Cdc48 has been implicated as a Ub-selective chaperone in other processes (Jentsch and Rumpf, 2007), this was the first indication that it regulates chromatin-bound proteins. Subsequently, multiple groups have demonstrated that proteasomal degradation of chromatin-bound substrates often requires extraction by Cdc48; examples include stalled RNAPII (Verma et al., 2011), proteins

involved in DNA repair (Acs et al., 2011; Meerang et al., 2011), and replication licensing factor Cdt1(Raman et al., 2011). In a related observation, at the end of mitosis Cdc48 was shown to remove Aurora B kinase from chromatin independently of proteolysis (Ramadan et al., 2007). In all of these cases, poly-ubiquitination of the substrate appeared to be a prerequisite for Cdc48 action.

In order to understand the underlying mechanism of how ubiquitination of activators regulates transcription, we have used a model system established previously by Salghetti *et al.* They demonstrated that in *Saccharomyces cerevisiae* the heterologous TA LexA-VP16 is poly-ubiquitinated and rapidly degraded, and that this process is coupled to transcription activation (Salghetti et al., 2001). Here we report that, in contrast, mono-Ub fused to LexA-VP16 inhibits transcription by preventing stable interactions between the activator and DNA. Cdc48 and its cofactors inhibit transcription most likely by extracting LexA-VP16 from DNA in a Ub-dependent manner and without subsequent proteolysis. Surprisingly, fusion with a single Ub is sufficient to recruit Cdc48 to LexA-VP16 and to prevent transcription. We show that this mode of regulation by Cdc48 applies in yeast and mammalian cells to native TAs that are known to be oligo-ubiquitinated but not degraded.

2.2 Experimental Procedures

2.2.1 Yeast strains and plasmids

Manipulations of *S. cerevisiae* employed standard techniques. Table A1.1 lists strains used in this study. The reporter gene *LacZ* under the control of four tandem LexA operators and the *GAL1* minimal promoter (pSH1834, Invitrogen) was cloned into pM4297 or

pM4366 (Voth et al., 2001) and then integrated into the *HO* locus of each strain. Site-specific integration was verified by PCR. Where indicated, the hybrid LexA operator with the sequence **CCGT**ACATCCAT**ACAG** replaced the four tandem wild-type operators.

For analysis of Met4 localization, a *CEN* plasmid expressing ^{3xHA}Met4 from the native *MET4* promoter was transformed into strains with endogenous *MET4* disrupted. The 3xHA tag was inserted in-frame at nucleotide 45 of the *MET4* open-reading frame (Lee et al., 2010).

For LV and Ub-LV activators, *CEN* pRS vectors with promoters of different strengths were used to achieve different expression levels (ATCC 87669). The Ub-LV activators initially were expressed from the *ACT1* promoter (Salghetti et al., 2001). Because LV is toxic in yeast, low expression levels were preferred and the *CYC1* promoter was used. For comparisons, activators were always expressed from the same promoter; nonetheless, similar results were obtained for Ub-LV proteins regardless of which promoter was used. Point mutations were made using the QuickChange® II XL Site-Directed Mutagenesis Kit (Stratagene) and verified by sequencing.

2.2.2 β-galactosidase assay

Yeast were grown to mid-log phase in liquid culture. An equivalent of 1 ml at 0.1 OD_{600} of cells was pelleted and resuspended in 100 ml of 140 mM Pipes (pH 7.2), 2.5% Triton X-100, and 0.5 mM fluorescein di-b-D-galactopyranoside (FDG) in wells of a 96-well plate (Hoffman et al., 2002). β-Galactosidase activity was quantified as the rate of FDG hydrolysis monitored continuously on a BioTek Synergy microplate reader for 1 h at 37 °C (Ex 485 nm, Em 530 nm).

2.2.3 Cell culture, transfections and treatments

MDA-MB-231 cells were maintained in DMEM medium supplemented with 10% fetal bovine serum (FBS), 1% Glutamax (Invitrogen) and 1% pen/strep (Life Technologies). For TGFβ-response experiments, cells were serum-starved overnight before treatment with 100 pM TGFβ (R&D) or 10 μM DBeQ (Life Sensors) or both.

2.2.4 Cycloheximide chase

Cycloheximide-chase experiments were performed essentially as described (Gardner et al., 2005). Briefly, yeast grown to an OD600 of 0.8-1.0 were treated at time-zero with 50 μg/ml cycloheximide and shaking was continued at 30 °C. Culture aliquots (4 ml) were removed at indicated times, centrifuged, and the cells were lysed by vortexing with glass beads in a buffer containing 1% SDS, 8 M urea, 10 mM MOPS (pH 6.8), 10 mM EDTA, and protease inhibitors. Cell lysates were analyzed by SDS-PAGE and immunoblotting.

2.2.5 RNA analysis

Total RNA from yeast was isolated by hot acid-phenol extraction (Collart and Oliviero, 2001). Total RNA from human MDA-MB-231 cells was isolated using the Aurum Total RNA Mini kit (BioRad) following the manufacturer's instructions. 1 μg (yeast) or 0.25 μg (human) purified RNA was used in reverse-transcription reactions using the iScript cDNA synthesis kit (BioRad). Relative amounts of each transcript were determined by real-time PCR using gene-specific primers (Table A1.2) and normalized against ACT1 (yeast) or GAPDH (human) mRNA. Data shown are averages of three independent experiments.

2.2.6 Chromatin Immunoprecipitation

ChIP assays in yeast were performed essentially as described (Li et al., 2007) except that 20 µl Protein G Dynabeads (Life Technologies) were used for each immunoprecipitation sample. Immunoprecipitated DNA was quantified by real-time PCR with iQ SYBR Green SuperMix (BioRad); primer sequences are shown in Table A1.2. Occupancy levels were calculated as the ratio of immunoprecipitated to input DNA. When the experiments involved temperature shifts, occupancy levels were further normalized to the inactive *GAL1* gene, or to the *RPL11* gene whenever galactose was used for yeast growth, in order to account for potential global effects of the temperature change. All data shown are averages of three independent experiments.

ChIP assays in mammalian cells followed the Upstate ChIP Assay Kit (17-295) protocol with a few modifications. One 10 cm dish (~5x106 cells) of MDA-MB-231 cells grown to 70-80% of confluence was used for each ChIP. Crosslinking was done with 1% formaldehyde at room temperature for 10 min. After washing with PBS, cells were resuspended in 0.5 ml cell lysis buffer (5 mM PIPES, pH 8, 85 mM KCl, 1% NP40) and incubated on ice for 20 min. Nuclei were then isolated by centrifugation at 2500 x g and lysed in 0.2 ml ChIP lysis buffer (50 mM Tris, pH 8, 10 mM EDTA, 1% SDS). Sonication of crosslinked chromatin with a Diagenode Bioruptor was done to generate DNA fragments of 100-500 bp. Subsequent steps followed the Upstate ChIP Assay Kit protocol except that a mixture of 10 µl Protein G Dynabeads and 10 µl Protein A Dynabeads (Life Technologies) was used in each IP instead of agarose beads. Protease inhibitors (Sigma P8340) were freshly added to all the lysis buffers. All data shown are averages of two independent experiments.

2.2.7 Cell fractionation

Cell fractionation of MDA-MB-231 cells was carried out by the REAP method (Suzuki et al., 2010). Isolation of yeast nuclei was carried out by first treating yeast with zymolase to remove the cell wall. Treated cell pellet was resuspended at 2.5x106 cells/ml in 20 mM PIPES, pH 6.5, 18% Ficoll 400, 0.5 mM MgCl2, supplemented with protease inhibitors. The nuclei were released by dounce homogenization and the homogenate was layered on top of twice volume of 20 mM PIPES, pH 6.5, 20% glycerol and 0.5 mM $MgCl_2$. After centrifugation at 11,500 rpm for 30 min at 4 °C, the pellet contains the nuclei and the supernatant is the cytoplasmic fraction. The nuclei were finally resuspended in 20 mM HEPES, pH 7.5, 1 mM $MgCl_2$, 100 mM CH_3CO_2K, 10% glycerol, 400 mM NaCl and treated with 0.05 µg/µl DNAse I at room temperature for 10 min.

2.2.8 Antibodies

Antibodies used in this study were anti-LexA (Millipore 06-719), anti-HA-12CA5 (Roche 1583816), anti-CTD-8WG16 (Abcam ab817 and Covance MMS-126R), anti-Smad2 (Invitrogen 51-1300), anti-Smad3 (Invitrogen 51-1500), anti-GAPDH (Sigma G9545), anti-TBP (gift from Dr. Laurie Stargell), rabbit anti-Yuh1 (available from a previous study), anti-tubulin (Sigma T9026), anti-Smad2/3 in ChIP analysis (BD 610842), anti-P-Smad2/3 (Abcam ab52903), anti-c-Jun (Santa Cruz sc1694), anti-VCP (Abcam ab11433), anti-Flag-M2 (Sigma F3165) and anti-Myc (clone 9E10, Millipore 05-419).

2.3 Results

2.3.1 Transcription activation by the Ub-LexA-VP16 fusion requires its deubiquitination

LexA-VP16 (LV) is a potent TA composed of the bacterial LexA DNA binding domain and the activation domain from Herpes Simplex Virus protein VP16. LV in yeast is poly-ubiquitinated by Met30, an SCF E3 Ub ligase, and rapidly degraded by the proteasome (Salghetti et al., 2001). This Ub-dependent degradation of LV is coupled to transcription activation. However, by fusing mono-Ub to the N-terminus of LV, Salghetti et al. found that Ub-LV can activate transcription independently of Met30. It is well known that eukaryotic Ub genes encode precursor forms of Ub that are co-translationally processed by deubiquitinating enzymes (DUBs) (Ozkaynak et al., 1984). The Ub C-terminal glycine (G76) is crucial for this processing as well as for subsequent conjugation and deconjugation. To produce stable Ub-fusion proteins *in vivo*, Ub G76 often is replaced with a larger amino acid in order to resist cleavage by DUBs. Fortuitously, we found that the activation potency of Ub-LV depends on the amino acid introduced at the Ub-76 position. When the C-terminus of Ub in Ub-LV was mutated to alanine (Ub(A76)-LV), Ub-LV activates transcription, in agreement with the report by Salghetti *et al*. However, when it was changed to valine, Ub(V76)-LV failed to activate transcription in either the presence or absence of Met30 (Figure 2.1A).

To test if deubiquitination efficiency was a determinant of transcriptional output, we mutated Ub G76 or the residue immediately after it. In yeast, when this 77th residue is a proline, deubiquitination is inhibited (Bachmair et al., 1986). Among four Ub-LV fusions with different linker residues, we observed that transcription potency correlated with the predicted deubiquitination efficiency; either V76 or P77 dramatically inhibited

transcription (Figure 2.1B). Accordingly, we observed substantial deubiquitination of Ub(A76)-LV but not Ub(V76)-LV (Figures 2.1C and 2.1D). These results strongly suggest that deubiquitination of the activator is required for transcription. Thus, Ub modification of at least some transcription factors is likely to be highly dynamic, as stable ubiquitination can prevent transcription activation.

2.3.2 Ub hydrophobic patch mutations restore transcription activation by Ub(V76)-LV

The difference between Ub(A76)-LV and Ub(V76)-LV in transcription activation was unexpected. A possible explanation was that the fused Ub caused rapid turnover of the activator, thereby limiting its abundance in yeast. We found that, on the contrary, both Ub(A76)-LV and Ub(V76)-LV are stable and that Ub(V76)-LV accumulates to even higher levels (Figures 2.1C and 2.1D). Therefore, the Ub moiety in Ub(V76)-LV inhibits transcription in a proteolysis-independent manner. To test if the Ub has a specific effect and does not act simply as a bulky attachment that interferes sterically, we mutated residues within the Ub hydrophobic patch, a commonly used surface for Ub–protein interactions. L8A, L8W or H68D modifications to this surface each greatly enhanced the Ub(V76)-LV-dependent transcription of *LacZ* (Figure 2.2A). Ub(L8A,V76)-LV activated transcription to a level similar to LV alone (Figure 2.3A). These results suggested that interaction of the Ub hydrophobic patch with one or more endogenous Ub receptors prevents transcription activation. Interestingly, the transcription activation by Ub(L8A,V76)-LV was accompanied by rapid degradation of the fusion protein (Figure 2.3B); this observation confirms the coupling between activator turnover and transcription that was described previously (Salghetti et al., 2001).

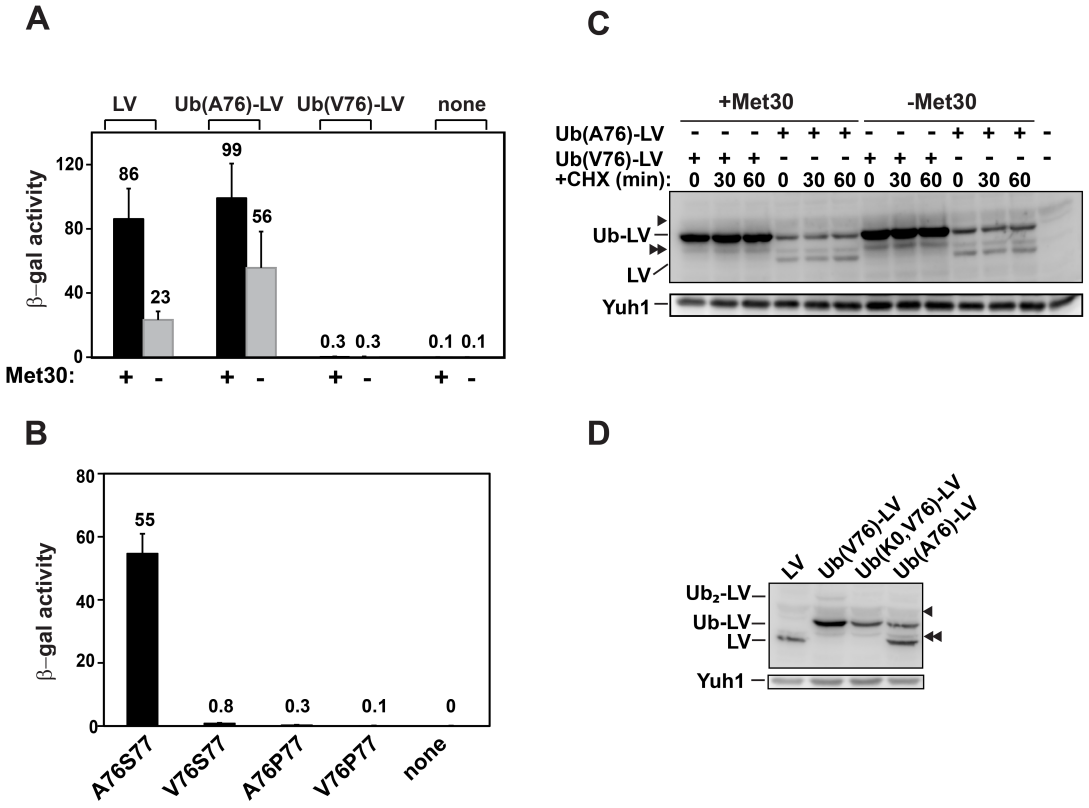

Figure 2.1. Deubiquitination of the Ub-LV fusion is needed for transcription activation.

(A) A *LacZ* reporter gene under the control of a 4x*LexA* operator and minimal *GAL1* promoter was integrated into yeast strains with and without endogenous *MET30* (YTY358 and YTY224). The strains were transformed with an empty vector (none) or a *CEN* plasmid expressing LV or Ub-LV fusions from the *CYC1* promoter, and *LacZ* transcription was measured as b-galactosidase activity. Mean values and standard deviations (error bars) are from three independent experiments. **(B)** Ub-protein linker residues (i.e., either Ub-76 or the subsequent residue) affect transcription activation by Ub-LV fusions. Ub-LV fusions with different linker residues were expressed in wild-type yeast with an integrated reporter gene (YTY076); transcription was measured as b-galactosidase activity. **(C)** Ub(A76)-LV and Ub(V76)-LV are both long-lived in yeast. Yeast strains in (A) were treated with cycloheximide. At the indicated times, aliquots were taken and whole-cell lysates were analyzed by SDS-PAGE and immunoblotting with anti-LexA and (as a loading control) anti-Yuh1 antibodies. Note the appearance of LV in yeast expressing Ub(A76)-LV but not the yeast with Ub(V76)-LV. The arrowhead denotes a non-specific band; the double-arrowhead denotes a degradative fragment of Ub-LV. **(D)** Steady-state levels of LV and Ub-LV activators. Whole-cell lysates were analyzed by as in (C). "K0" denotes the Ub mutant in which all seven lysines were mutated to arginines. Ub_2-LV indicates a di-ubiquitinated form of LV observed in yeast expressing Ub(V76)-LV but not Ub(K0,V76)-LV.

In addition to changes in the hydrophobic patch, we constructed mutants in which all seven lysines in Ub were mutated to arginines. Because the N-termini of these constructs (methionine followed by aspartate) are likely to be acetylated (Polevoda and Sherman, 2003) and the Ub lacks lysine sites for ubiquitination, Ub(K0,V76)-LV is trapped in a mono-ubiquitinated state (Figure 2.1D; for the role of Met30 in Ub-LV ubiquitination, see Discussion). As shown in Figure 2.2A, the Ub(K0) mutations did not affect the transcriptional potency of the Ub(V76)-LV activators; thus, a poly-Ub chain is not required to recruit the putative Ub receptor(s). We observed similar effects when Ub(V76) was fused to a different LexA-activation domain construct, LexA-Gal4AD (Figure 2.3C), and when the position of Ub(V76) in the fusion protein was C-terminal to LexA or LV (Figure 2.3D).

To rule out that the fused Ub causes mislocalization of the activator, we fractionated yeast cells and found that even more Ub(V76)-LV was in the nucleus than Ub(L8A,V76)-LV, which activates transcription potently (Figure 2.2B). We also expressed Ub(V76)-LV as a GFP fusion and found by microscopy that it localized diffusely throughout the yeast cytoplasm and nucleus (Figure 2.2C). These results show that fusion with Ub(V76) did not cause LV either to be excluded from the nucleus or sequestered in specific cellular compartments.

2.3.3 Ub prevents the LV transcription activator from stably binding to DNA

Next we investigated chromatin localization of Ub-LV by chromatin immunoprecipitation (ChIP) (Figure 2.2D). Although we could clearly detect Ub(V76)-LV at the promoter of the *LacZ* reporter gene (~5-fold above background), substantially higher

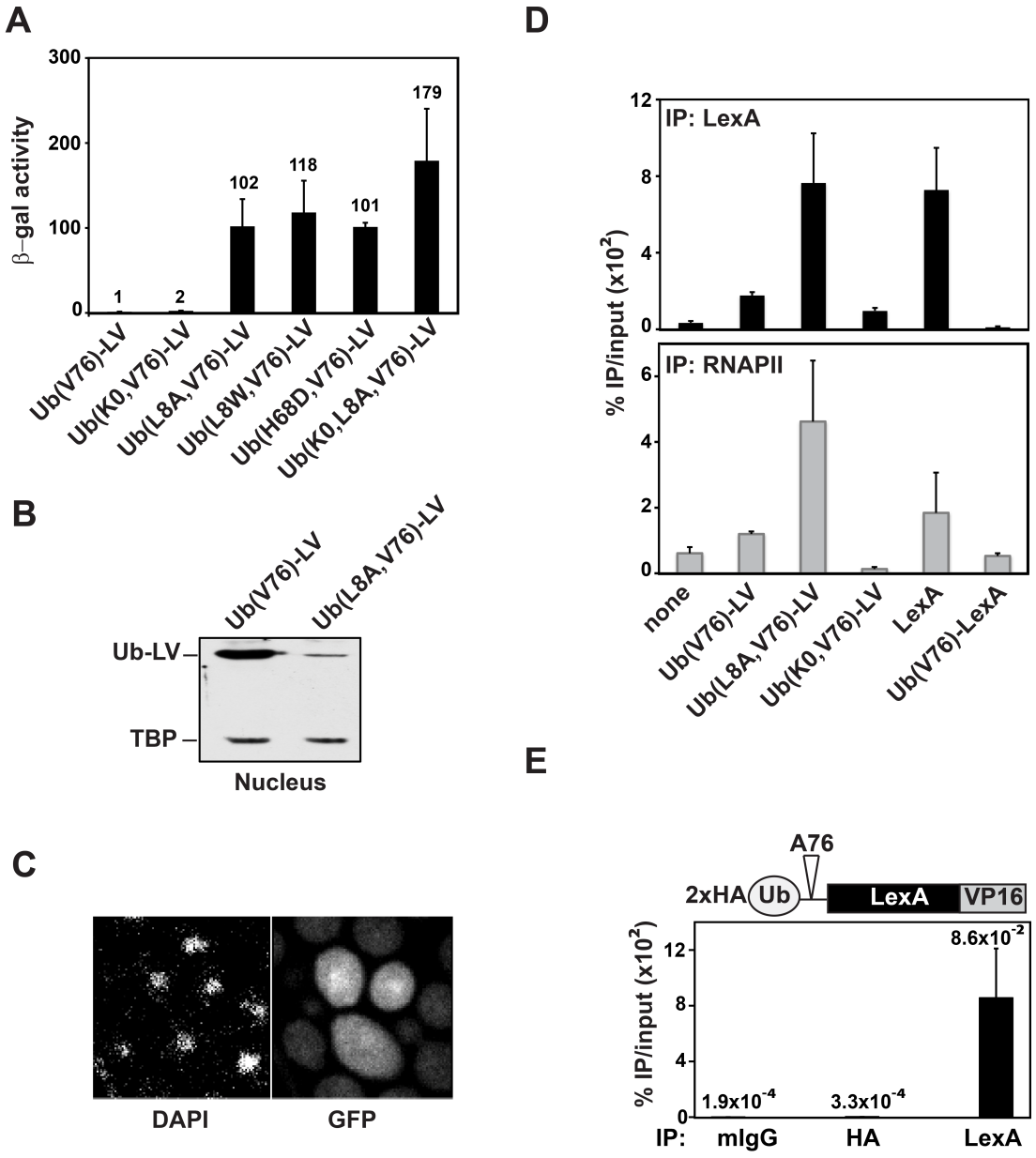
A
β–gal activity
300
200
100
0
1
2
102
118
101
179
Ub(V76)-LV
Ub(K0,V76)-LV
Ub(L8A,V76)-LV
Ub(L8W,V76)-LV
Ub(H68D,V76)-LV
Ub(K0,L8A,V76)-LV
B
Ub(V76)-LV
Ub(L8A,V76)-LV
Ub-LV
TBP
Nucleus
C
DAPI
GFP
D
IP: LexA
IP: RNAPII
% IP/input (x10²)
12
8
4
0
6
4
2
0
none
Ub(V76)-LV
Ub(L8A,V76)-LV
Ub(K0,V76)-LV
LexA
Ub(V76)-LexA
E
A76
2xHA
Ub
LexA
VP16
% IP/input (x10²)
12
8
4
0
8.6x10⁻²
1.9x10⁻⁴
3.3x10⁻⁴
IP:
mIgG
HA
LexA

Figure 2.2. N-terminal fused Ub prevents stable activator-DNA interactions.
(A) Mutations in the Ub hydrophobic patch restore transcription activation by LV. YTY076 yeast were transformed with a plasmid expressing Ub(V76)-LV or the indicated mutated versions from the *ACT1* promoter, and transcription of the *LacZ* reporter was measured as b-galactosidase activity. **(B)** Ub(V76)-LV is detected in the nucleus. Nuclei from yeast expressing either Ub(V76)-LV or Ub(L8A, V76)-LV were isolated and nuclear proteins were analyzed by SDS-PAGE and immunoblotting. **(C)** Ub(V76)-LV is localized diffusely both in the nucleus and the cytoplasm. Shown are confocal microscopy images of wild-type yeast expressing Ub(V76)-LV-GFP. Nuclei were stained with DAPI. **(D)** The N-terminal fused Ub inhibits promoter occupancy by LexA or LV *in vivo*. YTY076 was transformed with an empty vector or a plasmid expressing LexA or various LexA fusions. Occupancy of the LexA-operator or the promoter within the reporter gene was evaluated by ChIP analysis with anti-LexA or anti-RNAPII antibody, respectively. Error bars represent standard deviations of mean values from three independent experiments. Note that LexA alone may recruit small amounts of RNAPII non-specifically, but no transcription of *LacZ* was detected (data not shown). **(E)** YTY076 was transformed with a plasmid expressing N-terminal HA-tagged Ub(A76)-LV. ChIP with anti-HA (detecting Ub(A76)-LV) and anti-LexA (detecting Ub(A76)-LV and LV) antibodies revealed that only deubiquitinated LV was stably bound to DNA. Note that anti-HA and anti-LexA ChIP worked similarly well (see Figure 3D).

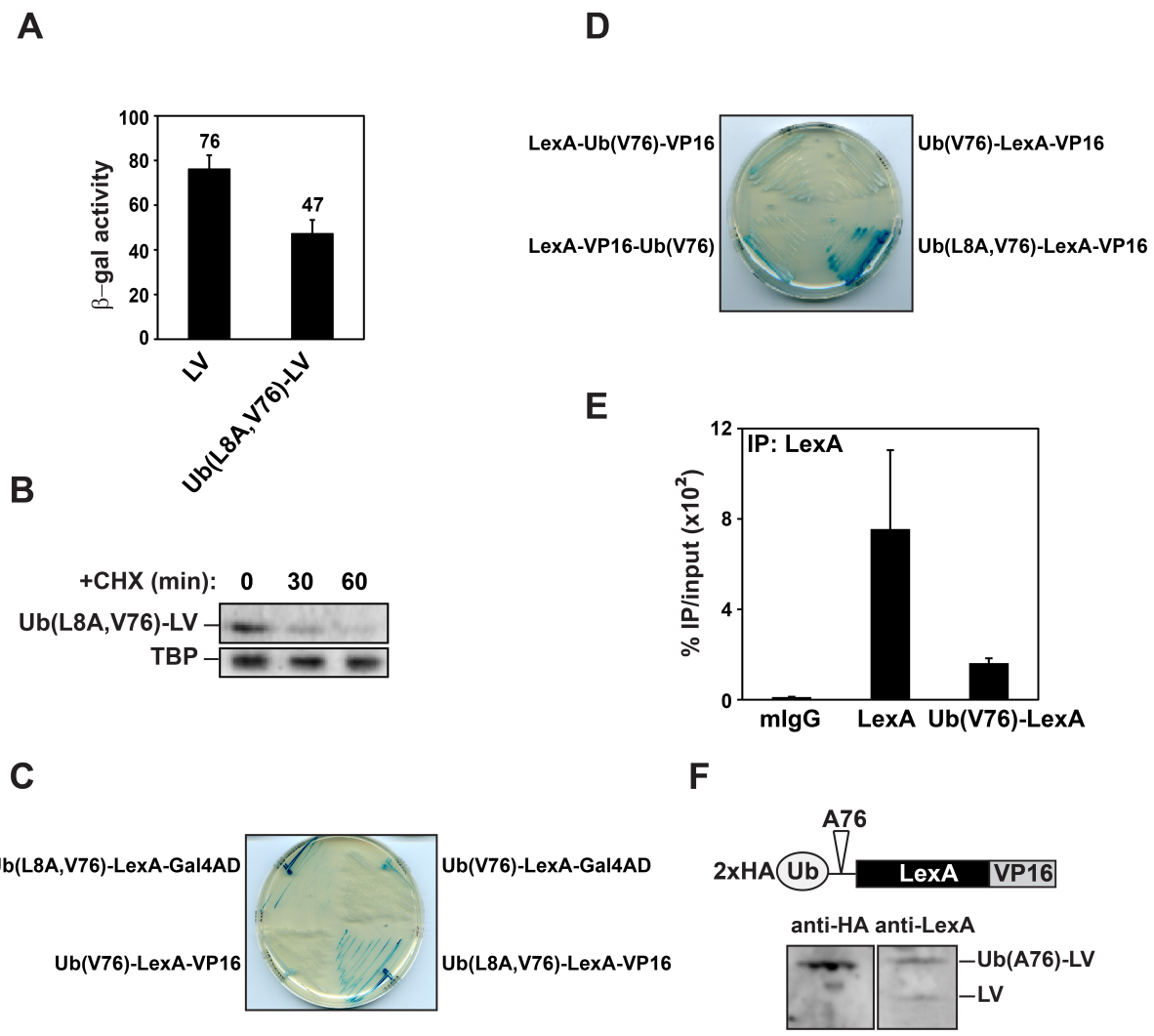
A
100
80
60
40
20
0
β–gal activity
76
47
LV
Ub(L8A,V76)-LV
B
+CHX (min): 0 30 60
Ub(L8A,V76)-LV
TBP
C
Ub(L8A,V76)-LexA-Gal4AD
Ub(V76)-LexA-Gal4AD
Ub(V76)-LexA-VP16
Ub(L8A,V76)-LexA-VP16
D
LexA-Ub(V76)-VP16
Ub(V76)-LexA-VP16
LexA-VP16-Ub(V76)
Ub(L8A,V76)-LexA-VP16
E
IP: LexA
% IP/input (x10²)
12
8
4
0
mIgG
LexA
Ub(V76)-LexA
F
A76
2xHA
Ub
LexA
VP16
anti-HA anti-LexA
Ub(A76)-LV
LV

Figure 2.3. Attachment of Ub to LexA-based activators inhibits transcription activation.

(A) Ub(L8A,V76)-LV activates transcription to a similar level as LV. Wild-type yeast with an integrated LacZ reporter gene (YTY076) was transformed with a plasmid expressing LV or Ub(L8A,V76)-LV from the *CYC1* promoter. Transcription of the reporter gene was measured as β-galactosidase activity. **(B)** Wild-type yeast with an integrated LacZ reporter gene (YTY076) was transformed with a plasmid expressing Ub(L8A,V76)-LV from the ACT1 promoter. Cycloheximide-chase experiments showed that the L8A mutation leads to rapid turnover of the activator, which correlates with high transcription potency. **(C)** The VP16 activation domain was replaced with the Gal4 activation domain (Gal4AD). The YTY076 strain was transformed with a plasmid expressing the indicated activator, then streaked onto X-gal containing plates. A similar inhibitory effect was observed when Ub(V76) was fused to the N-terminus of LexA-Gal4AD. Note that blue-colored colonies were typically very small; that is expected because the transcription potency of the LV activator is known to correlate with toxicity to the cells (Berger et al.,1992). We also routinely used Ub(L8A,V76)-LV as a positive control for transcription activation because the expression of LV is very toxic in yeast. **(D)** Ub(V76) was inserted either between LexA and VP16 or placed C-terminal to LexA-VP16. Transcription of the reporter gene was assessed as described in (C). Regardless of the position of the Ub(V76), it inhibited transcription activation by LexA-VP16. **(E)** A 4xLexA operator sequence was integrated into the HO locus of yeast (YTY615) and its occupancy by LexA or Ub(V76)-LexA was analyzed by ChIP. Even in the absence of promoter and reporter gene sequences, the Ub fusion prevented LexA from stably binding to DNA. This indicates that the transcription machinery is not required for the inhibitory effect of the fused Ub(V76). **(F)** Shown is the schematic of a Ub(A76)-LV construct with a 2xHA N-terminal tag. This plasmid was transformed into yeast and cell lysates were analyzed by SDS-PAGE and immunoblotting. Anti-HA antibody detected only the full-length Ub(A76)-LV, whereas anti-LexA antibody detected both Ub(A76)-LV and the deubiquitinated form, LV.

levels were detected with the hydrophobic patch mutant, Ub(L8A,V76)-LV. Consistently, RNAPII levels at the promoter tracked with reporter gene activity. Promoter occupancy by LexA without the activation domain was similar to that of Ub(L8A,V76)-LV. In contrast, the Ub(V76)-LexA fusion was not detected at the promoter. To further demonstrate that the inhibitory effect of the attached Ub moiety is independent of both the activation domain and the transcription machinery recruited by the activation domain, we removed the promoter and ORF regions of the *LacZ* reporter gene, leaving only the 4xLexA operator site. We obtained similar results in that occupancy at this site by LexA alone was much higher than by Ub(V76)-LexA (Figure 2.3E).

In the case of Ub(A76)-LV, our results (Figure 2.1) implicated a role for deubiquitination in transcription activation. We introduced a 2xHA-tag at the N-terminus of the fusion. Anti-HA antibody can detect only the Ub-fusion form of LV, whereas anti-LexA antibody additionally can detect LV alone (Figure 2.3F). ChIP analysis revealed that only the deubiquitinated form was at the reporter gene (Figure 2.2E), underscoring the requirement of deubiquitination for activator function.

2.3.4 Cdc48 and its cofactors Ufd1 and Npl4 extract Ub(V76)-LV from DNA

Cdc48 has been shown to extract poly-ubiquitinated proteins from chromatin (Wilcox and Laney, 2009), but there was no clear evidence that mono-ubiquitinated proteins can be extracted similarly. However, mono- or oligo-ubiquitination of a processed form of Spt23 can lead to Cdc48-dependent extraction from its dimerization partner protein embbeded in the ER (Rape et al., 2001). Thus, we considered Cdc48 to be a good candidate responsible for preventing Ub(V76)-LV from stably binding to DNA. In yeast strains with temperature-

sensitive proteins expressed from the *cdc48-3*, *ufd1-1*, or *npl4-2* alleles, transcription activation by Ub(V76)-LV was evident even at the semi-permissive temperature (30 °C) (Figure 2.4A). We confirmed that at the non-permissive temperature (37 °C) Ub(V76)-LV occupancy at the *LacZ* promoter is restored in both *cdc48-3* and *ufd1-1* strains, and that the increased activator occupancy corresponds to increased RNAPII occupancy (Figure 2.4B). To test whether the ATPase activity of Cdc48 is required to inhibit transcription activation by Ub(V76)-LV, we introduced the $cdc48^{QE}$ mutant which carries a Q-to-E substitution in the D1 ATPase domain (Ye et al., 2003). Overexpression of $cdc48^{QE}$ activated transcription of *LacZ* as measured by both mRNA levels and β-galactosidase activities (Figure 2.4C). To prove that Cdc48 inactivation promotes binding of the intact Ub-LV fusion, we took advantage of the N-terminal HA tag in 2xHA-Ub(V76)-LV. At the non-permissive temperature, we observed increased activator occupancy by ChIP analyses with both anti-HA and anti-LexA (Figure 2.4D); thus, full-length Ub(V76)-LV can bind to the promoter.

The results above suggest a scenario in which the segregase activity of Cdc48 and its cofactors prevent Ub(V76)-LV from stably binding to DNA. When we performed ChIP analysis of a tagged form of Cdc48 expressed from the native CDC48 locus, we found that Cdc48 occupancy at the *LacZ* promoter was significantly higher in cells expressing Ub(V76)-LV than Ub(L8A,V76)-LV (Figure 2.4E). Thus, Cdc48 most likely acts directly on promoter-bound ubiquitinated activator and strips it from the DNA in a continuous cycle. This could explain why low levels of Ub(V76)-LV are detectable at the promoter (Figure 2.4D).

Mono-ubiquitination of the Gal4 activator was shown to play important roles in *GAL* gene transcription, where it was proposed to prevent the 19S RP from stripping Gal4 from

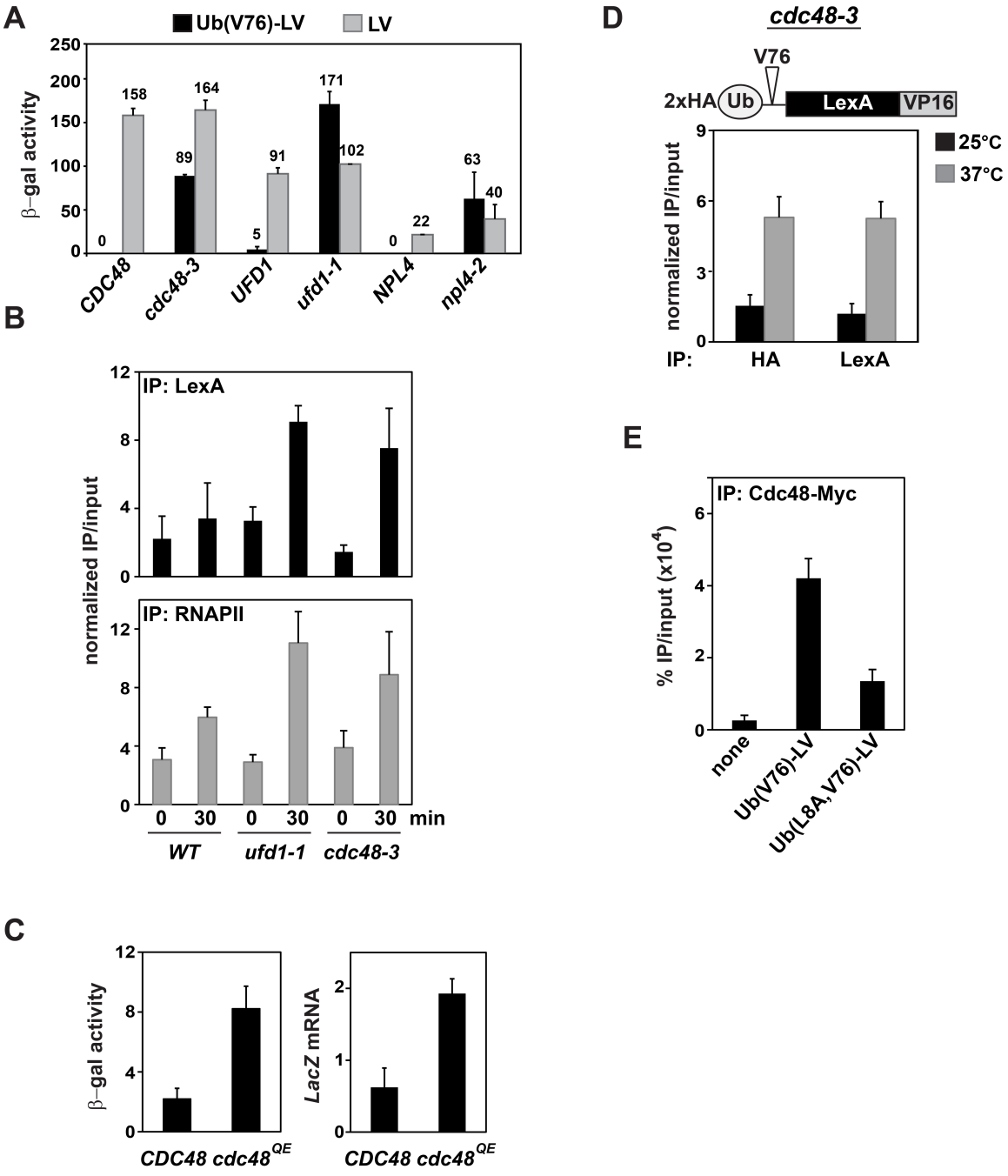
A
Ub(V76)-LV
LV
β–gal activity
250
200
150
100
50
0
158
164
89
91
5
171
102
0
22
63
40
CDC48
cdc48-3
UFD1
ufd1-1
NPL4
npl4-2
B
IP: LexA
IP: RNAPII
normalized IP/input
12
8
4
0
0 30 0 30 0 30 min
WT
ufd1-1
cdc48-3
C
β–gal activity
LacZ mRNA
CDC48 cdc48QE
CDC48 cdc48QE
D
cdc48-3
V76
2xHA
Ub
LexA
VP16
25°C
37°C
normalized IP/input
9
6
3
0
IP:
HA
LexA
E
IP: Cdc48-Myc
% IP/input (x10^4)
6
4
2
0
none
Ub(V76)-LV
Ub(L8A,V76)-LV

Figure 2.4. Cdc48 and its cofactors Ufd1 and Npl4 extract Ub(V76)-LV from DNA.
(A) A *LacZ* reporter gene as in Figure 1 was integrated into yeast expressing temperature-sensitive *cdc48-3*, *ufd1-1*, or *npl4-2* alleles, or into wild-type isogenic control strains. These were transformed with a *CEN* plasmid expressing Ub(V76)-LV or LV from the *ADH* promoter, and transformants were grown at the semi-permissive temperature (30 °C). Transcription of the reporter gene was measured as b-galactosidase activity. **(B)** The yeast strains in (A) were grown at 25 °C to log phase before shifting to 37 °C for 30 min. ChIP analysis with anti-LexA antibody showed increased promoter occupancy by Ub(V76)-LV upon inactivation of Ufd1 or Cdc48. Similar increases were observed for RNAPII occupancy. Occupancy at the reporter-gene promoter was normalized to occupancy at the inactive *GAL1* locus. **(C)** Wild-type Cdc48 or $Cdc48^{QE}$ under the control of a *GAL* promoter was over-expressed in YTY076 upon addition of galactose. Transcription of the reporter gene was measured as β-galactosidase activity (upper panel) or quantified by qPCR and normalized against that of *ACT1* (lower panel). **(D)** *cdc48-3* yeast were transformed with a plasmid expressing N-terminal HA-tagged Ub(V76)-LV. ChIP analysis with anti-HA and anti-LexA antibodies showed increased promoter occupancy by intact Ub(V76)-LV fusion upon inactivation of Cdc48. **(E)** Cdc48 was tagged with C-terminal 13xMyc at the endogenous *CDC48* locus. ChIP analysis using anti-Myc antibody showed that Cdc48 is recruited to the reporter gene by Ub(V76)-LV in a Ub-dependent manner.

the DNA (Archer et al., 2008; Ferdous et al., 2007). To investigate whether the 19S RP has a role in the regulation of Ub(V76)-LV, we measured reporter-gene activities in yeast strains with point mutations in five of the six 19S RP ATPase subunits (Rubin et al., 1998). None of the ATPase mutations affected Ub(V76)-LV-dependent *LacZ* expression except for *rpt5R* (Figure 2.5A). However, the *rpt5R* mutation did not affect promoter occupancy by either Ub(V76)-LV or RNAPII (Figure 2.5B). Therefore, the increased β-galactosidase activity we observed is most likely due to indirect effects of the mutation, such as an increased half-life of the β-galactosidase. We conclude that the 19S RP ATPases are unlikely to play a role in the transcriptional regulation afforded by the Ub(V76) fusion to LV.

2.3.5 Mono-Ub is sufficient to prevent transcription activation by LexA-VP16

Due to the dynamic and structurally diverse character of modifications by Ub, the number of Ub molecules attached to native substrates usually is not known. Our experimental system uniquely allowed us to address whether mono-Ub is sufficient to promote Cdc48-dependent remodeling of the substrate. In our previous experiments, the *LacZ* reporter gene had four upstream LexA operators and therefore could accommodate binding of up to four dimeric Ub-LV molecules. To limit the number of Ub-LV binding sites, we took advantage of a LexA mutant that recognizes an altered operator sequence (Dmitrova et al., 1998). $LexA^{408}$, which has three amino acid substitutions (P40A, N41S, A42S), was co-expressed with wild-type LV in a yeast strain that contained a *LacZ* reporter gene constructed with a single hybrid *LexA* operator recognized only by the $LexA^{408}$:LexA heterodimer (Figure 2.6A). As expected for this hybrid operator, LV activated *LacZ* transcription only when $LexA^{408}$ also was expressed (Figure 2.6B). However, surprisingly,

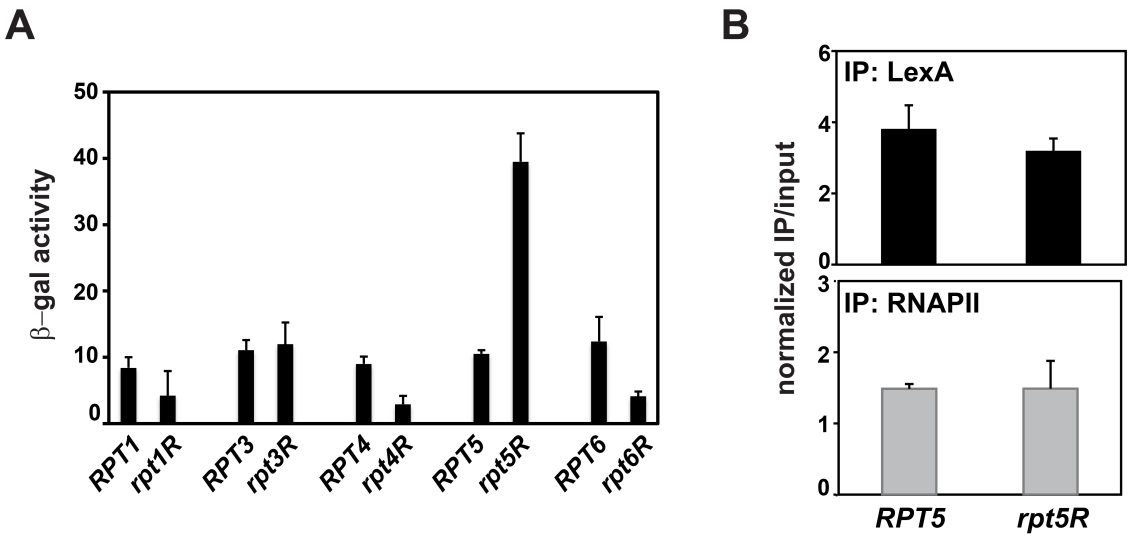

Figure 2.5. The proteasome ATPases encoded by RPT1, 3, 4, 5 or 6 are not required for the inhibitory effect of the fused Ub(V76) on transcription activation by LV.
(A) In each of the rptR strains, one of the proteasome ATPases bears a K to R substitution in the Walker A motif (Rubin et al., 1998). A *LacZ* reporter gene (as described in Figure 2.1) was integrated into each of the mutant strains as well as their isogenic wild-type controls. After introducing a plasmid expressing Ub(V76)-LV, transcription of the reporter gene in each strain was measured as β-galactosidase activity. Only the *rpt5R* strain showed increased reporter gene activity. The *rpt2R* strain was not analyzed because it is inviable. **(B)** Occupancy of the reporter gene promoter by Ub(V76)-LV or RNAPII was analyzed by ChIP with anti-LexA or anti-RNAPII (8WG16) antibodies. The *rpt5R* mutation did not increase promoter occupancy by the activator, suggesting that proteasome ATPases are not responsible for the inhibitory effect of the Ub moiety in Ub(V76)-LV. ChIP signals were normalized to the inactive *GAL1* locus.

transcription was completely abolished when Ub(K0,V76) was fused to LV, but was restored when L8A was introduced as an additional mutation into the Ub moiety. Consistently, Ub(K0,V76)-LV showed low promoter occupancy in comparison with LV (Figure 2.6C). These results demonstrate that, for LexA, a single mono-Ub is sufficient to prevent stable binding to the operator.

Cdc48's participation in diverse biological processes is made possible in part by an arsenal of substrate-recruiting adaptor proteins that interact with mono- or poly-Ub. The yeast genome encodes seven non-essential Cdc48 substrate adaptors that contain the Ub-regulatory-X (UBX) domain (Schuberth and Buchberger, 2008). In addition, Ufd1 and Npl4 are essential, highly-conserved Cdc48 adaptors. Using the *LacZ* reporter-gene assay, we found that only deletion of *ubx1* or *ubx2* resulted in moderately increased reporter-gene activity (Figure 2.6D). However, partial inactivation of *ufd1* or *npl4* by growth at 30 °C had much more pronounced effects. Therefore Ufd1 together with Npl4 are most likely sufficient to direct Cdc48 to DNA-bound Ub(V76)-LV, although we cannot rule out that UBX proteins have roles that were masked by functional redundancy among them.

2.3.6 Cdc48 helps to maintain *MET* gene repression through oligo-ubiquitinated Met4

The transcription activator Met4 is a master regulator of sulfur metabolism in yeast. In limiting methionine, Met4 activates transcription of a large number of genes (generally termed *MET* genes) involved in the synthesis of sulfur-containing metabolites. Under non-inducing conditions, Met4 inactivation is required for cell proliferation; this is achieved through ubiquitination by the SCF^{Met30} E3 Ub ligase (Kaiser et al., 2000) (Figure 2.7). Interestingly, Met4 is modified by a K48-linked oligo-Ub chain, yet escapes proteasome

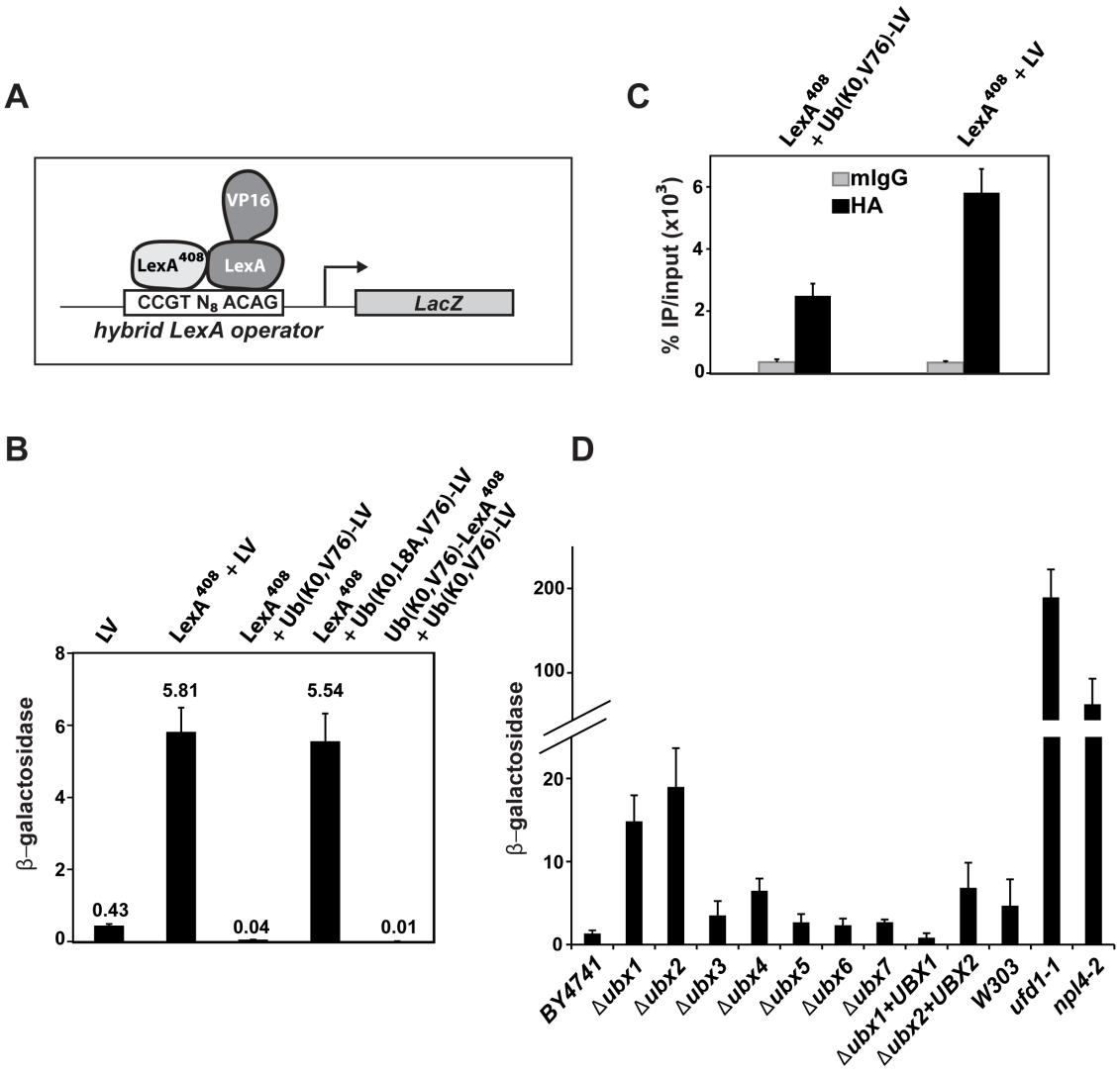
A
VP16
LexA408
LexA
CCGT N8 ACAG
LacZ
hybrid LexA operator
B
LV
LexA408 + LV
LexA408 + Ub(K0,V76)-LV
LexA408 + Ub(K0,L8A,V76)-LV
Ub(K0,V76)-LexA408 + Ub(K0,V76)-LV
β–galactosidase
0.43
5.81
0.04
5.54
0.01
C
LexA408 + Ub(K0,V76)-LV
LexA408 + LV
mIgG
HA
% IP/input (x10^3)
D
β–galactosidase
BY4741
Δubx1
Δubx2
Δubx3
Δubx4
Δubx5
Δubx6
Δubx7
Δubx1+UBX1
Δubx2+UBX2
W303
ufd1-1
npl4-2

Figure 2.6. A single Ub is sufficient to inhibit transcription activation by LV.
(A) Schematic of a hybrid LexA operator recognized specifically by the LexA^{408}:LexA heterodimer. LexA^{408} (bearing P40A, N41S, A42S mutations) binds to the left half of the operator, whereas wild-type LexA binds to the right half (Dmitrova et al., 1998). **(B)** A *LacZ* reporter gene with the hybrid LexA operator was integrated into wild-type yeast. This strain was then transformed with different combinations of plasmids expressing LexA^{408}, LexA-VP16, or their Ub-fusions, from the *CYC1* promoter. Transcription of the reporter gene was observed only when LexA^{408} and LexA-VP16 were expressed together. A single Ub(K0,V76) attached to LV abolished transcription activation as measured by b-galactosidase activity; inhibition by the attached Ub was reversed by L8A mutation at the Ub hydrophobic patch. **(C)** ChIP analysis with anti-HA antibodies shows that Ub(K0,V76)-LV has lower promoter occupancy than LV. An HA-tag was inserted between LexA and VP16. **(D)** The *LacZ* reporter gene was integrated into wild-type (*BY4741*) yeast or strains with one of the seven *UBX* genes deleted. The *LacZ* reporter was also integrated into temperature-sensitive *ufd1-1*, *npl4-2* strains and the isogenic wild-type strain (*W303*). These were transformed with a *CEN* plasmid expressing Ub(V76)-LV from the *ADH* promoter, grown at 30 °C to log phase, and *LacZ* transcription was measured as b-galactosidase activity. Plasmids expressing either Ubx1 or Ubx2 were able to rescue the phenotypes of *Dubx1* or *Dubx2* strains, respectively.

degradation because the chain is shielded by intramolecular association with Ub-binding domains (Ouni et al., 2011 and references therein). However, even without proteolysis, ubiquitination of Met4 is sufficient to prevent *MET* gene expression. In another layer of regulation, Met4 mediates ubiquitination of cofactors that recruit Met4 to its target genes (Ouni et al., 2010). Ubiquitination of these cofactors, such as Met32, leads to proteasome degradation which further prevents Met4-dependent *MET* gene activation and Met32-dependent cell cycle arrest.

How ubiquitination of Met4 maintains *MET* genes in a repressed state has been unclear. We hypothesized that Cdc48 may help to keep oligo-ubiquitinated Met4 from binding to target gene promoters under non-inducing conditions. As shown in Figures 2.8A and 2.8B, transcription of three such target genes, *MET17*, *MET3* and *CYS3*, increased upon inactivation of Cdc48 or its cofactor Ufd1, whereas no change was observed in control gene (*ACT1)* transcription (Figure 2.9A) or in the presence of wild-type Cdc48 (Figure 2.9B). Consistently, we also observed increased promoter occupancy by Met4 and RNAPII upon inactivation of Ufd1 (Figure 2.8C).

As expected, Met4 ubiquitination was largely unaffected by inactivation of Cdc48 (Figures 2.9C and 2.10A). However, Met4-dependent transcription is more complex in that Met4 itself lacks intrinsic DNA-binding activity and is targeted to specific genes through cofactors such as Met32. Although Met32 undergoes proteasome-dependent degradation, we found that Met32 turnover was not affected by inactivation of Cdc48 (Figure 2.10A). Moreover, upon inactivation of Ufd1, although increased promoter occupancy by Met4 mirrored the recruitment of RNAPII, the kinetics of promoter occupancy by Met32 showed a different pattern (compare Figures 2.8C and 2.8D). These results suggest that, to maintain

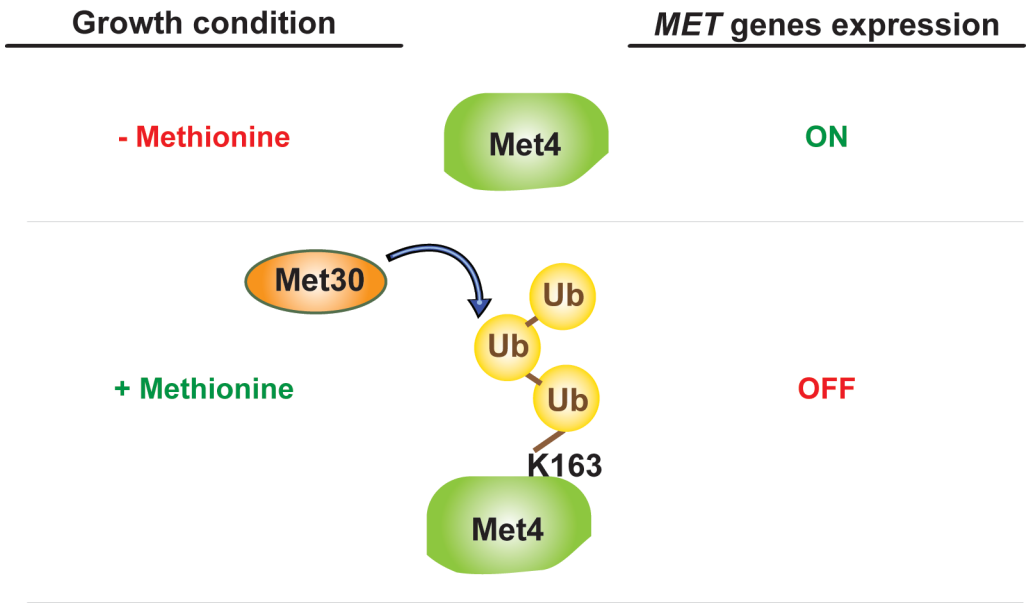

Figure 2.7. Regulation of *MET* genes expression by oligo-ubiquitination of the transcriptional activator Met4. In limiting methionine, Met4 activates transcription of a large number of genes (*MET* genes), involved in the synthesis of sulfur-containing metabolites. Under non-inducing conditions, when methionine intracellular concentrations are high, the SCF^{Met30} E3 Ub ligase ubiquitinates Met4 on Lysine 163. Although this ubiquitination does not target Met4 for degradation, is sufficient to prevent *MET* gene expression.

MET gene repression, Cdc48 acts on oligo-ubiquitinated Met4 and not the DNA-binding cofactor Met32.

To further demonstrate that the repressive effect of Cdc48 depends on Met4 oligo-ubiquitination, we compared the effects of Cdc48 inactivation with and without Met30. Without Met30, Met4 is not ubiquitinated and activates transcription potently (Kaiser et al., 2000). Our model predicts that Cdc48 has a repressive role only when Met4 is ubiquitinated. Indeed, inactivation of Cdc48 increased *MET* gene expression only in the presence of Met30 (Figure 2.11A), and Met4 occupancy at the *MET17* promoter was increased by Cdc48 inactivation only in strains expressing Met30 (Figure 2.11B). Met30 deletion led to marked increases in *MET* gene transcription (Figure 2.11A); this was accompanied by higher promoter occupancy by Met4 and RNAPII, but lower occupancy by Cdc48 (Figure 2.11C). In contrast, the levels of the DNA-binding co-factor, Met32, which was transiently overexpressed from a p*GAL* promoter, remained constant (Figures 2.11C and 2.9D).

Oligo-ubiquitination of Met4 is on a single residue, K163 (Flick et al., 2004) (Figure 2.7). When *MET4* was replaced with the *met4(K163R)* allele, *MET* genes were de-repressed as previously reported (Figures 2.9E and 2.9F). With *met4(K163R),* inactivation of Cdc48 no longer stimulated *MET* gene expression (Figure 2.11D). Unlike wild-type Met4, Met4(K163R) is rapidly degraded, perhaps as a consequence of transcription activation. As a control, we show that inactivation of Cdc48 does not affect the turnover of Met4(K163R) (Figure 2.10B). Importantly, although Met4(K163R) has higher occupancy at the *MET17* promoter and recruits more RNAPII, it fails to recruit Cdc48 (Figure 2.11E). Taken together, these results strongly support our model in which the oligo-Ub signal on Met4

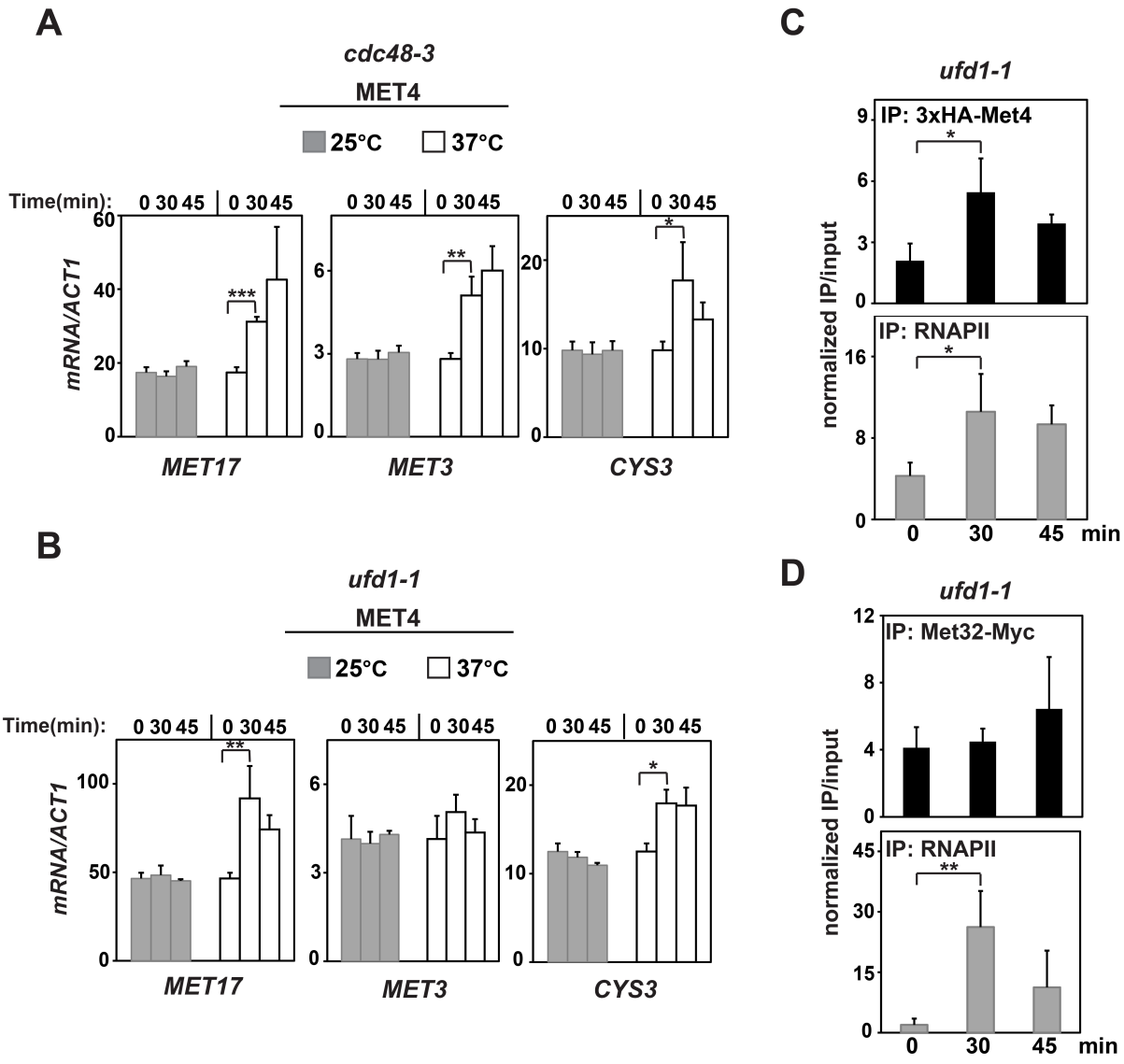
A
cdc48-3
MET4
25°C
37°C
Time(min): 0 30 45 | 0 30 45
mRNA/ACT1
MET17
MET3
CYS3
B
ufd1-1
MET4
25°C
37°C
Time(min): 0 30 45 | 0 30 45
mRNA/ACT1
MET17
MET3
CYS3
C
ufd1-1
IP: 3xHA-Met4
IP: RNAPII
normalized IP/input
0 30 45 min
D
ufd1-1
IP: Met32-Myc
IP: RNAPII
normalized IP/input
0 30 45 min

Figure 2.8. Cdc48 and Ufd1 contribute to the maintenance of *MET* gene repression. **(A)** and **(B)** *cdc48-3* and *ufd1-1* strains expressing 3xHA-Met4 from the native *MET4* promoter were grown at 25 °C in SD-URA medium containing 0.13 mM methionine. At log phase, half of the culture was shifted to 37 °C for the indicated times and *MET17, MET3* and *CYS3* transcripts were assayed by qRT-PCR. *p* values were determined by Students' t-test (* $p<0.05$; ** $p<0.01$; *** $p<0.001$). **(C)** The *ufd1-1* strain described in (B) was grown at 25 °C to log phase and shifted to 37 °C for the indicated times. Met4 and RNAPII occupancies at the *MET17* promoter were monitored by ChIP. ChIP signals were normalized to the silent *GAL1* locus. **(D)** Met32 was C-terminally tagged with 13xMyc at the endogenous *MET32* locus in the *ufd1-1* strain. This strain was grown in YPD at 25 °C to log phase and shifted to 37 °C for the indicated times. Met32 occupancy at the *MET17* promoter was monitored by ChIP with anti-Myc antibodies. Although RNAPII occupancy and Met4 occupancy increased upon Ufd1 inactivation, Met32 occupancy did not change significantly. By 45 min at 37 °C, occupancy by RNAPII and Met4 had decreased.
See also Figures S3 and S5.

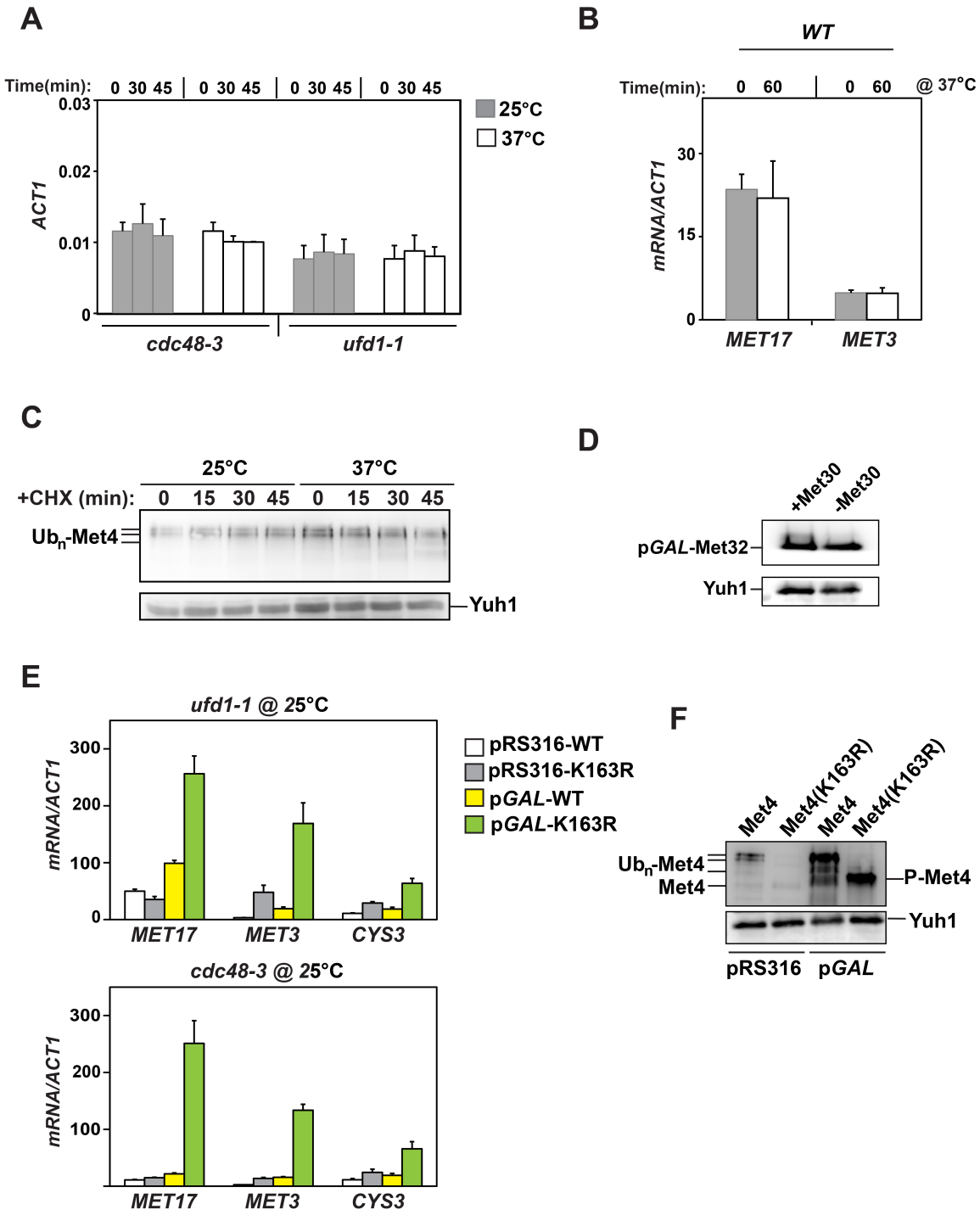
A
Time(min): 0 30 45 | 0 30 45 | 0 30 45 | 0 30 45
25°C
37°C
ACT1
0.03
0.02
0.01
0
cdc48-3
ufd1-1
B
WT
Time(min): 0 60 | 0 60 @ 37°C
mRNA/ACT1
30
15
0
MET17
MET3
C
25°C
37°C
+CHX (min): 0 15 30 45 0 15 30 45
Ubn-Met4
Yuh1
D
+Met30
-Met30
pGAL-Met32
Yuh1
E
ufd1-1 @ 25°C
mRNA/ACT1
300
200
100
0
MET17
MET3
CYS3
pRS316-WT
pRS316-K163R
pGAL-WT
pGAL-K163R
cdc48-3 @ 25°C
mRNA/ACT1
300
200
100
MET17
MET3
CYS3
F
Met4
Met4(K163R)
Met4
Met4(K163R)
Ubn-Met4
Met4
P-Met4
Yuh1
pRS316
pGAL

Figure 2.9. Cdc48 and Ufd1 help to maintain MET gene repression through oligo-ubiquitinated Met4. (A) *ACT1* expression was not altered upon temperature shift in *cdc48-3* and *ufd1-1* yeast. These strains were grown at 25 °C into log phase and then half of the culture was shifted to 37 °C. At the indicated times, aliquots were taken and *ACT1* mRNA levels were quantified by qRT-PCR. **(B)** *MET17* and *MET3* expression were not altered by the temperature shift in wild-type yeast. **(C)** Met4 ubiquitination was largely unaffected by inactivation of Cdc48. *cdc48-3* yeast expressing 3xHA-Met4 from the native MET4 promoter were grown in SD-URA medium at 25 °C. Upon addition of cycloheximide (CHX), half of the culture was shifted to 37 °C. Aliquots were removed at the indicated times and cell lysates were analyzed by SDS-PAGE and immunoblotting. Yuh1 protein served as an internal loading control. **(D)** *cdc48-3Δmet32* or *cdc48-3Δmet32Δmet30* strains were transformed with p*GAL*-Met32-Flag and grown to log phase at 25 °C. Expression of Met32 was induced for 2 h and whole-cell lysates were prepared and analyzed by SDS-PAGE and imunoblotting with anti-Flag and anti-Yuh1 antibodies. Met32 has similar steady-state levels in these strains. **(E)** Blocking oligo-ubiquitination of Met4 increases transcription of *MET* genes. *ufd1-1* and *cdc48-3* strains lacking endogenous Met4 were transformed with CEN plasmids expressing 3xHA-tagged wildtype Met4 or Met4(K163R) from either the native *MET4* promoter (pRS316) or the inducible *GAL1* promoter (p*GAL*). Transformants carrying the pRS316 plasmids were grown at 25 °C in SD-URA medium and *MET17*, *MET3* and *CYS3* transcripts were analyzed from log phase culture. Transformants carrying the p*GAL* plasmids were grown at 25 °C in SC-URA+Raffinose medium to log phase and induced with galactose for 2 h before RNA was collected for qRT-PCR. **(F)** The *ufd1-1* strains were constructed and cultured as described in (E). Met4 protein levels were analyzed by SDS-PAGE and immunoblotting with anti-HA and anti-Yuh1 antibodies.

recruits Cdc48, which in turn represses transcription by removing Met4 from *MET* gene promoters.

Surprisingly, although deletion of Met30 increased *MET17* transcription 20-fold, promoter occupancy by Met4 increased only 3-fold (Figure 2.11C). In the presence of Met30, inactivation of Ufd1 or Cdc48 led to similar increases in promoter occupancy by Met4 (Figures 2.8C and 2.11B), yet *MET17* transcription increased only 1.7-fold (Figures 2.8A and 2.8B). Because Cdc48 inactivation has only these small effects on steady-state transcript levels, we tested if *MET* gene repression is affected more profoundly during the transition from limiting to abundant methionine. Figure 2.12 shows that full repression is achieved within 15 min regardless of whether Cdc48 or Ufd1 is active. However, *MET* transcripts were maintained at up to 6-fold higher levels when Cdc48 or Ufd1 was inactivated, suggesting that the Cdc48 pathway functions in the maintenance phase of repression. Unlike with *MET17* or *MET3*, we observed significant derepression of *SAM1* and *SAM2,* genes encoding enzymes that synthesize *S*-adenosylmethione. These data suggest that Met4 target genes are differentially regulated and that transcriptional output is determined by factors in addition to Met4 and RNAPII recruitment, such as elongation factors or chromatin-remodeling activities. Ubiquitination of Met4 may regulate these uncharacterized activities in addition to lowering promoter occupancy through Cdc48.

2.3.7 p97 mediates Ub-dependent inactivation of receptor-activated Smads (R-Smads) independently of proteolysis

In human cells, mono-ubiquitination of R-Smads attenuates TGFβ signaling without promoting R-Smad degradation (Inui et al., 2011; Tang et al., 2011). Inui *et al.* suggested

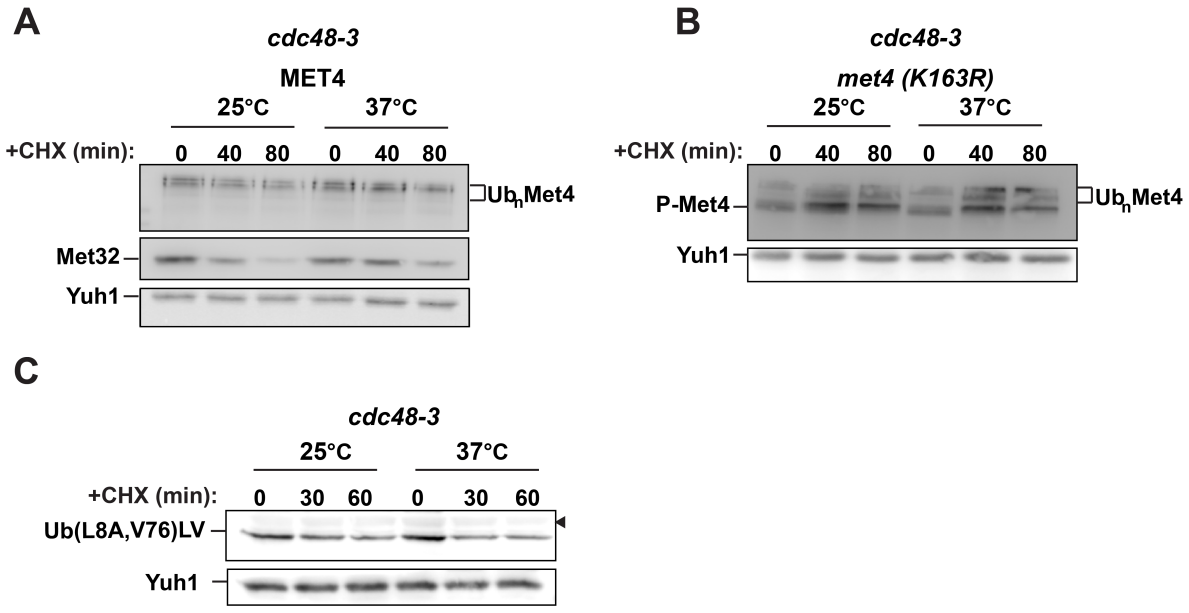

Figure 2.10. Cdc48 inactivation does not affect the half-lives of Met32, Met4(K163R), or Ub(L8A,V76)-LV.
(A) *cdc48-3Δmet4Δmet32* yeast (YTY613) were transformed with p*GAL*-Met32-Flag and pRS316-3xHA-Met4. Transformants were grown to log phase at 25 °C. Expression of *Met32* was induced for 2 h with galactose before addition of cycloheximide and half of the culture was shifted to 37 °C. Aliquots were removed at the indicated times and cell lysates were analyzed by SDS-PAGE and immunoblotting. **(B)** *cdc48-3Δmet4* yeast (YTY531) were transformed with p*GAL*-Met4(K163R) as described in Figure 2.9E. Met4(K163R) levels were analyzed as described in (A). **(C)** The *cdc48-3* strain with an integrated *LacZ* reporter gene (YTY380) was transformed with a plasmid expressing Ub(L8A,V76)-LV from the *ACT1* promoter. Cycloheximide-chase experiments, performed at the permissive (25 °C) or the non-permissve temperature (37 °C), showed that Ub(L8A,V76)-LV degradation is independent of Cdc48.

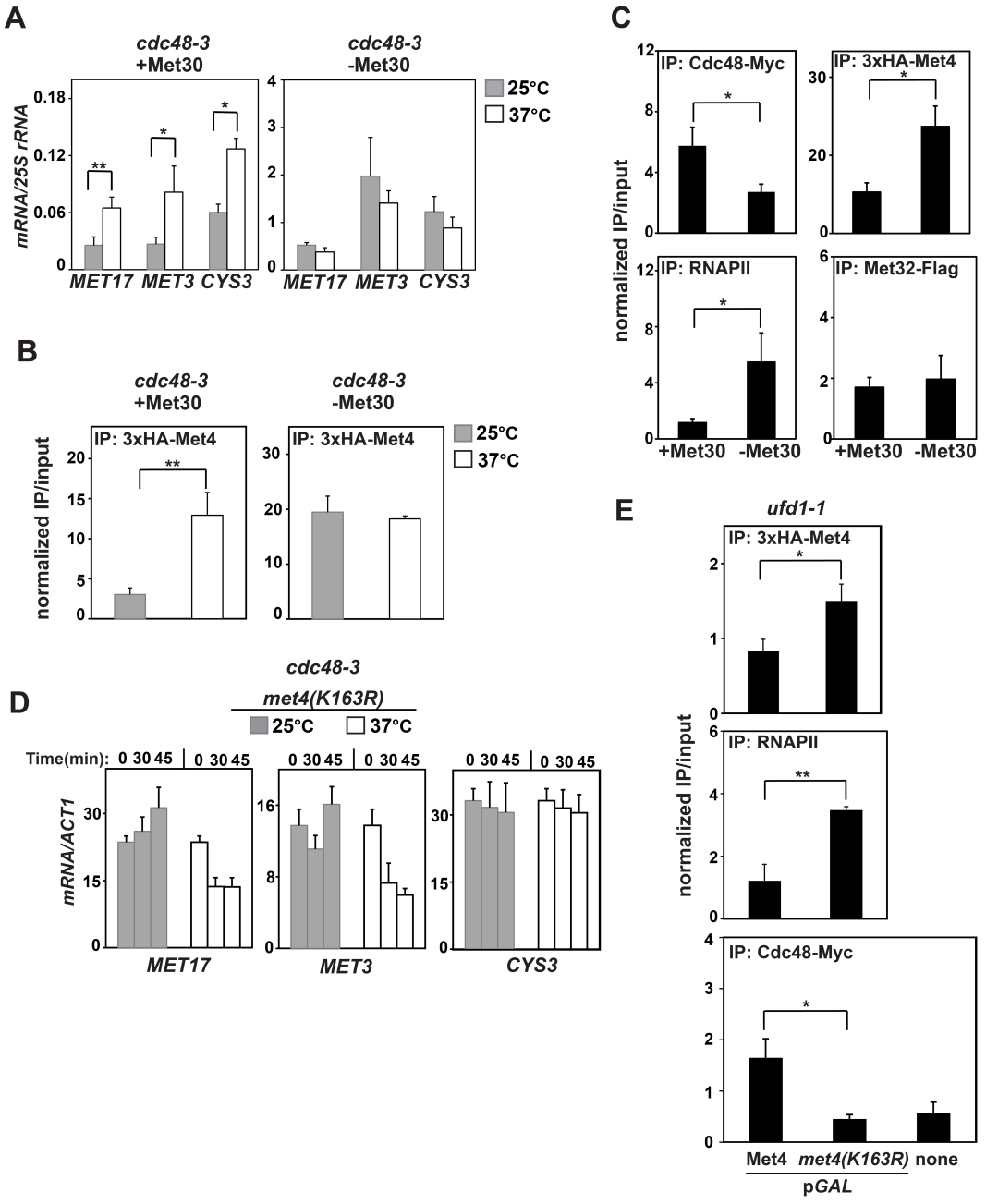
A
cdc48-3
+Met30
cdc48-3
-Met30
25°C
37°C
mRNA/25S rRNA
MET17 MET3 CYS3
B
cdc48-3
+Met30
cdc48-3
-Met30
IP: 3xHA-Met4
normalized IP/input
C
IP: Cdc48-Myc
IP: 3xHA-Met4
IP: RNAPII
IP: Met32-Flag
normalized IP/input
+Met30 -Met30
D
cdc48-3
met4(K163R)
Time(min): 0 30 45 0 30 45
mRNA/ACT1
MET17
MET3
CYS3
E
ufd1-1
IP: 3xHA-Met4
IP: RNAPII
IP: Cdc48-Myc
normalized IP/input
Met4 met4(K163R) none
pGAL

Figure 2.11. Cdc48 represses *MET* genes through oligo-ubiquitinated Met4.
(A) Cdc48 represses *MET* genes only in the presence of *MET30*. *cdc48-3Δmet32* and *cdc48-3Δmet32Δmet30* strains were grown in SD-URA medium at 25 °C. At log phase, expression of p*GAL*-Met32-Flag was induced for 2 h followed by shifting half of the culture to 37 °C for 45 min. Expression of endogenous *MET17, MET3* and *CYS3* genes was assayed by qRT-PCR and normalized to *25S rRNA*. **(B)** Cdc48 lowers promoter occupancy by Met4 only in the presence of *MET30*. Strains described in (A) were modified to express 3xHA-Met4 from the native *MET4* promoter. These were grown as in (A) and ChIP analysis of Met4 occupancy at the *MET17* promoter was performed. ChIP signals were normalized to the *RPL11* locus. **(C)** For ChIP analysis of *MET17* promoter occupancy by Cdc48, Met4, Met32 and RNAPII in the presence and absence of Met30, *Δmet32* and *Δmet32Δmet30* strains transformed with p*GAL*-Met32-Flag were modified to either express Cdc48-13xMyc at the endogenous *CDC48* locus or 3xHA-Met4 from its native promoter. ChIP signals were normalized to the *RPL11* locus. **(D)** Cdc48 does not repress *MET* genes in the presence of Met4(K163R). Expression of *MET17*, *MET3* and *CYS3* were analyzed as in Figure 5A except that wild-type Met4 was replaced with Met4(K163R). **(E)** 3xHA-tagged Met4 or Met4(K163R) were expressed from the *GAL* promoter for 40 min and then cells were fixed for ChIP analysis. Whereas Met4(K163R) occupancy was higher than Met4 at the *MET17* promoter and correlated with greater recruitment of RNAPII (top and middle panels, respectively), less Cdc48 (Myc-tagged at the endogenous *CDC48* locus) was recruited by Met4(K163R).

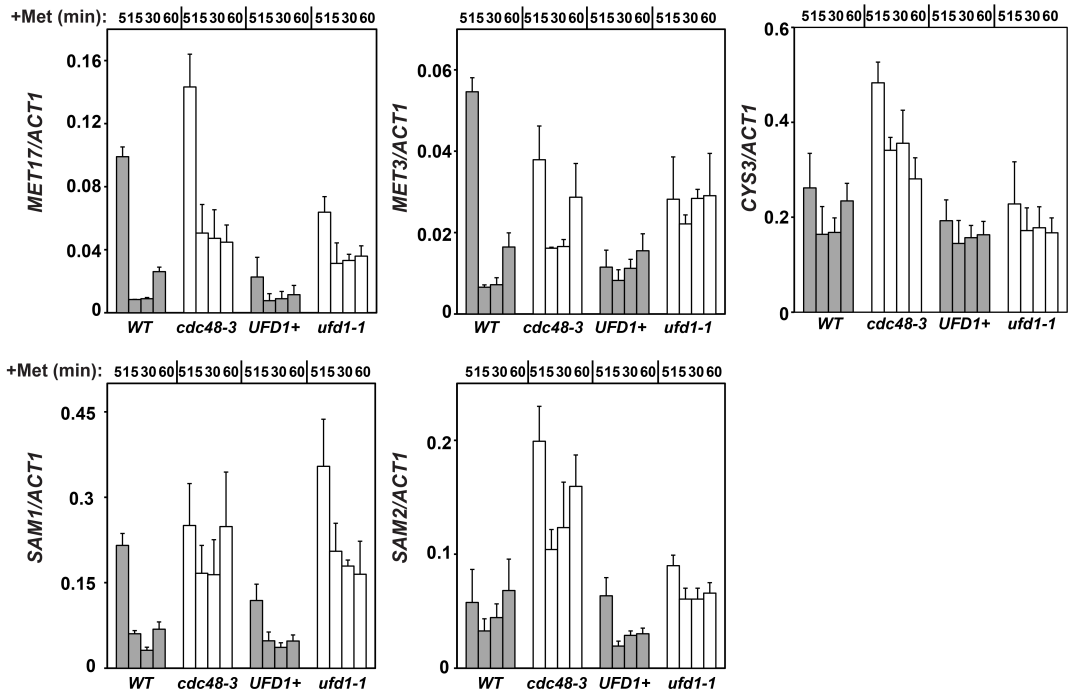

Figure 2.12. Cdc48 and Ufd1 function in the maintenance phase of MET gene repression. Yeast strains as indicated were grown in minimal medium to log phase at 25 °C followed by continual shaking at 37 °C for 30 min. At time zero, 1 mM methionine was added and aliquots of cultures were collected at the times indicated following methionine addition. Transcript levels were analyzed by quantitative RT-PCR and normalized to levels of *ACT1*. For each transcript, its level at zero-time was set to 1.

that ubiquitination sterically interferes with DNA binding, whereas Tang *et al.* proposed that ubiquitination sterically blocks formation of active Smad3/Smad4 complexes. Although both groups invoked "steric hindrance" models for the repressive effect of mono-ubiquitination, they reported different sites of ubiquitination. Based on our observations with LexA-VP16 and Met4 in yeast, we tested whether the Cdc48 homolog, p97, mediates extraction of ubiquitinated Smad from its interaction with DNA or proteins. We treated MDA-MB-231 human breast cancer cells with the p97-specific inhibitor DBeQ (Chou et al., 2011) and monitored expression of Smad target genes *CTGF* and *IL-11.* Inhibition of p97 increased Smad2/3-mediated transcription both with and without added TGFβ (Figure 2.13A). Within the 2 h period of treatment, the transcription enhancement by DBeQ alone was similar to that of TGFβ, the native signaling ligand (compare lanes 2 and 3). This suggests that p97 plays a major role in maintaining the Smad target genes in a repressed state. In addition, we found no evidence that inhibition of p97 increased the nuclear pool of Smad2/3 or phospho-Smad2/3 (Figure 2.13B); rather, a combination of TGFβ and DBeQ treatments slightly decreased nuclear Smad2/3 levels. Therefore, it is unlikely that p97 inhibition affects the signaling process upstream of transcription. By ChIP we found that inhibition of p97 dramatically increased promoter occupancy by Smad2/3 with or without TGFβ treatment (Figure 2.13C). These data support a model in which p97 helps to repress Smad target genes by preventing DNA binding of ubiquitinated R-Smads. Upon TGFβ signaling, Usp15 deubiquitinates Smad2/3 (Inui et al., 2011), which would lead to p97 dissociation and transcription activation. Interestingly, Smad4, a coactivator of R-smads, similarly has been reported to undergo mono-ubiquitination (Wang et al., 2008). Smad4 mono-ubiquitination disrupts its interaction with Smad2. Therefore, inhibition of p97 by

DBeQ also may promote binding of the Smad4 coactivator, which would lead to enhanced transcription of Smad target genes.

Smad regulation via p97-dependent extraction differs signficantly from the steric hindrance models proposed by Inui et al. and Tang et al. Although they are not mutually exclusive, those models depend heavily on where the Smad2/3 transcription factors are ubiquitinated, a point that remains unclear in light of the different results reported (Inui et al., 2011; Tang et al., 2011). In contrast, p97-dependent extraction is likely to be less sensitive to the ubiquitination site(s). However, we cannot rule out that p97 acts on other factors that affect promoter occupancy by Smad2/3. R-Smads undergo complex post-translational modifications, including oligo and poly-ubiquitination, that depend on cell type, expression levels of the Smads, and the strength and persistence of the stimuli. Whether steric hindrance or p97-dependent extraction by Ub are major contributors to Smad regulation will require future experiments in which these models are compared under uniform conditions.

2.4 Discussion

The functional outcome of ubiquitination is thought to depend on the number of Ubs attached to the substrate and the types of Ub-Ub linkages in polyUb chain(s) that may be formed. However, the dynamic and often very heterogeneous nature of Ub modifications make the structures and consequences of (poly)Ub signals difficult to define. Adding to this complexity is the fact that, typically, only a small fraction of a substrate protein is ubiquitinated. With TAs, at least two pools exist for any particular activator: one free and one bound to chromatin. Because antibodies against specific ubiquitinated proteins

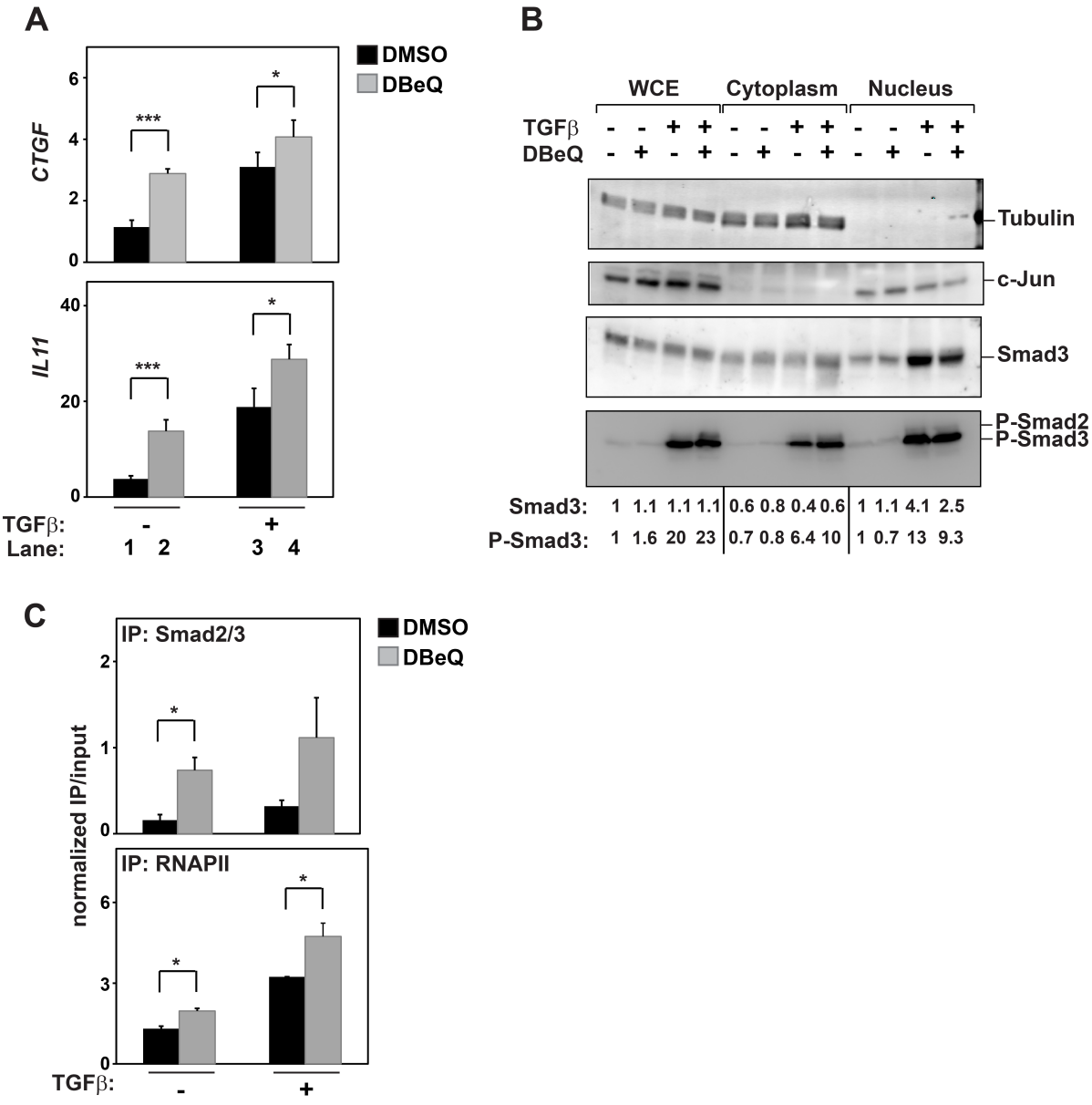
A
DMSO
DBeQ
CTGF
IL11
TGFβ:
Lane:
1 2 3 4
B
WCE
Cytoplasm
Nucleus
TGFβ
DBeQ
Tubulin
c-Jun
Smad3
P-Smad2
P-Smad3
Smad3: 1 1.1 1.1 1.1 0.6 0.8 0.4 0.6 1 1.1 4.1 2.5
P-Smad3: 1 1.6 20 23 0.7 0.8 6.4 10 1 0.7 13 9.3
C
IP: Smad2/3
IP: RNAPII
normalized IP/input
TGFβ:

Figure 2.13. p97 inhibits R-Smad-mediated transcription independently of proteolysis.(A) MDA-MB-231 cells were treated with either 100 pM TGFb alone or in combination with 10 mM DBeQ, a p97 inhibitor. After 2 h, mRNAs from *CTGF* and *IL11* were analyzed by qRT-PCR and normalized to *GAPDH* mRNA. Error bars represent standard deviations of mean values from three independent experiments. **(B)** Smad2/3 protein levels and cellular localization were not altered by DBeQ treatment. Cells were treated as in (A) and whole-cell extract (WCE), cytoplasmic and nuclear fractions were analyzed by SDS-PAGE and immunoblotted for total Smad3 and phospho-Smad2/3 (P-Smad2/3). Tubulin and c-Jun were used as cytosolic and nuclear markers, respectively. Numbers shown are band intensities normalized to tubulin for WCE and cytoplasm lanes, and to c-Jun for nucleus lanes. **(C)** Cells were treated as in (A) and Smad2/3 and RNAPII occupancies at the *CTGF* promoter, encompassing TGFβ-responsive elements, were monitored by ChIP. ChIP signals were normalized to an intergenic region. DBeQ treatment resulted in elevated promoter occupancy by Smad2/3 and RNAPII. Error bars represent standard deviations of mean values from two independent experiments.

generally are unavailable, for most TAs it has not been possible to determine which pool is ubiquitinated. These factors compound the difficulty in determining the direct consequence of ubiquitination.

Dynamics of activator ubiquitination—Using LexA-VP16 as a model transcription activator fused with various forms of Ub, we have demonstrated that mono-ubiquitination can lead to transcription inhibition by recruiting the AAA^+ ATPase Cdc48. Our results with Ub(V76)-LV differ from those of a previous study (Salghetti et al., 2001) that had employed Ub(A76)-LV. We found that the widely-used Ub(A76)-protein fusion undergoes substantial deubiquitination *in vivo*, making it difficult to differentiate whether the intact fusion or the deubiquitinated product is responsible for the observed function. With Ub-LV, the ubiquitinated activator does not bind to the promoter stably (Figure 2.2E) and mutations at the Ub-LV junction demonstrated that deubiquitination is required for transcription (Figure 2.1B). Ub-conjugate reversibility is similarly important for the physiological regulation of Met4 and R-Smad transcription activators. Interestingly, subsequent transcription activation frequently leads to poly-ubiquitination and degradation of the activator, as was previously shown for LV and Smad2/3 (Salghetti et al., 2001; Gao et al., 2009). This is a common strategy to turn off signaling events. Ub(V76)-LV is stable in wild-type yeast (Figure 2.1C), which suggests that fusion to Ub(V76) prevents poly-ubiquitination of LV by Met30. We think that this is a consequence of the timing and regulation of Ub attachment. A characteristic of transcription-coupled poly-ubiquitination is that the activator is "marked" for ubiquitination, typically via phosphorylation by coactivator(s) that are part of the transcription machinery (Lipford et al., 2005). In this way, activator ubiquitination and degradation are orchestrated to follow one or more

rounds of transcription. In the case of Ub(V76)-LV, because the transcription factor is synthesized with the Ub signal already attached, the lifetime of DNA-bound Ub(V76)-LV may be too brief to recruit the transcription machinery needed to mark the activator for Met30-dependent ubiquitination. In the cases of Met4 and Smad2/3, mono- or oligo-ubiquitination is independent of the transcription machinery and prevents transcription by destabilizing activator-DNA interactions even before higher-order transcription complexes can assemble. Thus, the activators we examined here exemplify how mono- and poly-ubiquitination regulate two different phases of transcription with different consequences. Notably, although Cdc48 mediates the inhibitory effect of mono- or oligo-ubiquitination, in the cases of Ub(L8A,V76)-LV and Met4(K163R), it does not appear to be required for the degradation of the poly-ubiquitinated transcription factors (Figure 2.10).

An unexpected role for mono-ubiquitination and Cdc48 in inhibiting transcription—The 26S proteasome often employs the segregase activity of Cdc48 to remove poly-ubiquitinated proteins from tightly-bound partners. This has been demonstrated recently for multiple chromatin-bound proteins that include yeast a2 and RNAPII, which directly interact with DNA (Verma et al., 2011; Wilcox and Laney, 2009), and Cdt1, Aurora kinase B, and L3MBTL1, which are bound to chromatin or its associated proteins (Acs et al., 2011; Ramadan et al., 2007; Raman et al., 2011). In most cases, Cdc48 is recruited by poly-Ub, yet the fates of the substrates differ. Whereas Aurora Kinase B is released as a stable protein, other substrates are degraded by the proteasome. How specificity of Cdc48 is governed and what properties determine the different fates of substrates are key unanswered questions.

To our surprise, for LexA, a single Ub is sufficient to recruit Cdc48 and promote dissociation from DNA. Cdc48 and many of its cofactors bind to Ub (Ye, 2006), but

specificity for mono- or poly-Ub is not well characterized. Yeast Ufd1 interacts with both mono- and poly-Ub, but its affinity for mono-Ub is quite weak (Park et al., 2005). We think it is unlikely that mono-Ub is the only feature that Cdc48 and its cofactors recognize in this process. First, the mono-Ub moiety by itself is not a very distinctive signal. *In vivo*, a large pool of Ub exists in a dynamic equilibrium of conjugated and unconjugated states; all of these are potential competitors for binding to Cdc48:Ufd1:Npl4 complexes. Secondly, Ub(V76)-LV in our experimental system was expressed at high levels from either the *ACT1* or *ADH* promoters and was found to be broadly distributed in both the cytoplasm and the nucleus (Figure 2.2D). In all of our reporter gene assays, a single LexA operator-driven *LacZ* gene was inserted at the endogenous *HO* locus. Therefore, there was a large pool of Ub(V76)-LV not associated with chromatin that in principal would have been available to compete with DNA-bound Ub(V76)-LV for binding by Cdc48:Ufd1:Npl4. Nonetheless, despite the high potency of the LV activator, transcription activation by Ub(V76)-LV was barely detectable. Thus, the Cdc48 machinery was remarkably efficient in preventing activation despite the high total concentration of Ub(V76)-LV and other mono-Ub conjugates.

Modification at DNA damage foci with the Ub-like protein SUMO recently was found to recruit Cdc48 activity via a SUMO-interacting motif (SIM) in the Ufd1 adaptor protein (Bergink et al., 2013; Hannich et al., 2005; Nie et al., 2012). We therefore investigated possible involvement of SUMO in the regulation of Ub(V76)-LV. Neither inactivation of SUMO (Figure 2.14A) nor deletion of the SIM motif from Ufd1 (Figure 2.14B) significantly affected *LacZ* transcription. Thus, SUMO does not contribute to the Cdc48-mediated transcription repression in this system. In addition to Ub, other features of the chromatin

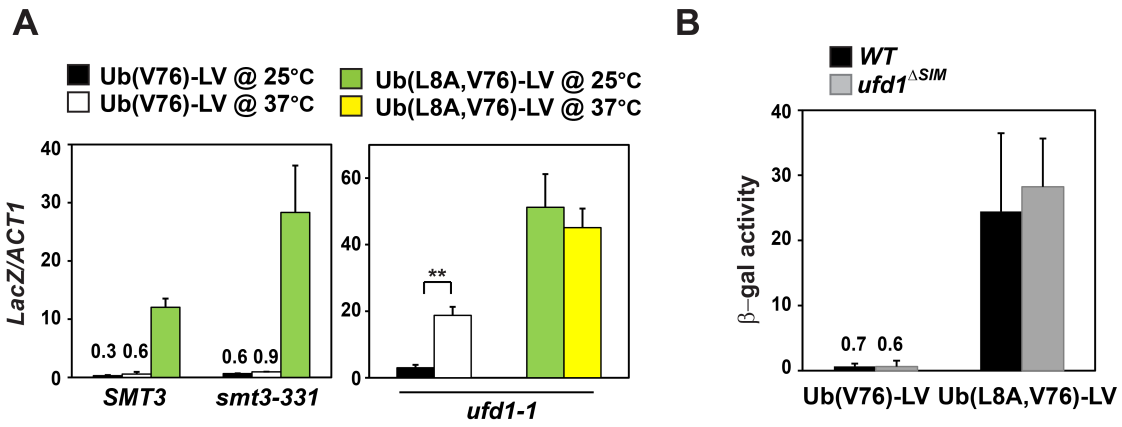

Figure 2.14. SUMO does not contribute to stripping of Ub(V76)-LV from DNA. (A) Yeast carrying a temperature-sensitive allele of SUMO, strain *smt3-331*, and its isogenic wild-type strain (*SMT3*) were transformed with a CEN plasmid containing the reporter gene *LacZ* and either the Ub(V76)-LV or Ub(L8A,V76)-LV transcription activator. Transformants were grown at the permissive temperature (25 °C) into log phase and then half of each culture was shifted to the non-permissive temperature (37 °C) for 30 min. Expression of the reporter gene was analyzed by qRT-PCR. No significant differences in Ub(V76)-LV-dependent *LacZ* expression were observed for *smt3-331* or *SMT3*; as expected, Ub(L8A,V76)-LV activated the reporter gene significantly in both strains. As a control, *LacZ* expression was analyzed similarly in the *ufd1-1* strain. The results are consistent with inhibitory roles for Ub and Ufd1 in Ub(V76)-LV-dependent transcription.
(B) Deletion of the SIM motif at the genomic *UFD1* locus was made as described (Bergink et al., 2013). Wild-type (YTY076) and *ufd1ΔSIM* (YTY616) yeast were transformed with a plasmid expressing either Ub(V76)-LV or Ub(L8A,V76)-LV, and transcription of the reporter gene in each strain was measured as β-galactosidase activity.

environment might help to recruit Cdc48 to the promoter. One possibility is that Cdc48 or its cofactor(s) has intrinsic affinity for naked DNA, which is commonly found at yeast UAS and promoter regions, as well as at sites of DNA damage. Low-affinity, non-specific interactions with DNA or chromatin in combination with specific interactions with Ub may explain how Cdc48 recognizes Ub(V76)-LV with high specificity. In addition, proteins involved in transcriptional regulation may interact with Cdc48 that, in combination with Ub, is able to recruit Cdc48 efficiently. Further studies will be required to explore these possibilities.

Although Ub is best known as a signal for protein degradation, non-proteolytic functions of Ub are gaining recognition. In the cases of the transcriptional activators described here, either degradation or non-proteolytic extraction by Cdc48 could, in principal, accomplish "down-regulation". Why, then, do these systems employ a non-proteolytic mechanism? Unlike ubiquitination coupled to degradation, ubiquitination coupled to non-proteolytic extraction has the potential advantage of preserving the functional activator protein. This latter scenario could facilitate rapid switching between "on" and "off" states of transcription. We expect that this mode of nonproteolytic extraction would be particularly useful when substantial new protein synthesis is difficult or detrimental. For example, in the yeast *MET* gene network, deubiquitination of Met4 could promote rapid activation of the pathway even when overall protein synthesis is limited by methionine depletion. Although the ubiquitination substrates we have described here all are transcription factors, we envision that Cdc48 can act similarly on other mono- or oligo-ubiquitinated proteins if an additional targeting element(s) is present.

CHAPTER 3: CHROMATIN REMODELING BY THE HUMAN INO80 COMPLEX

[3]Nucleosomes reduce the accessibility of DNA and inherently inhibit processes that involve DNA transactions, such as transcription, DNA repair, and DNA replication. Thus, eukaryotic cells have evolved mechanisms to modulate chromatin structure. The three primary modulators of chromatin dynamics are histone post-translational modifications (PTMs), histone variants, and ATP-dependent chromatin-remodeling enzymes. The INO80 complex is a chromatin-remodeler evolutionarily conserved from yeast to human. Previous studies with the yeast INO80 complex (yINO80) have shown that it can mobilize nucleosomes along DNA, i.e., slide nucleosomes, as well as catalyze the exchange of nucleosomal H2A.Z-H2B with free H2A-H2B dimers.

Here, we examine how histone variants or PTMs modulate the nucleosome sliding activity of the human INO80 complex (hINO80) *in vitro*. Our results suggest that nucleosomes containing H2A.Z or the H3 acetylation mimic (H3-K56Q) are mobilized by hINO80 with faster kinetics compared to canonical unmodified nucleosomes and their effects are additive. In contrast, ubiquitination of H2A or H2B has no significant effect. Given that nucleosomes containing H2A.Z and H3-K56Ac are frequently observed at promoters and DNA damage sites, our findings provide the first biochemical basis for the observed roles of hINO80 both in transcriptional regulation and DNA repair in mammalian cells.

[3] I heavily contributed to experimental conception, data collection and analysis of experiments presented in this chapter. Ben Schmitt carried out the experiments in Figures 3.1, 3.3D and 3.9 under my supervision. He also contributed to determination of the sliding rates for H3(K56Q) and H2A.Z/H3(K56Q) nucleosomes in Figure 3.7.

3.1 Introduction

The eukaryotic genetic material is packaged in the nucleus into arrays of nucleosomes. The canonical nucleosome includes 146 bp of DNA wrapped 1.65 times around an octameric histone core, comprised of two histone H2A-H2B dimers and one histone $(H3\text{-}H4)_2$ tetramer (Luger et al., 1997). Although packaging of DNA is necessary for maintaining its compaction in the nucleus, nucleosomes act as barriers for all DNA-related processes, including transcription, DNA replication and repair. As a consequence, eukaryotic cells have evolved different strategies to facilitate the assembly and disassembly of nucleosomes in a spatial and temporal regulated fashion. Among these strategies are the utilization of histone variants, histone PTMs and ATP-dependent chromatin remodelers (reviewed in (Bannister and Kouzarides, 2011; Becker and Horz, 2002; Gerhold and Gasser, 2014; Sevilla and Binda, 2014; Weber and Henikoff, 2014)). These strategies work cooperatively to maintain essential genomic functions required for cell identity and viability, at the same time create opportunities for cells to respond to the variable environment as needed. How histone variants, modifications and chromatin remodelers collaborate to elicit a defined biological response is still a major unanswered question in chromatin biology.

Ino80 is a member of the Snf2 family of helicase-like proteins that are ATP-dependent motors that drive many types of chromatin transactions (Flaus et al., 2006). In eukaryotic organisms ranging from yeast to man, Ino80 is part of a large multi-subunit complex that functions in transcription, DNA repair and DNA replication (reviewed in (Conaway and Conaway, 2009)). Genome-wide studies in *S. cerevisiae* have revealed that yINO80 regulates expression of ~20% of yeast genes (Jonsson et al., 2004; Mizuguchi et al.,

2004; van Attikum et al., 2004). *In vitro* biochemical characterization as well as *in vivo* genome-wide studies suggest that its function is intimately linked to the histone variant H2A.Z (Papamichos-Chronakis et al., 2011; Yen et al., 2013). *In vitro* yINO80 catalyzes the exchange of nucleosomal H2A.Z-H2B dimer with free H2A-H2B dimer (Papamichos-Chronakis et al., 2011). *In vivo* it localizes to the NFR (Nucleosome Free Region), which is flanked by nucleosomes enriched in H2A.Z (Yen et al., 2013). Yeast cells that lack Ino80 show global mislocalization of H2A.Z-containing nucleosomes (Papamichos-Chronakis et al., 2011). This can be seen as spurious incorporation of H2A.Z at some genomic loci in *Δino80*, together with the drop of H2A.Z incorporation at regions that are typically enriched in H2A.Z.

The biochemical properties of yINO80 suggest that its action antagonizes a related chromatin-remodeling complex SWR-C, which is also recruited to the NFR (Yen et al., 2013). SWR-C deposits H2A.Z by exchanging nucleosomal H2A-H2B dimers with free H2A.Z-H2B dimers (Luk et al., 2010). Interestingly, the +1 nucleosome, localized adjacent to the NFR, exhibits a higher turnover rate relative to all other nucleosomes across the genome (Dion et al., 2007; Yen at al., 2013). Therefore it has been suggested that, by localizing to the NFR, INO80 and SWR-C enhance adjacent nucleosome turnover via dynamic cycling of H2A.Z (Dion et al., 2007; Yen et al., 2013). This model implies that INO80 and SWR-C are recruited to the same NFR and +1 nucleosome turnover should decrease in the absence of either remodeler. Currently this evidence is lacking.

hINO80 contains a set of core subunits shared with yINO80 and several metazoan-specific subunits (Cai et al., 2007; Jin et al., 2005). Similar to yINO80, hINO80 has been reported to slide nucleosomes *in vitro* (Jin et al., 2005; Shen et al., 2000). However, to date

histone dimer exchange activity has not been demonstrated for hINO80. Functionally, it has been reported that hINO80 is required for self-renewal of mouse embryonic stem cells (ESCs), as well as for reprogramming and embryonic development (Wang et al., 2014). In ESCs, hINO80 selectively occupies promoters of core pluripotency genes and promotes their expression. Because, depletion of INO80 led to reduced DNaseI sensitivity at regions co-occupied by INO80 and ESC master transcription factors, such as Oct4, Nanog and Sox2, it suggests that INO80 promotes transcription by maintaining an open chromatin structure (Wang et al., 2014). How and whether hINO80 directly promotes open chromatin structure are not yet understood.

Promoters of actively transcribed genes in mammals contain nucleosomes that are enriched in both H2A.Z and acetylated H3 at K56 (Barski et al., 2007; Xie et al., 2009). Interestingly, H3K56Ac has a major impact on the H2A.Z exchange reactions *in vitro*. This modification abrogates the specificity of ySWR-C, leading to promiscuous exchange of H2A.Z and H2A (Figure 1.6C) (Watanabe et al., 2013). In the case of yINO80, H3K56Ac stimulates replacement of nucleosomal H2A.Z with H2A. Whether similar observations will apply to mammalian INO80 and mammalian histones remains unclear. Nevertheless, interplay between H2A.Z and H3K56Ac is likely to have a major impact on nucleosome dynamics at mammalian gene promoters.

In an effort to understand how hINO80 regulates transcription, we have characterized the nucleosome sliding activity of hINO80 and examined how histone variant H2A.Z and PTMs modulate its activity, including H2A ubiquitination, H2B ubiquitination and H3K56 acetylation. We found that hINO80 mobilizes nucleosomes containing H2A.Z or H3K56Q significantly faster than canonical unmodified nucleosomes in an ATP-dependent

manner. In contrast, ubiquitination of H2A and H2B had little effect. Interestingly, the effects of H2A.Z and H3K56Q are additive, leading to ~13-fold faster sliding rate than canonical unmodified nucleosomes. These findings have strong mechanistic implications in the function of hINO80 in transcription and DNA repair events.

3.2 Experimental procedures

3.2.1 Immunoaffinity purification of the hINO80 complex

The hINO80 complex was immunoaffinity purified from cells stably expressing the Flag-tagged hINO80 subunits CCDC95 or Ies2. Generation of these stable cell lines and preparation of nuclear extracts have been previously described (Cai et al., 2006; Yao et al., 2008). Once thawed, the nuclear extract was diluted with Buffer A (10 mM HEPES, pH 7.9, 1.5 mM $MgCl_2$, 10 mM KCl and freshly added 0.5 mM DTT, 200 μM PMSF and Protease Inhbitors) in order to adjust the salt concentration to 0.3 M, and clarified by ultracentrifugation at 100,000x*g* for 30 min at 4 °C. Anti-Flag (M2) agarose (Sigma) was equilibrated with Flag Wash Buffer (Buffer A supplemented with 0.3 M NaCl and 0.2% Triton-X-100) before incubation with the nuclear extract with rotation overnight. The resin was then washed four times with Flag Wash Buffer and once with Elution Base Buffer (10 mM Na HEPES, pH 7.9, 1.5 mM $MgCl_2$, 0.1 M NaCl, 0.05% Triton-X-100, 0.2 mM EDTA, 0.5 mM DTT and 5% glycerol). Bound proteins were eluted by incubation with 0.2 mg/ml 3xFlag peptide in Elution Base Buffer for 30 min at 4 °C; elution was repeated three times and the eluates were combined, supplemented with 2 mM DTT and flash frozen in liquid nitrogen. The quality of purified hINO80 complex was evaluated by SDS-PAGE and silver-staining (Figure 3.1A), whereas the quantity was determined by immuno-blotting with

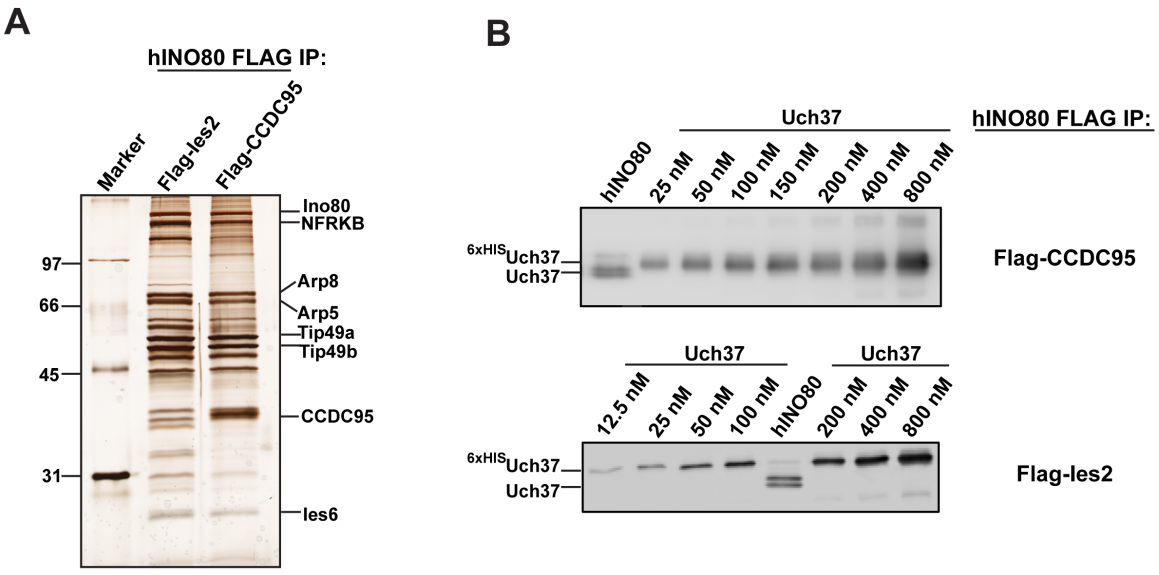

Figure 3.1. Purification of the human INO80 complex.
(A) hINO80 complex was affinity-purified through Flag-CCDC95 or Flag-Ies2 subunit from HeLa nuclear extracts and analyzed by SDS-PAGE and silver-staining. **(B)** Concentrations of the purified hINO80 complexes were determined based on the amount of Uch37 subunit, which was determined by western-blotting, using recombinant ^{6xHIS}Uch37 as standards.

anti-Uch37 antibodies and known quantities of recombinant Uch37 as quantitation standards (Figure 3.1B).

3.2.2 DNA-dependent ATPase assay

Because INO80 is an ATP-dependent chromatin remodeler, determination of its ATPase activity allows us to normalize the activity of hINO80 from different preps. A 207 bp DNA fragment was used to stimulate hINO80 ATPase activity, which was monitored using a fluorescent phosphate sensor, 7-Diethylamino-3-(((2-maleimidyl)-ethyl)amino)carbonyl) coumarin-labeled phosphate binding protein (MDCC-PBP) (Figure 3.2A) (Brune et al., 1994). Upon inorganic phosphate (Pi) binding, the fluorescence of MDCC-PBP increases and can be monitored continuously using a BioTek Synergy microplate reader (λ ex = 430 nm, λ em = 460 nm). The ATP was pre-treated with "Pi-mop"(0.04 units/ml purine nucleoside phosphorylase (PNPase) and 0.1 mM 7-methylguanosine (7-MEG)). 0.5 μM MDCC-PBP was incubated with 40 μM ATP in Reaction Buffer (25 mM HEPES, pH 7.6, 0.5 mM EGTA, 100 mM NaCl, 0.1 mM EDTA, 0.02% NP-40, 0.1 mg/ml BSA, 2 mM $MgCl_2$, 5% glycerol) for 15 min at 25°C. hINO80 was added at a concentration of 2 nM and incubated for 15 min at 25°C. 15 nM 207mer was added to stimulate the ATPase activity of hINO80. The increase in fluorescence was monitored continuously for up to 20 min (Figure 3.2B).

3.2.3 Generation of ubiquitinated histone mimics

Human recombinant histones H2A, H2A.Z, H2B, H3, H3.3, H4 and the site-specific histone mutants (H2A K119C, H2B K120C, H2A.Z K121C, H3 K56Q) were expressed and

purified as described (Dyer et al., 2004). Point mutations were made using the QuickChange® II XL Site-Directed Mutagenesis Kit (Stratagene) and verified by sequencing. Generation of ubiquitin-histone mimics was previously described (Long et al., 2014a).

3.2.4 Generation of labeled DNA for nucleosome assembly

The 216 bp DNA fragment, containing a lateral 601 positioning sequence (147 bp) and labeled with the fluorophore Cy5 or Atto532 (Figure 3.3C), was obtained by PCR amplification using the following primers:

Forward primer: 5' Cy5/Atto532-ACAGGATGTATATATCTGACACGTGCCTGG 3'

Reverse primer: 5' TGACCAAGGAAAGCATGATTCTTCACAC 3'

1 ng of pGEM 601 was used as template in a 100 µl PCR reaction containing 450 nM of each forward and reverse primers, 0.2 mM dNTPs, 5 µl DMSO, 1X Choice Taq buffer and 0.5 µl Choice Taq Polymerase (Denville). The amplification cycle was as follows:

1. Initial denaturation: 4 min at 94 °C
2. Denaturation: 30 sec at 94 °C
3. Annealing: 30 sec at 61 °C
4. Extension: 30 sec at 72 °C
    - Repeat steps 2-4 35 times
5. Final extension: 10 min at 72 °C
6. Cooling: hold at 12 °C

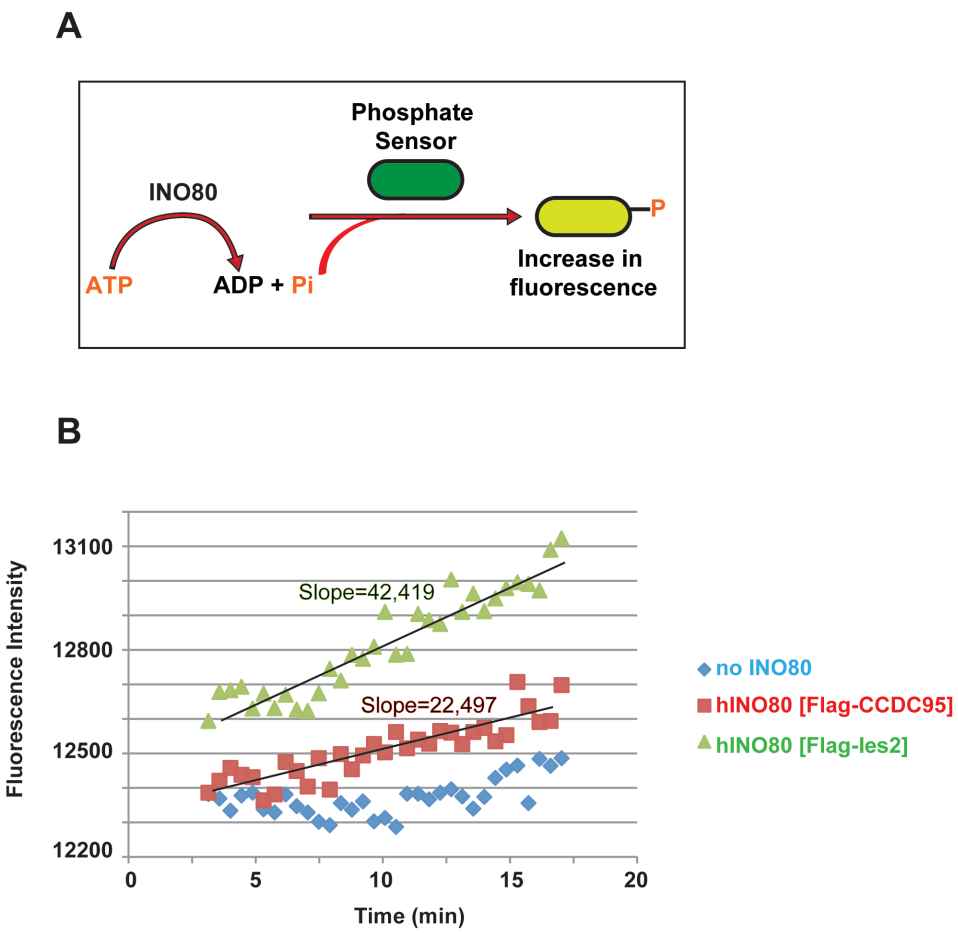

Figure 3.2. Determination of the ATPase activity of purified INO80 using a fluorescently-labeled phosphate sensor.
(A) ATP is hydrolyzed by INO80 into ADP and inorganic phosphate. Upon binding inorganic phosphate, fluorescence of the phosphate sensor (MDCC-PBP) increases and can be followed in real time. **(B)** Representative DNA-dependent ATPase assays were performed as described in Experimental procedures (3.2.2). The relative ATP-hydrolysis rates were determined by the slopes of fluorescence increase over time.

Typically, 50 PCR reactions were carried out and the products were purified on a Mono-Q column using a 0.5-1 M linear NaCl gradient over 40 column volumes in 20 mM Tris, pH 7.5, 0.1 mM EDTA. The Cy5-labeled 216 bp DNA fragment typically elutes at 0.8 M NaCl (Figure 3.3D). Peak fractions were combined and DNA was precipitated by adding 2.5 time of 100% ethanol, adjusting salt concentration to 0.3 M with NaOAc, followed by incubation at -20 °C for 2h. After incubation, the solution was transferred into 1.7 ml eppi tubes and centrifuged at 13,000 rpm for 30 min at 4 °. DNA pellets were washed twice with 70% ethanol, air dried, and resuspended in TE buffer (10 mM Tris, pH 8.0, 0.1 mM EDTA) to a final concentration of 30 μM.

3.2.5 Octamer and nucleosome assembly

Reconstitution of histone octamers containing Ub-histone mimics—Reconstitution of histone octamers was done as previously described by Dyer at al. (Dyer et al., 2004). Briefly, each lyophilized histone was dissolved in Unfolding Buffer (6 M guanidinium hydrochloride, 20 mM Tris pH 7.5, 5 mM DTT) to a concentration of approximately 50 mg/ml. Unfolding was allowed to proceed for 1 h prior to determining protein concentration by measuring the absorbance at 276 nm. For the Ub*histone mimic, as the eluates from the nickel column contain a mixture of Ub-containing species, the concentration of Ub*histone mimic was estimated by SDS-PAGE and Coomassie staining. Histone proteins were mixed at equal molar ratio to a final protein concentration of approximately 2 mg/ml, and dialyzed at 4 °C against at least three changes of 600 ml of Refolding Buffer (10 mM Tris pH 7.6, 2 M NaCl, 1 mM EDTA, 5 mM βME).

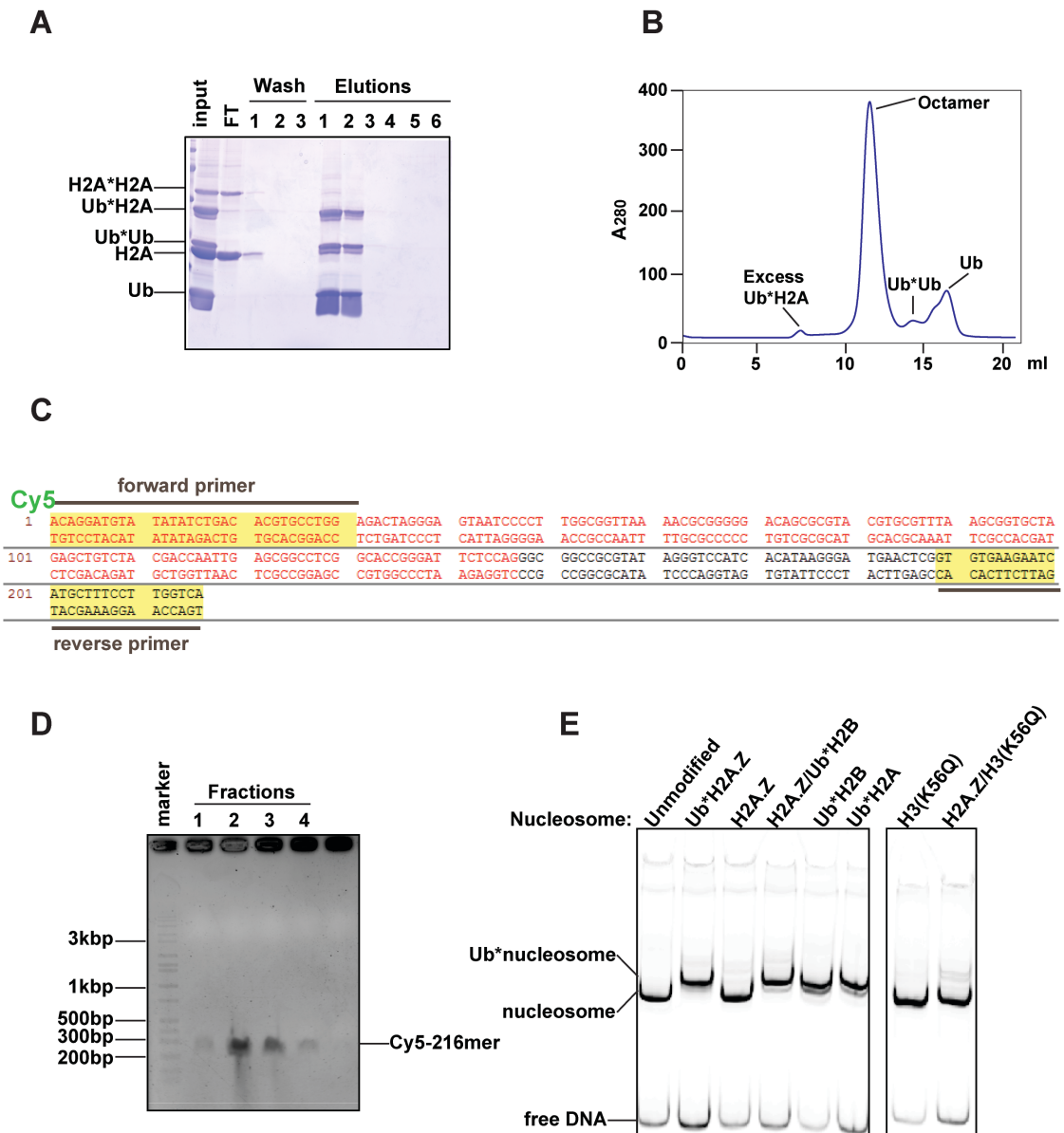
A
input
FT
Wash
1 2 3
Elutions
1 2 3 4 5 6
H2A*H2A
Ub*H2A
Ub*Ub
H2A
Ub
B
A280
400
300
200
100
0
0
5
10
15
20
ml
Octamer
Excess
Ub*H2A
Ub*Ub
Ub
C
Cy5
forward primer
1 ACAGGATGTA TATATCTGAC ACGTGCCTGG AGACTAGGGA GTAATCCCCT TGGCGGTTAA AACGCGGGGG ACAGCGCGTA CGTGCGTTTA AGCGGTGCTA
TGTCCTACAT ATATAGACTG TGCACGGACC TCTGATCCCT CATTAGGGGA ACCGCCAATT TTGCGCCCCC TGTCGCGCAT GCACGCAAAT TCGCCACGAT
101 GAGCTGTCTA CGACCAATTG AGCGGCCTCG GCACCGGGAT TCTCCAGGGC GGCCGCGTAT AGGGTCCATC ACATAAGGGA TGAACTCGGT GTGAAGAATC
CTCGACAGAT GCTGGTTAAC TCGCCGGAGC CGTGGCCCTA AGAGGTCCCG CCGGCGCATA TCCCAGGTAG TGTATTCCCT ACTTGAGCCA CACTTCTTAG
201 ATGCTTTCCT TGGTCA
TACGAAAGGA ACCAGT
reverse primer
D
marker
Fractions
1 2 3 4
3kbp
1kbp
500bp
300bp
200bp
Cy5-216mer
E
Nucleosome:
Unmodified
Ub*H2A.Z
H2A.Z
H2A.Z/Ub*H2B
Ub*H2B
Ub*H2A
H3(K56Q)
H2A.Z/H3(K56Q)
Ub*nucleosome
nucleosome
free DNA

Figure 3.3. Synthesis and purification of ubiquitin histone-mimics and preparation of ubiquitinated nucleosomes.
(A) Histone H2A(K119C) was crosslinked with ^{6xHIS}Ub(G76C) as described in Experimental procedures (3.2.4). Unreacted histones were removed Ni-NTA purification. Fractions from the nickel purification were analyzed by SDS-PAGE and Coomassie blue staining. FT: flow-through**. (B)** HPLC chromatogram of purification of Ub*H2A/H2B/H3/H4 octamers. Reconstituted histone octamers were injected on a Superdex 200 column. Absorbance at 280 nm was monitored over time and eluates were analyzed by SDS-PAGE and Coomassie blue staining. The ubiquitinated octamer eluted at ~12.5 ml. The Ub* H2A in excess, Ub*Ub and Ub were eluted at ~7.5 ml, ~14 ml and ~17 ml, respectively. **(C)** Schematic of the 216 bp DNA sequence used in nucleosome reconstitution for sliding experiments. The 601 positioning sequence is laterally positioned (colored in red). Forward and reverse primers used for amplification are highlighted in yellow. The forward primer is labeled with the Cy5 (or Atto532) fluorophore at the 5' end. **(D)** Cy5 end-labeled 216 bp DNA containing a lateral 601 positioning sequence were amplified by PCR and purified by anion-exchange HPLC on a Mono Q column. Peak fractions were analyzed by agarose gel electrophoresis and ethidium bromide staining. **(E)** Purified histone octamers were assembled into mononucleosomes with the 216mer DNA by salt dilution. The ratio of octamer:DNA was previously optimized to minimize the amounts of free DNA. The percentage of free DNA in these nucleosome preparations was typically 1-2%.

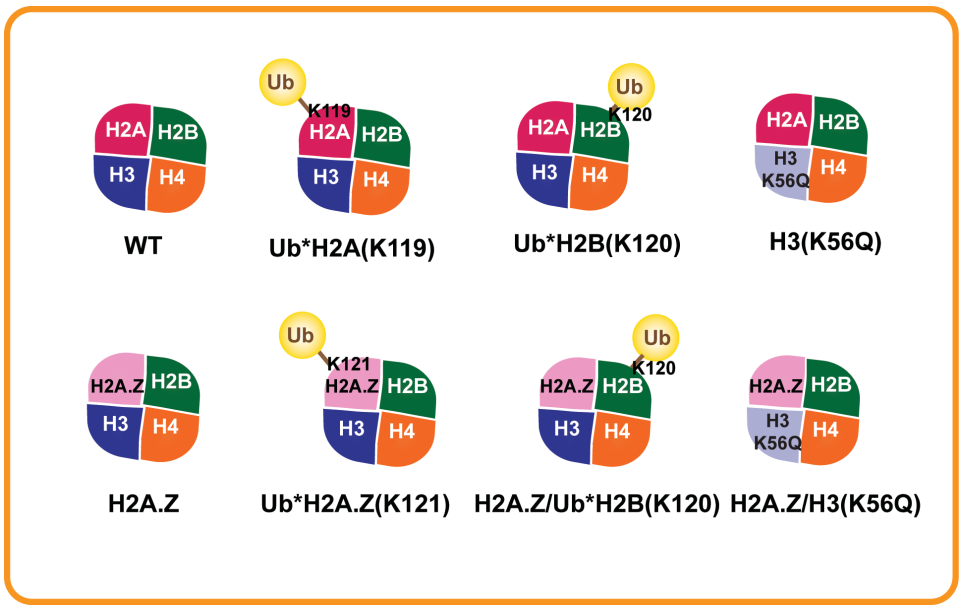

Figure 3.4. Illustration of the different nucleosomes used in sliding assays. Ubiquitinated histones were obtained by crosslinking ubiquitin to the indicated histones as described in (Long et., 2014a). * denotes the crosslink. All histones used in this study are recombinant human histones expressed and purified from *E. Coli.* For the purpose of this thesis, "WT" denotes nucleosomes containing human H2A, H2B, H3.3 and H4 histone. The H3.3 variant is always used because it is typically found in transcriptionally active regions of the genome.

After refolding, histone octamers were purified by gel filtration on a Superdex 200 column. High molecular weight aggregates elute in the void volume, whereas the much smaller Ub and Ub*Ub species elute later (Figure 3.3B). Purified octamers were concentrated to approximately 30-50 μM, supplemented with glycerol to 20% v/v, flash frozen in liquid nitrogen and stored at -80 °C in small aliquots.

Assembly of mononucleosomes—In vitro reconstitution of nucleosomes relies on the sequential binding of one $(H3\text{-}H4)_2$ tetramer and two H2A-H2B dimers onto the DNA. This may be achieved by salt gradient deposition or chaperone-assisted assembly. We employed the salt dilution method as described by McGinty at al. (McGinty et al., 2008). Reactions contain octamer and DNA mixed at a specific molar ratio at 2 M NaCl concentration, which was then diluted in the Initial Dilution Buffer (IDB) (10 mM Tris, pH 7.6, 1 mM EDTA, 1 mM DTT, 0.1 mg/ml BSA) in a stepwise fashion. To gradually lower the salt concentration, we added the following volumes of IDB to a 10 μl reaction, every 15 min, while incubating at 30°C: 3.3 μl, 6.7 μl, 5 μl, 3.6 μl, 4.7 μl, 6.7 μl, 10 μl, 30 μl and 20 μl to a salt concentration of 200 mM. Subsequently, the reaction was diluted two-fold with the Final Dilution Buffer (FDB) (10 mM Tris, pH 7.6, 1 mM EDTA, 20% glycerol, 0.1% NP-40, 0.1 mg/ml BSA), resulting a final salt concentration of 100 mM. An initial concentration of 2 μM DNA and octamer were typically used. Titrations of DNA:octamer ratios at 1:1, 1:1.1, 1:1.2, 1:1.3, 1:1.4, 1:1.5 and 1:1.6 were performed to determine the ideal ratio for different types of nucleosomes. Assembled nucleosomes were evaluated by a 6% TBE native gel electrophoresis and visualized by scanning on the Typhoon FLA 7000 instrument with excitation at 635 nm (for Cy5) or 532 nm (for Atto532) (Figure 3.3E).

3.2.6 ATP-dependent nucleosome sliding assay

To measure the ATP-dependent chromatin remodeling activity of INO80, we employed mononucleosomes assembled on Cy5-labeled 216 bp DNA fragments containing a 601-positioning sequence at one end of the DNA. The mononucleosome substrate (20 nM) was incubated with hINO80 (1 or 2 nM) and 1 mM ATP at 30 °C for varying amounts of time in a buffer containing 20 mM HEPES, pH 7.9, 50 mM NaCl, 10 mM $MgCl_2$, 2 mM DTT, 0.5 mM AEBSF, 100 μg/ml BSA, 10% glycerol and 0.05% Nonidet P-40. The reactions were terminated by addition of 0.3 mg/ml salmon sperm DNA, which competes with nucleosomes in binding to hINO80. 6% TBE native mini-gels (37.5:1 acrylamide:bis-acrylamide) were pre-run at 4 °C for 15 min at 125V in 0.2XTBE (45 mM Tris-borate, 1 mM EDTA). The reactions were then loaded on these gels, electrophoresed at 4 °C for 2.5 h at 125V, and visualized by scanning on the Typhoon™ FLA 9500 instrument at 635 nm (for Cy5) and 532 nm (for Atto532).

The position of the nucleosome on the 216 bp DNA affects electrophoretic mobility; laterally positioned nucleosomes migrate faster in the gel than more centrally positioned nucleosomes. Since INO80 chromatin remodeling complexes preferentially move mononucleosomes toward the center of a DNA fragment, remodeling activity can be readily monitored by the emergence of a population of nucleosomes that exhibits decreased electrophoretic mobility (Figure 3.4A).

Quantification of nucleosome remodeling gels—To determine the rate of sliding, the fluorescent intensities of nucleosome bands were quantified using ImageQuant (GE Life Sciences). Because some sliding products migrate closely to the starting material, we found

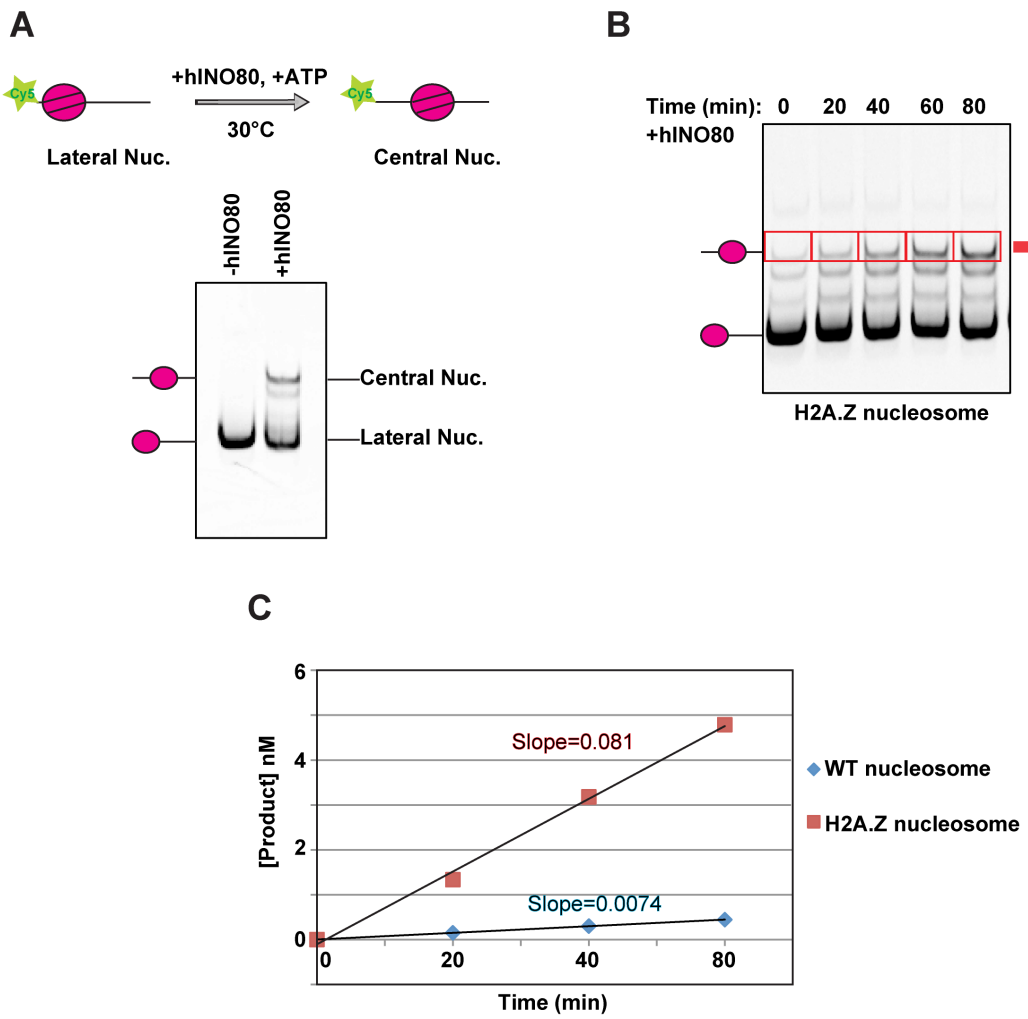

Figure 3.5. Nucleosome sliding by hINO80.
(A) hINO80 mobilizes nucleosomes from the lateral position towards the central position on a 216mer DNA in the presence of ATP. Nucleosome mobilization, i.e. sliding, can be monitored by 6% native-PAGE. Laterally positioned nucleosomes migrate faster than more centrally positioned nucleosomes. **(B)** A typical time-course of the sliding assay. The slowest migrating band (highlighted by a red box) represents centrally positioned nucleosomes that are used to monitor the rate of sliding. **(C)** For each time point, the percentage of central nucleosomes in each lane was quantified by fluorescence intensity. By plotting the amounts of central nucleosomes generated over time, the rate of sliding corresponds to the slope of the linear phase of the reaction.

that monitoring the top band, which represents the centrally positioned nucleosome, was most reproducible and its intensity increases linearly over time (Figure 3.4B). For the purpose of comparison, for each lane we quantified the intensity of the top band, normalized against the total nucleosome fluorescence, and calculated the amounts of centrally positioned nucleosome at each time point. These were plotted against time and fitted with a linear equation. The rate of sliding (nM/min) was the slope of the linear phase of the time course (Figure 3.4C). Sliding reactions with each nucleosome substrate were performed at least twice, with both hINO80 purified via Flag-CCDC95 and Flag-Ies2 subunit. The average and standard deviation of the rate obtained were plotted in Figure 3.7.

3.3 Results

hINO80 was immuno-purified from two different cell lines, stably expressing Flag-tagged versions of INO80 subunits CCDC95 or Ies2 (Figure 3.1A). Prior to the analysis for sliding activities, the protein concentration of hINO80 was determined by quantitative western blotting (Figure 3.1B). Additionally, we determined the DNA-dependent ATP hydrolysis activity for each preparation and normalized the amount of hINO80 based on its ATPase activity (Figure 3.2). Sliding assays with different nucleosomal substrates were performed at least twice with at least two different preparations of hINO80.

Previously, it was reported that yINO80 preferentially binds to nucleosomes with extranucleosomal DNA (> 20 bp) with an observed dissociation constant (K_d) of approximately 10 nM (Udugama et al., 2011). This affinity does not increase with longer lengths of extranucleosomal DNA, or when the extranucleosomal DNA is present on both

sides of the nucleosome core particle. However, 70 bp of extranucleosomal DNA are necessary for optimal nucleosome mobilization (Udugama et al., 2011). Therefore, we reconstituted the nucleosome substrates on a 216 bp DNA fragment with a lateral 601 positioning sequence (147 bp) (Figure 3.3C).

3.3.1 Ubiquitination of H2A or H2B does not affect the sliding activity of hINO80

Mono-ubiquitination of H2A or H2B in their C-terminal tails is involved in the regulation of transcription. Whereas mono-ubiquitination of H2A at lysine 119 has been associated with gene silencing (Fang et al., 2004), mono-ubiquitination of H2B at lysine 120 is mainly coupled to transcription activation (Nakanishi et al., 2009). In metazoans, the INO80 complex harbors a deubiquitylase subunit, Uch37 (Yao et al., 2008). The physiological substrate of Uch37 is not known and is a subject of intense study in our lab. Thus, we tested whether ubiquitination of histones modulate hINO80-mediated mobilization of nucleosomes.

Ubiquitinated histones can be obtained by *in vitro* ubiquitination using purified E1, E2 and cognate E3 enzymes or by purification from large number of cells. These strategies typically have low yields and the products obtained often are contaminated with non-specific ubiquitinated products or additional PTMs that are present on native histones. To circumvent these difficulties, we used a method that takes advantage of a highly reactive bifunctional thiol crosslinker, 1,3-dichloroacetone (Long et al., 2014a). Since neither Ub nor H2A or H2B contain naturally occurring cysteine residues, site-specific crosslinking can be implemented by introducing a cysteine at the C-terminus of Ub (G76C) and the native ubiquitination site of H2A (K119C) or H2B (K120C). The crosslinked product contains an

additional carboxylate group and is one C-C bond longer compared to the native isopeptide bond. These Ub-histone mimics (denoted Ub*histone) can be purified to homogeneity and assembled into octamers and nucleosomes (Figure 3.3).

Purified hINO80 mobilizes nucleosomes from a lateral position on the 216 bp DNA fragment to more central positions in an ATP-dependent manner, as previously reported (Figure 3.5A and data not shown). We found that nucleosomes containing either Ub*H2A or Ub*H2B were mobilized by hINO80 with similar rates as unmodified nucleosomes (Figure 3.6A and 3.7). These results suggest that, although Ub is a bulky modification, it does not affect how hINO80 interact or mobilize nucleosomes.

3.3.2 hINO80 slides H2A.Z and H3K56Q-containing nucleosomes with faster kinetics

Given the genetic evidence that links yINO80 to localization of H2A.Z across the yeast genome, we proposed to study mobilization of H2A.Z-containing nucleosomes by the hINO80 complex *in vitro*. We found that hINO80 slides H2A.Z-containing nucleosomes ~8-fold faster than canonical nucleosomes (Figure 3.6C and 3.7). In order to distinguish whether the difference in mobilization was due to higher affinity of hINO80 for H2A.Z-containing nucleosomes or to faster catalysis, we employed a competition-sliding assay. In this assay, differentially labeled nucleosomes (Cy5-H2A.Z nucleosome and Atto532-WT nucleosome) were incubated with hINO80 individually or simultaneously, and the sliding rate was determined. When both nucleosomes were incubated with hINO80, there was a 50% reduction in the sliding rate for each type of nucleosome (Figure 3.8). This result

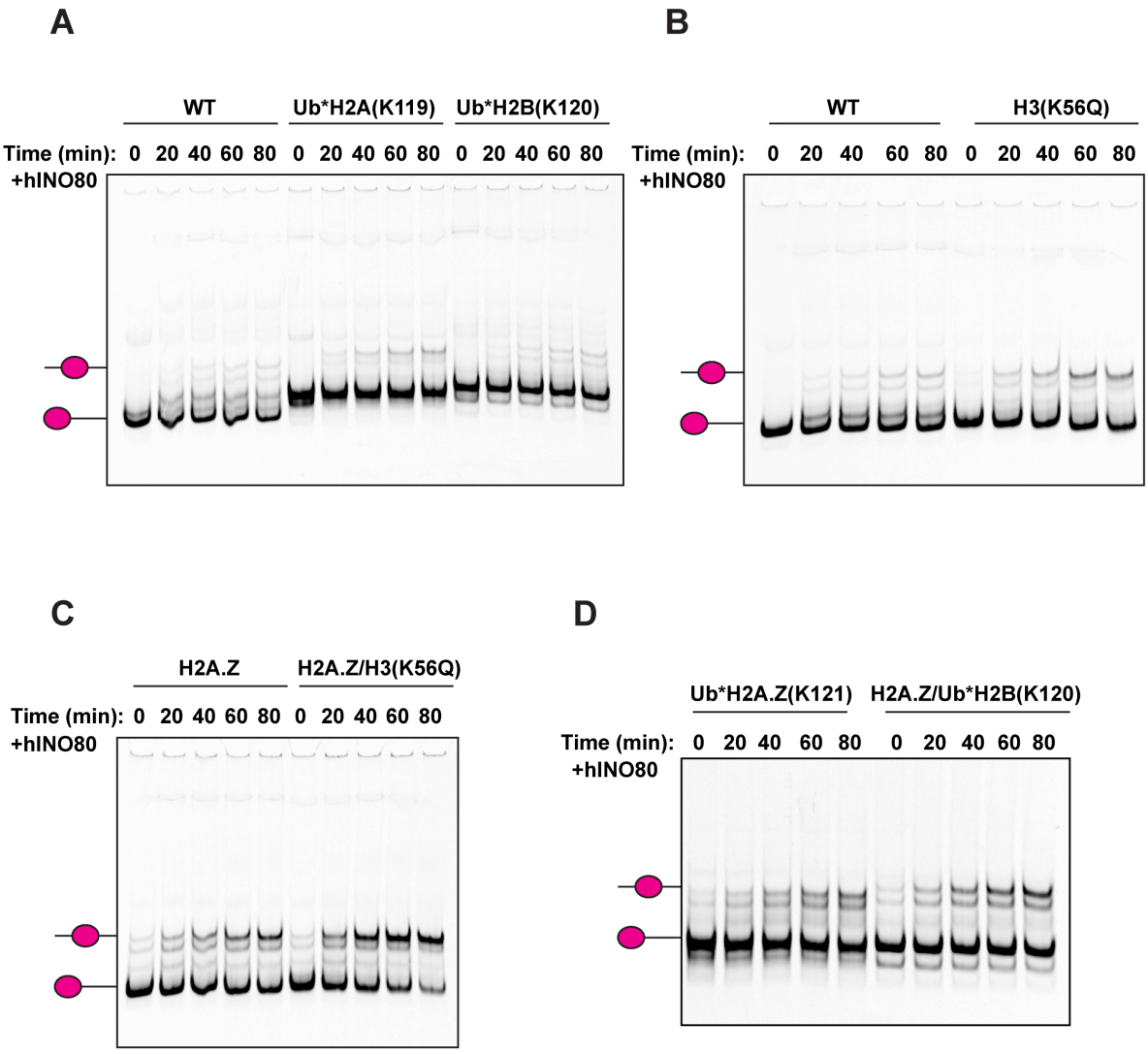

Figure 3.6. Histone modifications and variants have different effects on nucleosome sliding by hINO80.
(A) Nucleosome sliding assays were performed as described in Experimental procedures (3.2.6). WT, Ub*H2A(K119) or Ub*H2B(K120) nucleosomes were mobilized by hINO80 with similar kinetics. **(B)** Nucleosomes containing the acetylation mimic H3K56Q were mobilized by hINO80 ~5 times faster than WT nucleosomes. **(C)** H2A.Z nucleosomes were mobilized by hINO80 ~8 times faster than WT nucleosomes (compare with panel A). H3K56Q further enhances sliding of H2A.Z nucleosomes by hINO80. **(D)** Ub*H2A.Z(K121) or Ub*H2B(K120) inhibits sliding of H2A.Z nucleosomes by hINO80.

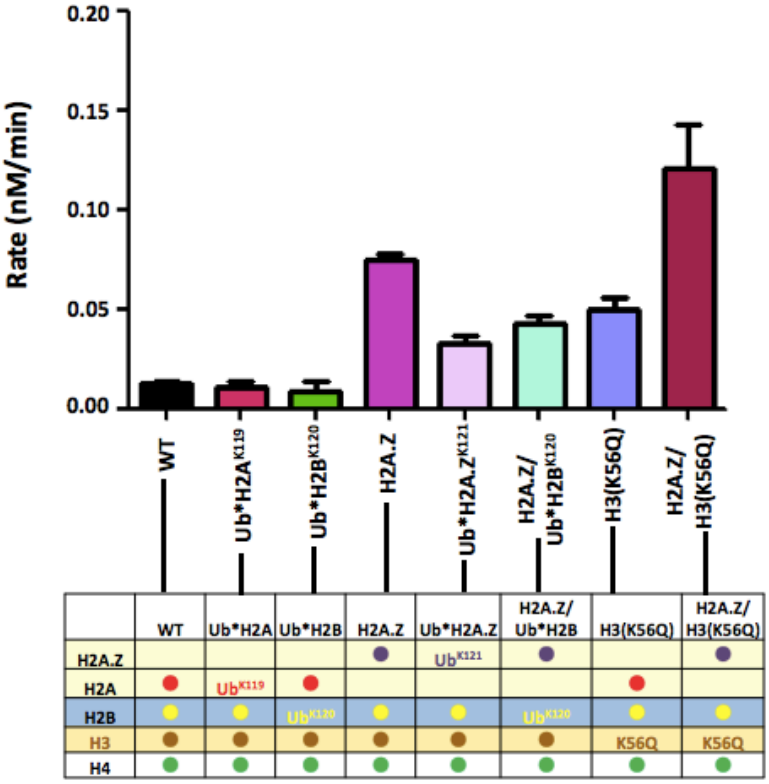

Figure 3.7. Summary of hINO80 sliding rates with different types of nucleosomes. The rate of formation of centrally positioned nucleosomes was measured as described in Experimental procedures (3.2.6) and Figure 3.4. Sliding reactions with each nucleosome substrate were performed at least twice, with both hINO80 purified via Flag-CCDC95 or Flag-Ies2 subunit. Shown are the average and standard deviation of the rates obtained.

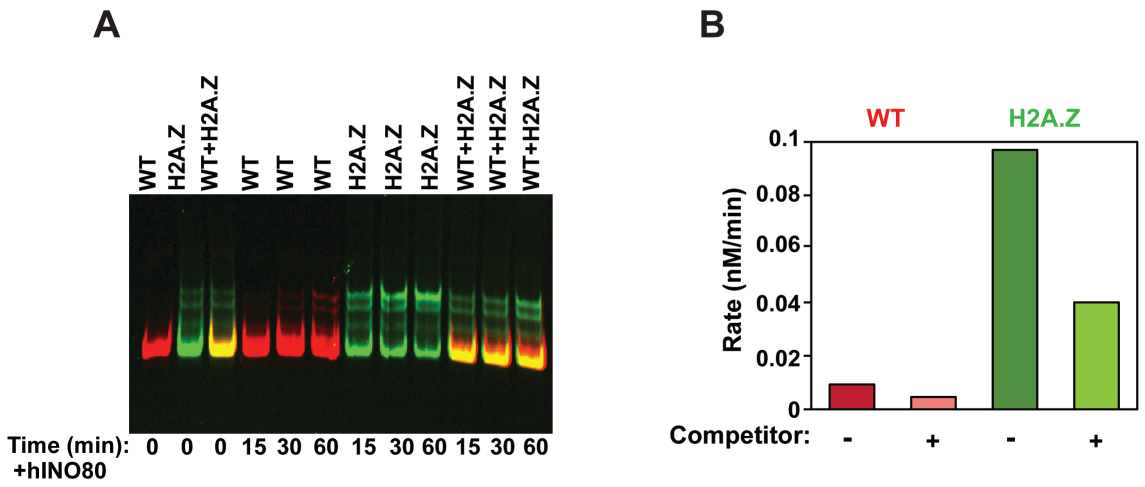

Figure 3.8. The increased sliding rate for H2A.Z nucleosomes is due to faster catalysis by hINO80.
(A) WT nucleosomes (red) were reconstituted with Atto532-labeled 216 bp DNA, whereas the H2A.Z nucleosomes (green) were reconstituted with Cy5-labeled 216 bp DNA. These nucleosomes (20 nM) were incubated with hINO80 (2 nM) individually or together sliding rate was measured for each type of nucleosome. **(B)** Shown are the sliding rates of each type of nucleosome, either when assayed by itself (- competitor) or mixed with the other type (+ competitor). When WT and H2A.Z nucleosomes were present at equal amounts, a 50% reduction in the rate of product was observed with each nucleosome, suggesting hINO80 binds WT and H2A.Z nucleosomes indiscriminately.

suggests that the faster mobilization observed for H2A.Z-containing nucleosomes is due to faster catalysis, rather than higher nucleosome binding affinity of hINO80.

Acetylation of H3K56 stimulates the dimer exchange activity of yINO80 *in vitro* (Watanabe et al., 2013). In order to unravel whether H3K56Ac modulates the nucleosome sliding activity of hINO80, we assembled nucleosomes containing H3 with a glutamine residue at position 56 to mimic acetylation (H3K56Q). We found that hINO80 slides H3(K56Q)-containing nucleosomes ~5-fold faster compared to unmodified nucleosomes (Figure 3.6B and 3.7). The observed stimulatory effect could be essential for efficient mobilization of nucleosomes harboring this PTM at gene promoter regions.

Previous work indicates that gene promoters in mammals are enriched in nucleosomes harboring both H2A.Z and H3K56Ac (Barski et al., 2007; Xie et al., 2009). Therefore, we proposed to assay sliding of nucleosomes harboring both H2A.Z and H3(K56Q), for possible cooperation. We found that sliding by hINO80 of H2A.Z/H3(K56Q)-containing nucleosomes was ~13-fold faster compared to that of canonical unmodified nucleosomes (Figure 3.6C and 3.7). Nucleosome sliding for H2A.Z or H3(K56Q)-containing nucleosomes is 8 and 5-fold faster than canonical unmodified nucleosomes, respectively. Thus, when these marks are present simultaneously the enhancement of the sliding activity of hINO80 is additive.

3.3.3 Ubiquitination of H2A.Z significantly inhibits nucleosome sliding by hINO80

Reminiscent of the canonical histone H2A, which is ubiquitinated on lysine 119, the H2A.Z variant is ubiquitinated at lysine 121 by the E3 ligase Ring1B, subunit of the polycomb repressive complex 1 (PRC1) in mammals (Cao et al., 2005). The mono-

ubiquitinated H2A.Z has been found to be deubiquitinated by Usp10 (Draker et al., 2011). Cellular localization experiments highlight that Ub-H2A.Z is found at transcriptionally silent facultative heterochromatin on the inactive X chromosome (Sarcinella et al., 2007), suggesting Ub-H2A.Z is a silencing mark. Furthermore, silencing of Usp10 results in elevated levels of Ub-H2A.Z, whereas loss of Ub-H2A.Z at *KLK3* and *PSA* promoters correlates with transcriptional activation (Draker et al., 2011). We found that hINO80 mobilized nucleosomes containing Ub*H2A.Z(K121) ~2 to 3-fold slower than H2A.Z-containing nucleosomes (Figure 3.6D and 3.7). Interestingly, nucleosomes containing H2A.Z in combination with Ub*H2B(K120) were also remodeled 2-fold slower compared to H2A.Z/H2B-containing nucleosomes (Figure 3.6D and 3.7). This suggests that, not only ubiquitination of H2A.Z, but also ubiquitination of other histones in H2A.Z-containing nucleosomes, decreases the sliding rate by hINO80. Ubiquitination of H2A.Z could provide a useful regulatory mechanism for establishing silencing chromatin loci, which could be promptly reversed by deubiquitination, followed by faster mobilization.

3.3.4 yISW1 remodels H2A or H2A.Z containing nucleosomes similarly

In order to investigate whether faster sliding kinetics of H2A.Z-containing nucleosomes is a unique property of hINO80, we performed similar assays with two remodeler complexes purified from yeast: yINO80 and yISW1. Like INO80, the ISWI family of remodelers also slides nucleosomes from lateral to central positions. They have been reported to function as molecular rulers for DNA linker length and position nucleosome arrays in regular spacing *in vitro* (Chaban et al., 2008; Dechassa et al., 2008; Yamada et al., 2011).

Purified yINO80 has very poor sliding activity with WT nucleosomes, which contain recombinant human histones. However, it slides H2A.Z-containing nucleosomes with similar efficiency as hINO80. This leads to a ~35 fold-difference in sliding rates between WT and H2A.Z nucleosomes with yINO80 (Figure 3.9A and 3.9C). We also observed an additive effect when H2A.Z and H3(K56Q) were combined in the same nucleosome (Figure 3.9A). In contrast, we did not observe a significant difference in remodeling of WT and H2A.Z nucleosomes by yISW1 (Figure 3.9B and 3.9C). These results strongly argue that the increased mobilization of H2A.Z-containing nucleosomes by INO80 is not due to an inherent property of H2A.Z nucleosomes. Rather, specific interactions between H2A.Z and INO80 likely account for more efficient remodeling.

It is important to keep in mind that *in vitro* reconstituted nucleosomes are homotypic, namely containing two copies of H2A.Z (H2A.Z/H2A.Z). *In vivo,* aside from homotypic nucleosomes there are also heterotypic nucleosomes, containing one copy of H2A.Z and one copy of H2A (H2A.Z/H2A). A detailed study in *Drosophila* has shown that homotypic nucleosomes are enriched at promoter regions and just downstream of the TSS of actively transcribed genes, whereas heterotypic nucleosomes are mainly found within gene bodies (Weber et al., 2010). This suggests that homotypic and heterotypic nucleosomes have distinctive properties and might facilitate different steps of transcription. Therefore, it would be interesting to investigate the sliding activity of hINO80 with heterotypic nucleosome substrates.

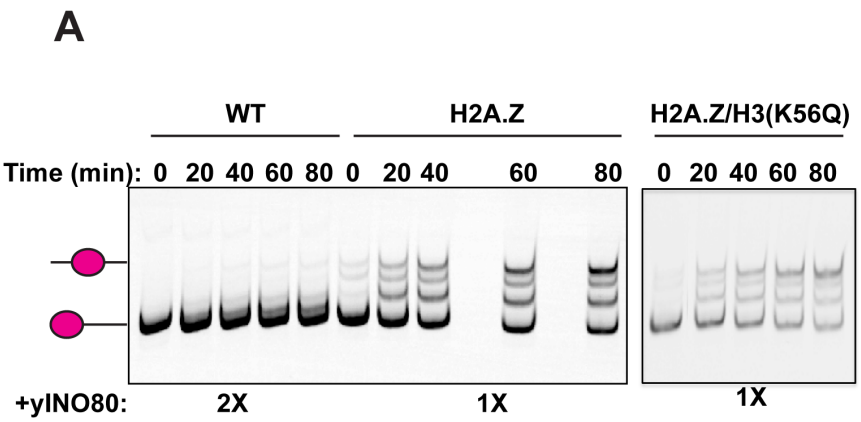
A
WT
H2A.Z
H2A.Z/H3(K56Q)
Time (min): 0 20 40 60 80 0 20 40 60 80 0 20 40 60 80
+yINO80: 2X 1X 1X
B
WT
H2A.Z
Time (min): 0 20 40 60 80 0 20 40 60 80
+ySW1
C
Normalized rate
40
30
20
10
0
yINO80
ySW1
Nucleosomes: WT H2A.Z

Figure 3.9. Nucleosome sliding by the yeast remodelers yINO80 and yISW1.
(A) Sliding of WT, H2A.Z and H2A.Z/H3K56Q nucleosomes by yINO80. For WT nucleosomes twice as much yINO80 was used in this assay. **(B)** Sliding of WT and H2A.Z nucleosomes by yISW1. **(C)** Shown are relative sliding rates between WT and H2A.Z nucleosomes. Whereas yINO80 slides H2A.Z nucleosomes with dramatically higher efficiency, yISW1 slides both types of nucleosomes (WT and H2A.Z) indiscriminately.

3.4 Discussion

Whereas there are multiple studies focused on characterizing the remodeling activities of the yeast INO80 complex, only few groups have investigated activities of the human INO80 complex. In particular, how histone variants and PTMs modulate the remodeling activity of hINO80 has not been explored. This is partly due to the difficulty in obtaining purified hINO80 complexes from mammalian cells with sufficient quantity and homogeneity. In addition, obtaining homogeneous preparations of nucleosomes harboring a particular PTM or histone variant can be technically challenging. We have been able to prepare hINO80 from two different cell lines: a HEK293 cell line stably expressing Flag-CCDC95 and a HeLa S3 cell line stably expressing Flag-Ies2 (Cai et al., 2006; Yao et al., 2008). By normalizing different hINO80 preps based on their ATPase activities, we consistently observed that hINO80 catalyzes sliding of H2A.Z-containing nucleosomes ~8-fold faster than canonical nucleosomes. The presence of H3 acetylation mimic, K56Q, further enhances the rate of sliding by ~5-fold. These properties suggest that H2A.Z/H3K56Ac-contaning nucleosomes are preferred substrates of hINO80.

yINO80 has also been reported to prefer H2A.Z/H3K56Ac-containing nucleosomes, but in a different type of biochemical assay. yINO80 catalyzes replacement of nucleosomal H2A.Z-H2B dimer with free H2A-H2B dimer (Papamichos-Chronakis et al., 2011). This activity is specific for H2A.Z nucleosomes, as it is unable to incorporate H2A-H2B dimers into H2A nucleosomes. The dimer exchange activity is also further stimulated by the presence of H3(K56Q) (Watanabe et al., 2013). We assayed yINO80 for its sliding activity with nucleosomes reconstituted with recombinant human histones. yINO80 mobilized H2A.Z nucleosomes at a similar rate as hINO80, but it had almost no activity against H2A

nucleosomes. In contrast, yISW1 mobilized H2A and H2A.Z-containing nucleosomes similarly. These results strongly argue that the increased mobilization of H2A.Z-containing nucleosomes by INO80 is not due to an inherent property of H2A.Z nucleosomes. The competition-sliding assay between H2A and H2A.Z nucleosomes revealed that the enhanced sliding of H2A.Z nucleosomes by hINO80 is driven by faster catalysis, rather than higher affinity. These findings suggest that specific interactions between INO80 and H2A.Z likely account for more efficient remodeling. Which regions of H2A.Z are involved in this interaction is an interesting question that we intend to address in the future.

Genetic evidence from yeast provides strong support for a role for yINO80 in regulating the localization of H2A.Z across the genome (Papamichos-Chronakis et al., 2011). *In vivo* analysis revealed elevated H2A.Z levels at the *KAR4* promoter region in the *Δino80* strain. Biochemical and genetic evidence suggest that yINO80 drives eviction of H2A.Z at the *KAR4* promoter to facilitate transcription activation. Work in embryonic stem cells (ESCs) has shown that H2A.Z is highly enriched at active and bivalent promoters (Wang et al., 2014). In these cells, hINO80 has been reported to occupy the proximal promoter regions of pluripotency genes and activate their expression by maintaining an open chromatin environment. Our *in vitro* data suggest that hINO80 could enhance promoter accessibility by enhanced mobilization of H2A.Z-containing nucleosomes. We plan to further explore this intriguing possibility by monitoring H2A.Z levels and positioning at these gene promoters upon perturbation of the hINO80 complex.

Another possibility is that the sliding activity that we observe *in vitro* is a surrogate for the dimer exchange activity that hINO80 could perform *in vivo.* We have not been able to detect dimer exchange by hINO80 *in vitro,* using the same experimental conditions

previously employed to demonstrate the dimer exchange activity for yINO80 (data not shown). It is possible that hINO80 requires other factors to catalyze dimer exchange, including other PTMs or unknown accessory proteins. Recently, the mammalian histone chaperone ANP32E was identified as a H2A.Z-specific chaperone, that can remove H2A.Z-H2B dimers from the nucleosome *in vitro* (Obri et al., 2014). Interestingly, structural evidence suggests that removal of H2A.Z-H2B by ANP32E requires the chaperone to compete with DNA ends in order to access the dimer, which could be facilitated by nucleosomal DNA end breathing *in vitro*. One attractive possibility is that ANP32E, or similar types of chaperones, could assist hINO80 in catalyzing H2A.Z-H2B dimer exchange *in vivo*, by capturing the released H2A.Z-H2B dimer, thus promoting replacement of H2A.Z by H2A.

CHAPTER 4: DISCUSSION AND PERSPECTIVES

4.1 Regulation of transcription by ubiquitination of transcriptional activators

[4]Transcriptional activators (TAs) regulate transcription by orchestrating time and locus-specific assembly of complex transcription machinery. One way in which these activators are controlled is by the covalent attachment of the conserved protein, ubiquitin (Ub), which can serve as either a proteolytic or non-proteolytic signal. For a subset of the activators, polyubiquitination-dependent degradation of the activator controls its abundance (reviewed in (Yao and Ndoja, 2012)). In these cases, transcription activation can require protein synthesis as well as internal or external stimulus. In contrast, other activators have been reported to undergo mono- or oligo-ubiquitination that does not lead to protein degradation (reviewed in (Yao and Ndoja, 2012)). The mechanisms by which monoubiquitination of TAs affect their activities have been poorly understood. In a recent study, we demonstrated that monoubiquitination of some TAs can inhibit transcription by recruiting the AAA+ ATPase Cdc48 (also known in metazoan organisms as p97 or valosin-containing protein, VCP), which then extracts the ubiquitinated activator from DNA (Ndoja et al., 2014).

4.1.1 A non-proteolytic function of Ub in transcription repression

Given the dynamic nature of Ub modification, it is often difficult to assess the direct effect of ubiquitination on TAs. Without specific antibodies that differentiate the ubiquitinated from non-ubiquitinated pool of activators, determining which pool is

[4] This chapter is related to Ndoja A. and Yao T. (2014) Microbial Cell 1 (7), 253-255. Published figures include 4.1.

chromatin-bound and responsible for driving transcription has generally not been possible. We were able to bypass these obstacles by employing the Ub-LV fusion protein. We found that Cdc48 was recruited to the promoter of the reporter gene in the presence of Ub-LV or Ub-LexA (without the VP16 activation domain), but not by Ub(L8A)-LV, which contains a point mutation in the hydrophobic patch. It is surprising that a single Ub attached to the activator was sufficient to recruit Cdc48 and elicit its segregase activity. After all, monoUb by itself is not a very distinctive signal *in vivo*, and competition by the large pool of unconjugated Ub in the cell is expected to weaken the interaction. We also observed substantial amounts of Ub-LV that are not bound to chromatin. These are all potential competitors for Cdc48:Ufd1:Npl4 complexes. Thus, chromatin-bound Ub-LV likely contains additional signals that contribute to recruitment of Cdc48. Through experiments that are detailed in Chapter 2, we ruled out some of the usual suspects, such as SUMO modifications or transcription coactivators that may bind to VP16. We speculate that Cdc48 or its cofactor(s) has intrinsic affinity for chromatin itself. Either naked DNA, which is commonly found at promoter regions in yeast, or nucleosomes might be additional targeting signals. Low-affinity, non-specific interactions with chromatin combined with specific interactions with monoUb could target Cdc48 efficiently to promoter-bound Ub-LV. However, we cannot rule out that other components of the transcription machinery may also contribute to Cdc48 recruitment. An increasing number of proteins have been found to interact with Cdc48/p97/VCP, and a VCP-interacting motif (VIM) was recently identified in multiple Cdc48-interacting proteins (Stapf et al., 2011). The yeast genome encodes dozens of proteins that have a consensus VIM, some of which are known players in the transcription process.

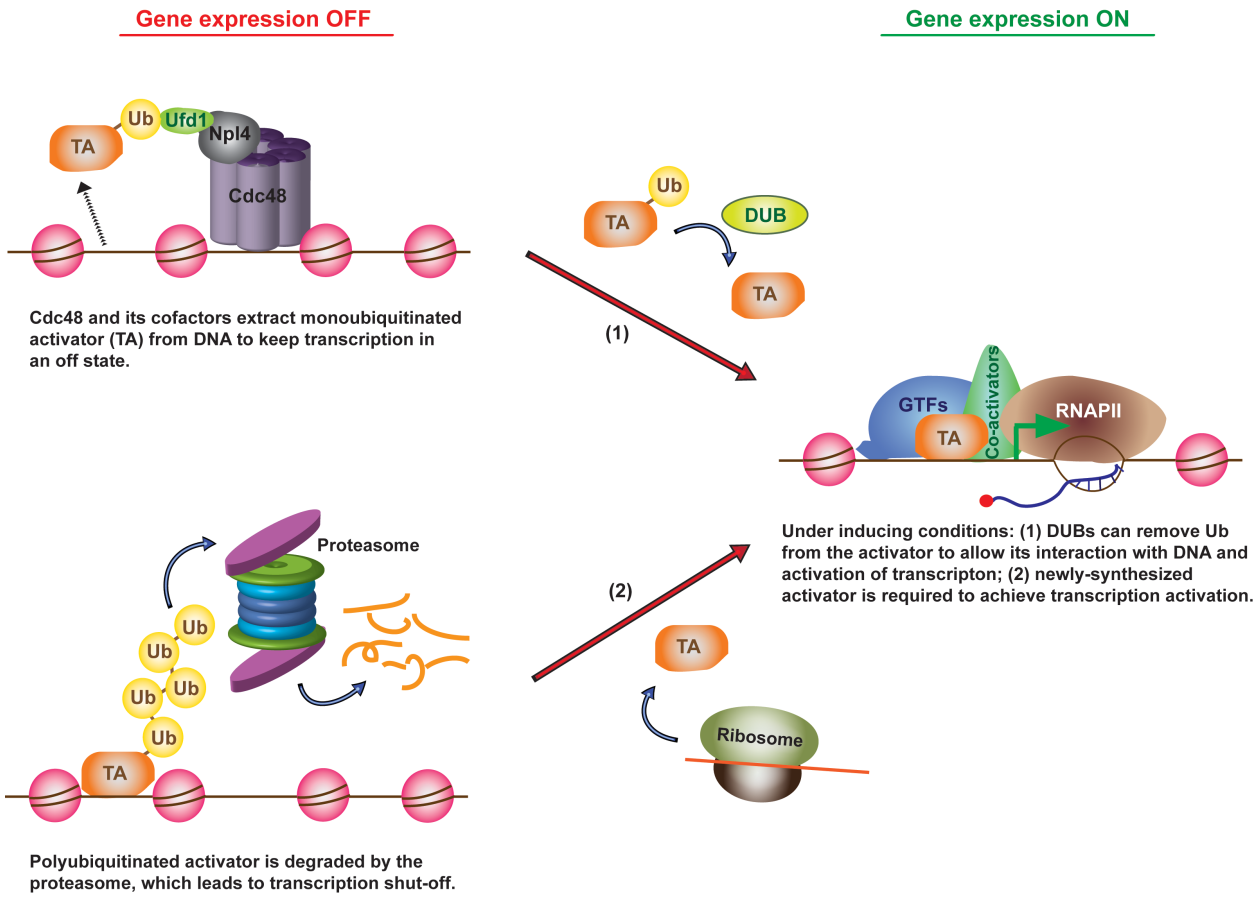

Figure 4.1. Ubiquitination of transcription activators down-regulates transcription through multiple routes.

It is satisfying that the mechanism revealed from the study of the artificial activator Ub-LV applies as well to native transcription activators such as Met4 and R-Smads. We expect that additional activators will be found to be regulated by a similar mechanism in the near future. One remaining question is why these systems employ a non-proteolytic route to achieve transcription downregulation. An obvious possibility is that mono- or oligo-ubiquitination is readily reversible: rapid induction of transcription by deubiquitination of the activator would not require new protein synthesis (Figure 4.1). In the case of the yeast *MET* gene network, this mode of regulation could be essential, as new protein synthesis can be limiting in an environment where methionine levels are low. Currently, the DUB that deubiquitinates Met4 upon methionine depletion has not been identified. In the case of R-Smads, Usp15 has been found to be necessary for transcription activation under inducing conditions (Inui et al., 2011). In these cases, how the DUBs are regulated in response to changing environments are interesting topics for future studies.

4.2 The INO80 chromatin-remodeling complex

DNA damage and aberrant chromosome replication are detrimental to genome integrity with serious effects to an organism's health and survival. During recent years it has become apparent that chromatin structure plays an essential in maintaining genome integrity. Elucidating the mechanism that is utilized to protect genome stability is an important step toward understanding and fighting diseases like cancer. ATP-dependent chromatin remodeling enzymes utilize the force generated by ATP-hydrolysis to alter the position and the composition of nucleosomes. Among them is the INO80 chromatin-remodeling complex, which has been found to participate in transcription, DNA repair and

DNA replication (reviewed in (Conaway and Conaway, 2009)). While none of the hINO80 subunits are significantly mutated in human cancers, they are involved in telomere stability and DNA damage repair pathways (Gospodinov et al., 2011; Wu et al., 2007). At least some of the functions of hINO80 at DNA damage sites are believed to be through its ability to regulate gene expression, because the expression of DNA damage repair genes, including *RAD54B* and *XRCC3*, are hINO80 dependent (Park et al., 2010). In agreement with a role for INO80 in mediating genome stability, INO80 heterozygous knockout mice have an increased incidence of soft tissues sarcomas compared to INO80 wild type mice (Min et al., 2013). Therefore, elucidating the mechanism of action of hINO80 is essential for moving the field forward towards characterization of new therapeutic targets.

In vitro biochemical studies have shown that yINO80 catalyzes exchange of nucleosomal H2A.Z-H2B dimers with H2A-H2B free dimers (Papamichos-Chronakis et al., 2011). This exchange activity is stimulated by acetylation of H3 at lysine 56 (Watanabe et al., 2013). Aside from mediating histone dimer exchange, yINO80 has also been reported to catalyze sliding of nucleosomes from a lateral to a central position on a DNA fragment (Udugama et al., 2011). *In vivo* yINO80 localizes to the nucleosome free region (NFR), and contacts the +1 nucleosome, which is enriched in H2A.Z (Yen et al., 2013). The action of yINO80 is antagonized by SWR-C, which deposits free H2A.Z-H2B dimers and removes nucleosomal H2A-H2B dimers (Luk et al., 2010). Similar to yINO80, SWR-C is also recruited to the NFR, adjacent to the +1 nucleosome (Yen et al., 2013). Given the size of these remodelers, the NFR region is not large enough to accommodate simultaneous binding of SWR-C and yINO80. Therefore, it is more likely that they are recruited to the NFR individually. One possibility is that conditions that favor transient recruitment of one

remodeler may result in conditions that favor recruitment of the other. For example, SWR-C recruitment could promote deposition of H2A.Z. Once SWR-C deposits two copies of H2A.Z, it would dissociate from the NFR, as saturation of a nucleosome with two molecules of H2A.Z has been shown to inhibit the SWR-C ATPase activity (Luk et al., 2010). Because H2A.Z-containing nucleosomes are yINO80 substrates, they could promote yINO80 recruitment. This would lead to H2A.Z removal. The "futile cycle" of reciprocal H2A.Z/H2A exchange catalyzed by SWR-C and yINO80 could promote enhanced nucleosome turnover (Yen et al., 2013). This feature of +1 nucleosomes might provide a way for rapid invasion by transcription factors and RNAPII, thus favoring transcription.

Whether these biochemical properties also apply to hINO80 is yet to be explored. In an effort to elucidate the sliding activity of hINO80 we immunoaffinity purified this remodeler from cell lines that stably express its Flag-tagged subunits CCDC95 and Ies2 (Cai et al., 2006; Jin et al., 2005). Similar to yINO80, the human counterpart supports nucleosome sliding in an ATP-dependent manner, and has been shown to mobilize nucleosomes from a lateral to a central position on a DNA fragment (Jin et al., 2005). Previously, the Conaway group assayed nucleosome sliding by hINO80 of nucleosomes harboring canonical, unmodified histones (Chen et al., 2013; Jin et al., 2005). *In vivo*, cooperation between chromatin remodelers, histone variants and PTMs offers diverse regulatory options in different DNA metabolic processes, such as transcription, DNA repair and replication. Therefore, in order to better understand how hINO80 mobilizes nucleosomes containing histone variants or histones with PTMs, we assayed the sliding activity of hINO80 versus H2A.Z-containing nucleosomes and nucleosomes containing histones with PTMs, such as ubiquitination and acetylation.

4.2.1 hINO80 slides H2A.Z-containing nucleosomes more efficiently

We found that hINO80 mobilized H2A.Z-containing nucleosomes more efficiently than canonical, unmodified nucleosomes. This is not due to increased affinity of hINO80 for H2A.Z-containing nucleosomes, as the sliding rate for both H2A.Z- and H2A-containing nucleosomes decreased by ~2-fold, when they were simultaneously incubated with hINO80. We also assayed yINO80 for its sliding activity with nucleosomes reconstituted with recombinant human histones. yINO80 mobilized H2A.Z nucleosomes at a similar rate as hINO80, but it had almost no activity against H2A nucleosomes. In contrast, yISW1 mobilized H2A and H2A.Z-containing nucleosomes similarly. These results strongly argue that the increased mobilization of H2A.Z-containing nucleosomes by INO80 is not due to an inherent property of H2A.Z nucleosomes. Specific interactions between INO80 and H2A.Z are likely to account for more efficient remodeling.

In addition, we found that nucleosomes containing the H3 acetylation mimic, K56Q, are slided by hINO80 with faster kinetics and the effects of H2A.Z and H3K56Q are additive. In mammalian cells, nucleosomes containing both H2A.Z and H3-K56Ac are found at promoter regions of actively transcribed genes and DNA damage sites (Barski et al., 2007; Xie et al., 2009). These nucleosomes have been shown to exhibit rapid turnover kinetics *in vivo* (Dion et al., 2007; Yen et al., 2013). Therefore, our results provide biochemical evidence that hINO80 participates in transcription and DNA repair processes via ATP-dependent mobilization of H2A.Z/H3-K56Ac-containing nucleosomes.

It has been reported that over-expression of H2A.Z is associated with breast cancer progression (Hua et al., 2008; Rangasamy, 2010). A study of breast tumor samples collected from over 500 patients revealed that the elevated levels of H2A.Z expression are

associated with the spread of the cancer to lymph nodes, metastasis, and decreased patient survival (Hua et al., 2008). It has been proposed that the molecular pathway and mechanism that links altered H2A.Z levels to tumorigenesis is by transcription regulation of *TFF1*, which is one of the major estrogen receptor induced genes (Prest et al., 2002). The product of *TFF1* has been used as a marker protein for breast cancer and ER-α positive tumors (Lacroix, 2006). H2A.Z is enriched at the promoter proximal region of *TFF1* upon estrogen signaling, and has been reported to facilitate recruitment of the transcription factor FoxA1 at the enhancer of the promoter region. Both H2A.Z and FoxA1 are required for recruitment of the transcriptional machinery and expression of *TFF1* in breast cancer cells (Lupien et al., 2008). The mechanism by which H2A.Z facilitates FoxA1 recruitment and subsequent activation of *TFF1* is not understood. Therefore, understanding how H2A.Z localization on chromatin is regulated is of foremost importance.

First of all, how is H2A.Z specificity achieved? SWR-C has been shown to interact with H2A.Z via its subunit Swc2 (Wu et al., 2005). The metazoan counterpart of Swc2, which is found in the human SRCAP and p400/Tip60 complexes, can also bind to H2A.Z (Wu et al., 2005). One possibility is that INO80 also makes specific contacts with H2A.Z through one or more of its subunits.

In mouse ESCs, it has been proposed that INO80 activates expression of pluripotency genes by maintaining an open chromatin environment and facilitating recruitment of RNAPII (Wang et al., 2014). Based on our *in vitro* results, we propose that hINO80 facilitates transcription by increasing mobilization of H2A.Z-containing nucleosomes at promoter regions in mammalian cells. hINO80 could accomplish this by sliding the nucleosomes away from the promoter region to expose DNA binding sites and

promote recruitment of transcription factors. Alternatively, hINO80 could promote removal of H2A.Z. Based upon this model, we hope to address two main questions: (1) What accounts for the H2A.Z-specificity? (2) Is H2A.Z localization on chromatin affected upon depletion of hINO80? Specific experiments designed to address these questions are detailed below.

4.2.2 What accounts for the H2A.Z specificity?

H2A.Z has ~60% sequence similarity with H2A. Among the differences, H2A.Z possesses a unique carboxy-terminal α-helix (αC) and C-terminal tail, which have been shown to be essential for H2A.Z function in *Drosophila melanogaster* (Clarkson et al., 1999). Consistent with this finding, they are also required for interaction with the yeast SWR-C chromatin remodeling complex as well as the H2A.Z-specific mammalian chaperone ANP32E (Obri et al., 2014; Wu et al., 2005). Therefore, the αC and the C-terminal tail represent good candidates for possible interaction regions between hINO80 and H2A.Z. To test this hypothesis, we have generated two different mutant versions of H2A.Z. In the first mutant, aminoacids ^{98}DSLI^{101} of the αC region of H2A.Z were substituted with the H2A corresponding aminoacids ^{95}NKLLG^{99}. In the second H2A.Z mutant, the entire C-terminal tail was deleted and substituted with the C-terminal tail of H2A. Next, we plan to assay the sliding activity of hINO80 versus nucleosomes containing either one of the two H2A.Z mutants, in order to understand whether any of these regions is responsible for the H2A.Z-specificity observed in case of hINO80. If any one of these regions accounts for the enhanced sliding of H2A.Z-containing nucleosomes, we expect to observe diminished hINO80-mediated sliding of the nucleosomes harboring the mutant H2A.Z histone.

4.2.3 Is H2A.Z localization on chromatin affected upon depletion of INO80?

Based on our model that hINO80 mediates mobilization of H2A.Z-containing nucleosomes, we hope to assess the effects of hINO80 depletion on genome-wide H2A.Z localization *in vivo.* To accomplish this task, we decided to deplete the hINO80 subunit Ies2, which has been reported to be required for the ATPase and nucleosome sliding activity of hINO80 (Chen et al., 2013). We chose to deplete Ies2 by generating cell lines stably expressing shRNA for Ies2, under the control of a doxycycline inducible promoter. One advantage to using this method over siRNA transfection is consistency from one experiment to another, as the cell population would exhibit similar levels of Ies2 depletion.

We are currently generating these stable cell lines by packaging Ies2 shRNA, encoding a puromycin resistance cassette, into lentiviruses, and infecting HeLa cells. Upon selection of puromycin-resistant cells, we will induce expression of shRNA for Ies2 by addition of doxycycline and monitor Ies2 protein levels through western-blot analysis and its mRNA levels through quantitative RT-PCR. Once we have obtained stable cell lines that show significant depletion of Ies2, we would like to perform a careful analysis of the genome-wide localization of H2A.Z by ChIP-Seq. If hINO80, as our *in vitro* data strongly suggest, is implicated in mobilization of nucleosomes containing the histone variant H2A.Z *in vivo*, impairment of its sliding activity would result in mislocalization of H2A.Z across the genome. As discussed in Chapter 3, the hINO80 sliding activity we observe *in vitro* could be a proxy for the dimer exchange it could perform *in vivo*. If this was the case we expect to observe higher H2A.Z occupancy at promoter regions upon Ies2 depletion.

REFERENCES

Acs, K., Luijsterburg, M.S., Ackermann, L., Salomons, F.A., Hoppe, T., and Dantuma, N.P. (2011). The AAA-ATPase VCP/p97 promotes 53BP1 recruitment by removing L3MBTL1 from DNA double-strand breaks. Nat Struct Mol Biol *18*, 1345-1350.

Albert, I., Mavrich, T.N., Tomsho, L.P., Qi, J., Zanton, S.J., Schuster, S.C., and Pugh, B.F. (2007). Translational and rotational settings of H2A.Z nucleosomes across the Saccharomyces cerevisiae genome. Nature *446*, 572-576.

Allen, M.D., Buchberger, A., and Bycroft, M. (2006). The PUB domain functions as a p97 binding module in human peptide N-glycanase. J Biol Chem *281*, 25502-25508.

Archer, C.T., Burdine, L., Liu, B., Ferdous, A., Johnston, S.A., and Kodadek, T. (2008a). Physical and functional interactions of monoubiquitylated transactivators with the proteasome. J Biol Chem *283*, 21789-21798.

Archer, C.T., Delahodde, A., Gonzalez, F., Johnston, S.A., and Kodadek, T. (2008b). Activation domain-dependent monoubiquitylation of Gal4 protein is essential for promoter binding in vivo. J Biol Chem *283*, 12614-12623.

Archer, C.T., and Kodadek, T. (2010). The hydrophobic patch of ubiquitin is required to protect transactivator-promoter complexes from destabilization by the proteasomal ATPases. Nucleic Acids Res *38*, 789-796.

Arnaudo, A.M., and Garcia, B.A. (2013). Proteomic characterization of novel histone post-translational modifications. Epigenetics & chromatin *6*, 24.

Auld, K.L., Brown, C.R., Casolari, J.M., Komili, S., and Silver, P.A. (2006). Genomic association of the proteasome demonstrates overlapping gene regulatory activity with transcription factor substrates. Mol Cell *21*, 861-871.

Baek, G.H., Cheng, H., Choe, V., Bao, X., Shao, J., Luo, S., and Rao, H. (2013). Cdc48: a swiss army knife of cell biology. Journal of amino acids *2013*, 183421.

Bannister, A.J., and Kouzarides, T. (2011). Regulation of chromatin by histone modifications. Cell research *21*, 381-395.

Barbaric, S., Luckenbach, T., Schmid, A., Blaschke, D., Horz, W., and Korber, P. (2007). Redundancy of chromatin remodeling pathways for the induction of the yeast PHO5 promoter in vivo. J Biol Chem *282*, 27610-27621.

Barski, A., Cuddapah, S., Cui, K., Roh, T.Y., Schones, D.E., Wang, Z., Wei, G., Chepelev, I., and Zhao, K. (2007). High-resolution profiling of histone methylations in the human genome. Cell *129*, 823-837.

Baumann, M., Pontiller, J., and Ernst, W. (2010). Structure and basal transcription complex of RNA polymerase II core promoters in the mammalian genome: an overview. Molecular biotechnology *45*, 241-247.

Becker, P.B., and Horz, W. (2002). ATP-dependent nucleosome remodeling. Annual review of biochemistry *71*, 247-273.

Bei, S.Z., Li, Y.A., Li, L., Pan, Z.Y., Li, G.X., Lan, B.X., Bao, Y.H., Yan, Q.Y., and Wang, Q. (1983). Electron microscopic studies on the chromatin of blastoderm nuclei and yolk granules beneath blastoderm of fertilized and unincubated chicken eggs. Scientia Sinica Series B, Chemical, biological, agricultural, medical & earth sciences / Chung-kuo k'o hsueh yuan, chu pan *26*, 708-715.

Bhat, K.P., and Greer, S.F. (2011). Proteolytic and non-proteolytic roles of ubiquitin and the ubiquitin proteasome system in transcriptional regulation. Biochim Biophys Acta *1809*, 150-155.

Bhat, K.P., Turner, J.D., Myers, S.E., Cape, A.D., Ting, J.P., and Greer, S.F. (2008). The 19S proteasome ATPase Sug1 plays a critical role in regulating MHC class II transcription. Mol Immunol *45*, 2214-2224.

Biegel, J.A., Fogelgren, B., Zhou, J.Y., James, C.D., Janss, A.J., Allen, J.C., Zagzag, D., Raffel, C., and Rorke, L.B. (2000). Mutations of the INI1 rhabdoid tumor suppressor gene in medulloblastomas and primitive neuroectodermal tumors of the central nervous system. Clinical cancer research : an official journal of the American Association for Cancer Research *6*, 2759-2763.

Billon, P., and Cote, J. (2013). Precise deposition of histone H2A.Z in chromatin for genome expression and maintenance. Biochim Biophys Acta *1819*, 290-302.

Boeger, H., Griesenbeck, J., and Kornberg, R.D. (2008). Nucleosome retention and the stochastic nature of promoter chromatin remodeling for transcription. Cell *133*, 716-726.

Boeger, H., Griesenbeck, J., Strattan, J.S., and Kornberg, R.D. (2004). Removal of promoter nucleosomes by disassembly rather than sliding in vivo. Mol Cell *14*, 667-673.

Bonisch, C., and Hake, S.B. (2012). Histone H2A variants in nucleosomes and chromatin: more or less stable? Nucleic Acids Res *40*, 10719-10741.

Bottomley, M.J. (2004). Structures of protein domains that create or recognize histone modifications. EMBO Rep *5*, 464-469.

Boyault, C., Gilquin, B., Zhang, Y., Rybin, V., Garman, E., Meyer-Klaucke, W., Matthias, P., Muller, C.W., and Khochbin, S. (2006). HDAC6-p97/VCP controlled polyubiquitin chain turnover. EMBO J *25*, 3357-3366.

Braun, B.C., Glickman, M., Kraft, R., Dahlmann, B., Kloetzel, P.M., Finley, D., and Schmidt, M. (1999). The base of the proteasome regulatory particle exhibits chaperone-like activity. Nat Cell Biol *1*, 221-226.

Bres, V., Kiernan, R.E., Linares, L.K., Chable-Bessia, C., Plechakova, O., Treand, C., Emiliani, S., Peloponese, J.M., Jeang, K.T., Coux, O.*, et al.* (2003). A non-proteolytic role for ubiquitin in Tat-mediated transactivation of the HIV-1 promoter. Nat Cell Biol *5*, 754-761.

Brune, M., Hunter, J.L., Corrie, J.E., and Webb, M.R. (1994). Direct, real-time measurement of rapid inorganic phosphate release using a novel fluorescent probe and its application to actomyosin subfragment 1 ATPase. Biochemistry *33*, 8262-8271.

Buchberger, A. (2013). Roles of Cdc48 in regulated protein degradation in yeast. Sub-cellular biochemistry *66*, 195-222.

Buchberger, A., Howard, M.J., Proctor, M., and Bycroft, M. (2001). The UBX domain: a widespread ubiquitin-like module. J Mol Biol *307*, 17-24.

Cai, Y., Jin, J., Gottschalk, A.J., Yao, T., Conaway, J.W., and Conaway, R.C. (2006). Purification and assay of the human INO80 and SRCAP chromatin remodeling complexes. Methods *40*, 312-317.

Cai, Y., Jin, J., Yao, T., Gottschalk, A.J., Swanson, S.K., Wu, S., Shi, Y., Washburn, M.P., Florens, L., Conaway, R.C.*, et al.* (2007). YY1 functions with INO80 to activate transcription. Nat Struct Mol Biol *14*, 872-874.

Cao, R., Tsukada, Y., and Zhang, Y. (2005). Role of Bmi-1 and Ring1A in H2A ubiquitylation and Hox gene silencing. Mol Cell *20*, 845-854.

Carrozza, M.J., Li, B., Florens, L., Suganuma, T., Swanson, S.K., Lee, K.K., Shia, W.J., Anderson, S., Yates, J., Washburn, M.P.*, et al.* (2005). Histone H3 methylation by Set2 directs deacetylation of coding regions by Rpd3S to suppress spurious intragenic transcription. Cell *123*, 581-592.

Chaban, Y., Ezeokonkwo, C., Chung, W.H., Zhang, F., Kornberg, R.D., Maier-Davis, B., Lorch, Y., and Asturias, F.J. (2008). Structure of a RSC-nucleosome complex and insights into chromatin remodeling. Nat Struct Mol Biol *15*, 1272-1277.

Chambers, A.L., Ormerod, G., Durley, S.C., Sing, T.L., Brown, G.W., Kent, N.A., and Downs, J.A. (2012). The INO80 chromatin remodeling complex prevents polyploidy and maintains normal chromatin structure at centromeres. Genes Dev *26*, 2590-2603.

Chandrasekharan, M.B., Huang, F., and Sun, Z.W. (2009). Ubiquitination of histone H2B regulates chromatin dynamics by enhancing nucleosome stability. Proc Natl Acad Sci U S A *106*, 16686-16691.

Chen, L., Cai, Y., Jin, J., Florens, L., Swanson, S.K., Washburn, M.P., Conaway, J.W., and Conaway, R.C. (2011). Subunit organization of the human INO80 chromatin remodeling complex: an evolutionarily conserved core complex catalyzes ATP-dependent nucleosome remodeling. J Biol Chem *286*, 11283-11289.

Chen, L., Conaway, R.C., and Conaway, J.W. (2013). Multiple modes of regulation of the human Ino80 SNF2 ATPase by subunits of the INO80 chromatin-remodeling complex. Proc Natl Acad Sci U S A *110*, 20497-20502.

Chi, Y., Huddleston, M.J., Zhang, X., Young, R.A., Annan, R.S., Carr, S.A., and Deshaies, R.J. (2001). Negative regulation of Gcn4 and Msn2 transcription factors by Srb10 cyclin-dependent kinase. Genes Dev *15*, 1078-1092.

Clarkson, M.J., Wells, J.R., Gibson, F., Saint, R., and Tremethick, D.J. (1999). Regions of variant histone His2AvD required for Drosophila development. Nature *399*, 694-697.

Collins, G.A., Lipford, J.R., Deshaies, R.J., and Tansey, W.P. (2009). Gal4 turnover and transcription activation. Nature *461*, E7; discussion E8.

Conaway, R.C., and Conaway, J.W. (2009). The INO80 chromatin remodeling complex in transcription, replication and repair. Trends Biochem Sci *34*, 71-77.

Dai, R.M., and Li, C.C. (2001). Valosin-containing protein is a multi-ubiquitin chain-targeting factor required in ubiquitin-proteasome degradation. Nat Cell Biol *3*, 740-744.

Davies, N., and Lindsey, G.G. (1994). Histone H2B (and H2A) ubiquitination allows normal histone octamer and core particle reconstitution. Biochim Biophys Acta *1218*, 187-193.

Dechassa, M.L., Zhang, B., Horowitz-Scherer, R., Persinger, J., Woodcock, C.L., Peterson, C.L., and Bartholomew, B. (2008). Architecture of the SWI/SNF-nucleosome complex. Mol Cell Biol *28*, 6010-6021.

DeLaBarre, B., and Brunger, A.T. (2003). Complete structure of p97/valosin-containing protein reveals communication between nucleotide domains. Nature structural biology *10*, 856-863.

Deshaies, R.J. (1999). SCF and Cullin/Ring H2-based ubiquitin ligases. Annual review of cell and developmental biology *15*, 435-467.

Dhalluin, C., Carlson, J.E., Zeng, L., He, C., Aggarwal, A.K., and Zhou, M.M. (1999). Structure and ligand of a histone acetyltransferase bromodomain. Nature *399*, 491-496.

Dion, M.F., Kaplan, T., Kim, M., Buratowski, S., Friedman, N., and Rando, O.J. (2007). Dynamics of replication-independent histone turnover in budding yeast. Science *315*, 1405-1408.

Dunican, D.S., McWilliam, P., Tighe, O., Parle-McDermott, A., and Croke, D.T. (2002). Gene expression differences between the microsatellite instability (MIN) and chromosomal instability (CIN) phenotypes in colorectal cancer revealed by high-density cDNA array hybridization. Oncogene *21*, 3253-3257.

Dyer, P.N., Edayathumangalam, R.S., White, C.L., Bao, Y., Chakravarthy, S., Muthurajan, U.M., and Luger, K. (2004). Reconstitution of nucleosome core particles from recombinant histones and DNA. Methods Enzymol *375*, 23-44.

Ebbert, R., Birkmann, A., and Schuller, H.J. (1999). The product of the SNF2/SWI2 paralogue INO80 of Saccharomyces cerevisiae required for efficient expression of various yeast structural genes is part of a high-molecular-weight protein complex. Molecular microbiology *32*, 741-751.

Faast, R., Thonglairoam, V., Schulz, T.C., Beall, J., Wells, J.R., Taylor, H., Matthaei, K., Rathjen, P.D., Tremethick, D.J., and Lyons, I. (2001). Histone variant H2A.Z is required for early mammalian development. Curr Biol *11*, 1183-1187.

Fang, J., Chen, T., Chadwick, B., Li, E., and Zhang, Y. (2004). Ring1b-mediated H2A ubiquitination associates with inactive X chromosomes and is involved in initiation of X inactivation. J Biol Chem *279*, 52812-52815.

Ferdous, A., O'Neal, M., Nalley, K., Sikder, D., Kodadek, T., and Johnston, S.A. (2008). Phosphorylation of the Gal4 DNA-binding domain is essential for activator mono-ubiquitylation and efficient promoter occupancy. Mol Biosyst *4*, 1116-1125.

Ferdous, A., Sikder, D., Gillette, T., Nalley, K., Kodadek, T., and Johnston, S.A. (2007). The role of the proteasomal ATPases and activator monoubiquitylation in regulating Gal4 binding to promoters. Genes Dev *21*, 112-123.

Fierz, B., Chatterjee, C., McGinty, R.K., Bar-Dagan, M., Raleigh, D.P., and Muir, T.W. (2011). Histone H2B ubiquitylation disrupts local and higher-order chromatin compaction. Nature chemical biology *7*, 113-119.

Finley, D. (2009). Recognition and processing of ubiquitin-protein conjugates by the proteasome. Annual review of biochemistry *78*, 477-513.

Flaus, A., Martin, D.M., Barton, G.J., and Owen-Hughes, T. (2006). Identification of multiple distinct Snf2 subfamilies with conserved structural motifs. Nucleic Acids Res *34*, 2887-2905.

Fleming, A.B., Kao, C.F., Hillyer, C., Pikaart, M., and Osley, M.A. (2008). H2B ubiquitylation plays a role in nucleosome dynamics during transcription elongation. Mol Cell *31*, 57-66.

Flick, K., Ouni, I., Wohlschlegel, J.A., Capati, C., McDonald, W.H., Yates, J.R., and Kaiser, P. (2004). Proteolysis-independent regulation of the transcription factor Met4 by a single Lys 48-linked ubiquitin chain. Nat Cell Biol *6*, 634-641.

Flick, K., Raasi, S., Zhang, H., Yen, J.L., and Kaiser, P. (2006). A ubiquitin-interacting motif protects polyubiquitinated Met4 from degradation by the 26S proteasome. Nat Cell Biol *8*, 509-515.

Ford, J., Odeyale, O., Eskandar, A., Kouba, N., and Shen, C.H. (2007). A SWI/SNF- and INO80-dependent nucleosome movement at the INO1 promoter. Biochemical and biophysical research communications *361*, 974-979.

Fritsch, O., Benvenuto, G., Bowler, C., Molinier, J., and Hohn, B. (2004). The INO80 protein controls homologous recombination in Arabidopsis thaliana. Mol Cell *16*, 479-485.

Frohlich, K.U., Fries, H.W., Rudiger, M., Erdmann, R., Botstein, D., and Mecke, D. (1991). Yeast cell cycle protein CDC48p shows full-length homology to the mammalian protein VCP and is a member of a protein family involved in secretion, peroxisome formation, and gene expression. J Cell Biol *114*, 443-453.

Ganguli, D., Chereji, R.V., Iben, J.R., Cole, H.A., and Clark, D.J. (2014). RSC-dependent constructive and destructive interference between opposing arrays of phased nucleosomes in yeast. Genome Res *24*, 1637-1649.

Geng, F., and Tansey, W.P. (2012). Similar temporal and spatial recruitment of native 19S and 20S proteasome subunits to transcriptionally active chromatin. Proc Natl Acad Sci U S A *109*, 6060-6065.

Geng, F., Wenzel, S., and Tansey, W.P. (2012). Ubiquitin and proteasomes in transcription. Annual review of biochemistry *81*, 177-201.

Gerhold, C.B., and Gasser, S.M. (2014). INO80 and SWR complexes: relating structure to function in chromatin remodeling. Trends in cell biology *24*, 619-631.

Gillette, T.G., Gonzalez, F., Delahodde, A., Johnston, S.A., and Kodadek, T. (2004). Physical and functional association of RNA polymerase II and the proteasome. Proc Natl Acad Sci U S A *101*, 5904-5909.

Glickman, M.H., Rubin, D.M., Coux, O., Wefes, I., Pfeifer, G., Cjeka, Z., Baumeister, W., Fried, V.A., and Finley, D. (1998). A subcomplex of the proteasome regulatory particle required for ubiquitin-conjugate degradation and related to the COP9-signalosome and eIF3. Cell *94*, 615-623.

Goldknopf, I.L., Taylor, C.W., Baum, R.M., Yeoman, L.C., Olson, M.O., Prestayko, A.W., and Busch, H. (1975). Isolation and characterization of protein A24, a "histone-like" non-histone chromosomal protein. J Biol Chem *250*, 7182-7187.

Gonzalez, F., Delahodde, A., Kodadek, T., and Johnston, S.A. (2002). Recruitment of a 19S proteasome subcomplex to an activated promoter. Science *296*, 548-550.

Gospodinov, A., Vaissiere, T., Krastev, D.B., Legube, G., Anachkova, B., and Herceg, Z. (2011). Mammalian Ino80 mediates double-strand break repair through its role in DNA end strand resection. Mol Cell Biol *31*, 4735-4745.

Groll, M., Ditzel, L., Lowe, J., Stock, D., Bochtler, M., Bartunik, H.D., and Huber, R. (1997). Structure of 20S proteasome from yeast at 2.4 A resolution. Nature *386*, 463-471.

Guillemette, B., Bataille, A.R., Gevry, N., Adam, M., Blanchette, M., Robert, F., and Gaudreau, L. (2005). Variant histone H2A.Z is globally localized to the promoters of inactive yeast genes and regulates nucleosome positioning. PLoS biology *3*, e384.

Hartley, P.D., and Madhani, H.D. (2009). Mechanisms that specify promoter nucleosome location and identity. Cell *137*, 445-458.

Hartmann-Petersen, R., Wallace, M., Hofmann, K., Koch, G., Johnsen, A.H., Hendil, K.B., and Gordon, C. (2004). The Ubx2 and Ubx3 cofactors direct Cdc48 activity to proteolytic and nonproteolytic ubiquitin-dependent processes. Curr Biol *14*, 824-828.

Hatch, C.L., Bonner, W.M., and Moudrianakis, E.N. (1983). Minor histone 2A variants and ubiquinated forms in the native H2A:H2B dimer. Science *221*, 468-470.

Henikoff, S. (2009). Labile H3.3+H2A.Z nucleosomes mark 'nucleosome-free regions'. Nat Genet *41*, 865-866.

Hershko, A., and Ciechanover, A. (1998). The ubiquitin system. Annual review of biochemistry *67*, 425-479.

Hicke, L. (2001). Protein regulation by monoubiquitin. Nat Rev Mol Cell Biol *2*, 195-201.

Higashi, T., Matsunaga, S., Isobe, K., Morimoto, A., Shimada, T., Kataoka, S., Watanabe, W., Uchiyama, S., Itoh, K., and Fukui, K. (2007). Histone H2A mobility is regulated by its tails and acetylation of core histone tails. Biochemical and biophysical research communications *357*, 627-632.

Hoch, D.A., Stratton, J.J., and Gloss, L.M. (2007). Protein-protein Forster resonance energy transfer analysis of nucleosome core particles containing H2A and H2A.Z. J Mol Biol *371*, 971-988.

Hogan, C.J., Aligianni, S., Durand-Dubief, M., Persson, J., Will, W.R., Webster, J., Wheeler, L., Mathews, C.K., Elderkin, S., Oxley, D.*, et al.* (2010). Fission yeast Iec1-ino80-mediated nucleosome eviction regulates nucleotide and phosphate metabolism. Mol Cell Biol *30*, 657-674.

Hong, L., Schroth, G.P., Matthews, H.R., Yau, P., and Bradbury, E.M. (1993). Studies of the DNA binding properties of histone H4 amino terminus. Thermal denaturation studies reveal that acetylation markedly reduces the binding constant of the H4 "tail" to DNA. J Biol Chem *268*, 305-314.

Hu, G., Cui, K., Northrup, D., Liu, C., Wang, C., Tang, Q., Ge, K., Levens, D., Crane-Robinson, C., and Zhao, K. (2013). H2A.Z facilitates access of active and repressive complexes to chromatin in embryonic stem cell self-renewal and differentiation. Cell stem cell *12*, 180-192.

Hua, S., Kallen, C.B., Dhar, R., Baquero, M.T., Mason, C.E., Russell, B.A., Shah, P.K., Liu, J., Khramtsov, A., Tretiakova, M.S.*, et al.* (2008). Genomic analysis of estrogen cascade reveals histone variant H2A.Z associated with breast cancer progression. Molecular systems biology *4*, 188.

Husnjak, K., Elsasser, S., Zhang, N., Chen, X., Randles, L., Shi, Y., Hofmann, K., Walters, K.J., Finley, D., and Dikic, I. (2008). Proteasome subunit Rpn13 is a novel ubiquitin receptor. Nature *453*, 481-488.

Ikeda, F., and Dikic, I. (2008). Atypical ubiquitin chains: new molecular signals. 'Protein Modifications: Beyond the Usual Suspects' review series. EMBO Rep *9*, 536-542.

Inui, M., Manfrin, A., Mamidi, A., Martello, G., Morsut, L., Soligo, S., Enzo, E., Moro, S., Polo, S., Dupont, S., *et al.* (2011). USP15 is a deubiquitylating enzyme for receptor-activated SMADs. Nat Cell Biol *13*, 1368-1375.

Iouzalen, N., Moreau, J., and Mechali, M. (1996). H2A.ZI, a new variant histone expressed during Xenopus early development exhibits several distinct features from the core histone H2A. Nucleic Acids Res *24*, 3947-3952.

Ishibashi, T., Dryhurst, D., Rose, K.L., Shabanowitz, J., Hunt, D.F., and Ausio, J. (2009). Acetylation of vertebrate H2A.Z and its effect on the structure of the nucleosome. Biochemistry *48*, 5007-5017.

Izban, M.G., and Luse, D.S. (1992). Factor-stimulated RNA polymerase II transcribes at physiological elongation rates on naked DNA but very poorly on chromatin templates. J Biol Chem *267*, 13647-13655.

Jacobs, S.A., and Khorasanizadeh, S. (2002). Structure of HP1 chromodomain bound to a lysine 9-methylated histone H3 tail. Science *295*, 2080-2083.

Jason, L.J., Finn, R.M., Lindsey, G., and Ausio, J. (2005). Histone H2A ubiquitination does not preclude histone H1 binding, but it facilitates its association with the nucleosome. J Biol Chem *280*, 4975-4982.

Jentsch, S., and Rumpf, S. (2007). Cdc48 (p97): a "molecular gearbox" in the ubiquitin pathway? Trends Biochem Sci *32*, 6-11.

Jiang, Y., Wang, X., Bao, S., Guo, R., Johnson, D.G., Shen, X., and Li, L. (2010). INO80 chromatin remodeling complex promotes the removal of UV lesions by the nucleotide excision repair pathway. Proc Natl Acad Sci U S A *107*, 17274-17279.

Jin, C., and Felsenfeld, G. (2007). Nucleosome stability mediated by histone variants H3.3 and H2A.Z. Genes Dev *21*, 1519-1529.

Jin, J., Cai, Y., Yao, T., Gottschalk, A.J., Florens, L., Swanson, S.K., Gutierrez, J.L., Coleman, M.K., Workman, J.L., Mushegian, A., *et al.* (2005). A mammalian chromatin remodeling complex with similarities to the yeast INO80 complex. J Biol Chem *280*, 41207-41212.

Jonsson, Z.O., Jha, S., Wohlschlegel, J.A., and Dutta, A. (2004). Rvb1p/Rvb2p recruit Arp5p and assemble a functional Ino80 chromatin remodeling complex. Mol Cell *16*, 465-477.

Joshi, A.A., and Struhl, K. (2005). Eaf3 chromodomain interaction with methylated H3-K36 links histone deacetylation to Pol II elongation. Mol Cell *20*, 971-978.

Kaiser, P., Flick, K., Wittenberg, C., and Reed, S.I. (2000). Regulation of transcription by ubiquitination without proteolysis: Cdc34/SCF(Met30)-mediated inactivation of the transcription factor Met4. Cell *102*, 303-314.

Kamura, T., Sato, S., Iwai, K., Czyzyk-Krzeska, M., Conaway, R.C., and Conaway, J.W. (2000). Activation of HIF1alpha ubiquitination by a reconstituted von Hippel-Lindau (VHL) tumor suppressor complex. Proc Natl Acad Sci U S A *97*, 10430-10435.

Kanno, T., Kanno, Y., Siegel, R.M., Jang, M.K., Lenardo, M.J., and Ozato, K. (2004). Selective recognition of acetylated histones by bromodomain proteins visualized in living cells. Mol Cell *13*, 33-43.

Kao, C.F., Hillyer, C., Tsukuda, T., Henry, K., Berger, S., and Osley, M.A. (2004). Rad6 plays a role in transcriptional activation through ubiquitylation of histone H2B. Genes Dev *18*, 184-195.

Kaplan, C.D., Laprade, L., and Winston, F. (2003). Transcription elongation factors repress transcription initiation from cryptic sites. Science *301*, 1096-1099.

Kim, J., Hake, S.B., and Roeder, R.G. (2005). The human homolog of yeast BRE1 functions as a transcriptional coactivator through direct activator interactions. Mol Cell *20*, 759-770.

Kim, S.Y., Herbst, A., Tworkowski, K.A., Salghetti, S.E., and Tansey, W.P. (2003). Skp2 regulates Myc protein stability and activity. Mol Cell *11*, 1177-1188.

Kodadek, T., Sikder, D., and Nalley, K. (2006). Keeping transcriptional activators under control. Cell *127*, 261-264.

Koegl, M., Hoppe, T., Schlenker, S., Ulrich, H.D., Mayer, T.U., and Jentsch, S. (1999). A novel ubiquitination factor, E4, is involved in multiubiquitin chain assembly. Cell *96*, 635-644.

Kohler, A., Schneider, M., Cabal, G.G., Nehrbass, U., and Hurt, E. (2008). Yeast Ataxin-7 links histone deubiquitination with gene gating and mRNA export. Nat Cell Biol *10*, 707-715.

Kuras, L., Rouillon, A., Lee, T., Barbey, R., Tyers, M., and Thomas, D. (2002). Dual regulation of the met4 transcription factor by ubiquitin-dependent degradation and inhibition of promoter recruitment. Mol Cell *10*, 69-80.

Kwak, H., Fuda, N.J., Core, L.J., and Lis, J.T. (2013). Precise maps of RNA polymerase reveal how promoters direct initiation and pausing. Science *339*, 950-953.

Lacroix, M. (2006). Significance, detection and markers of disseminated breast cancer cells. Endocrine-related cancer *13*, 1033-1067.

Lee, D., Ezhkova, E., Li, B., Pattenden, S.G., Tansey, W.P., and Workman, J.L. (2005). The proteasome regulatory particle alters the SAGA coactivator to enhance its interactions with transcriptional activators. Cell *123*, 423-436.

Lee, T.A., Jorgensen, P., Bognar, A.L., Peyraud, C., Thomas, D., and Tyers, M. (2010). Dissection of combinatorial control by the Met4 transcriptional complex. Mol Biol Cell *21*, 456-469.

Leon, A., and McKearin, D. (1999). Identification of TER94, an AAA ATPase protein, as a Bam-dependent component of the Drosophila fusome. Mol Biol Cell *10*, 3825-3834.

Li, B., Carey, M., and Workman, J.L. (2007). The role of chromatin during transcription. Cell *128*, 707-719.

Lipford, J.R., Smith, G.T., Chi, Y., and Deshaies, R.J. (2005). A putative stimulatory role for activator turnover in gene expression. Nature *438*, 113-116.

Liu, C.W., Millen, L., Roman, T.B., Xiong, H., Gilbert, H.F., Noiva, R., DeMartino, G.N., and Thomas, P.J. (2002). Conformational remodeling of proteasomal substrates by PA700, the 19 S regulatory complex of the 26 S proteasome. J Biol Chem *277*, 26815-26820.

Long, L., Furgason, M., and Yao, T. (2014a). Generation of nonhydrolyzable ubiquitin-histone mimics. Methods *70*, 134-138.

Long, L., Thelen, J.P., Furgason, M., Haj-Yahya, M., Brik, A., Cheng, D., Peng, J., and Yao, T. (2014b). The U4/U6 recycling factor SART3 has histone chaperone activity and associates with USP15 to regulate H2B deubiquitination. J Biol Chem *289*, 8916-8930.

Lorch, Y., Griesenbeck, J., Boeger, H., Maier-Davis, B., and Kornberg, R.D. (2011). Selective removal of promoter nucleosomes by the RSC chromatin-remodeling complex. Nat Struct Mol Biol *18*, 881-885.

Lorch, Y., LaPointe, J.W., and Kornberg, R.D. (1987). Nucleosomes inhibit the initiation of transcription but allow chain elongation with the displacement of histones. Cell *49*, 203-210.

Luger, K., Mader, A.W., Richmond, R.K., Sargent, D.F., and Richmond, T.J. (1997). Crystal structure of the nucleosome core particle at 2.8 A resolution. Nature *389*, 251-260.

Luk, E., Ranjan, A., Fitzgerald, P.C., Mizuguchi, G., Huang, Y., Wei, D., and Wu, C. (2010). Stepwise histone replacement by SWR1 requires dual activation with histone H2A.Z and canonical nucleosome. Cell *143*, 725-736.

Lupien, M., Eeckhoute, J., Meyer, C.A., Wang, Q., Zhang, Y., Li, W., Carroll, J.S., Liu, X.S., and Brown, M. (2008). FoxA1 translates epigenetic signatures into enhancer-driven lineage-specific transcription. Cell *132*, 958-970.

Marzluff, W.F., Gongidi, P., Woods, K.R., Jin, J., and Maltais, L.J. (2002). The human and mouse replication-dependent histone genes. Genomics *80*, 487-498.

Marzluff, W.F., Wagner, E.J., and Duronio, R.J. (2008). Metabolism and regulation of canonical histone mRNAs: life without a poly(A) tail. Nature reviews Genetics *9*, 843-854.

Mavrich, T.N., Ioshikhes, I.P., Venters, B.J., Jiang, C., Tomsho, L.P., Qi, J., Schuster, S.C., Albert, I., and Pugh, B.F. (2008). A barrier nucleosome model for statistical positioning of nucleosomes throughout the yeast genome. Genome Res *18*, 1073-1083.

McGinty, R.K., Kim, J., Chatterjee, C., Roeder, R.G., and Muir, T.W. (2008). Chemically ubiquitylated histone H2B stimulates hDot1L-mediated intranucleosomal methylation. Nature *453*, 812-816.

McNeill, H., Knebel, A., Arthur, J.S., Cuenda, A., and Cohen, P. (2004). A novel UBA and UBX domain protein that binds polyubiquitin and VCP and is a substrate for SAPKs. The Biochemical journal *384*, 391-400.

Meerang, M., Ritz, D., Paliwal, S., Garajova, Z., Bosshard, M., Mailand, N., Janscak, P., Hubscher, U., Meyer, H., and Ramadan, K. (2011). The ubiquitin-selective segregase VCP/p97 orchestrates the response to DNA double-strand breaks. Nat Cell Biol *13*, 1376-1382.

Metivier, R., Penot, G., Hubner, M.R., Reid, G., Brand, H., Kos, M., and Gannon, F. (2003). Estrogen receptor-alpha directs ordered, cyclical, and combinatorial recruitment of cofactors on a natural target promoter. Cell *115*, 751-763.

Meyer, H.H., Wang, Y., and Warren, G. (2002). Direct binding of ubiquitin conjugates by the mammalian p97 adaptor complexes, p47 and Ufd1-Npl4. EMBO J *21*, 5645-5652.

Min, J.N., Tian, Y., Xiao, Y., Wu, L., Li, L., and Chang, S. (2013). The mINO80 chromatin remodeling complex is required for efficient telomere replication and maintenance of genome stability. Cell research *23*, 1396-1413.

Mizuguchi, G., Shen, X., Landry, J., Wu, W.H., Sen, S., and Wu, C. (2004). ATP-driven exchange of histone H2AZ variant catalyzed by SWR1 chromatin remodeling complex. Science *303*, 343-348.

Molinari, E., Gilman, M., and Natesan, S. (1999). Proteasome-mediated degradation of transcriptional activators correlates with activation domain potency in vivo. EMBO J *18*, 6439-6447.

Morrison, A.J., Highland, J., Krogan, N.J., Arbel-Eden, A., Greenblatt, J.F., Haber, J.E., and Shen, X. (2004). INO80 and gamma-H2AX interaction links ATP-dependent chromatin remodeling to DNA damage repair. Cell *119*, 767-775.

Muller, J.M., Deinhardt, K., Rosewell, I., Warren, G., and Shima, D.T. (2007). Targeted deletion of p97 (VCP/CDC48) in mouse results in early embryonic lethality. Biochemical and biophysical research communications *354*, 459-465.

Muratani, M., Kung, C., Shokat, K.M., and Tansey, W.P. (2005). The F box protein Dsg1/Mdm30 is a transcriptional coactivator that stimulates Gal4 turnover and cotranscriptional mRNA processing. Cell *120*, 887-899.

Muratani, M., and Tansey, W.P. (2003). How the ubiquitin-proteasome system controls transcription. Nat Rev Mol Cell Biol *4*, 192-201.

Nakanishi, S., Lee, J.S., Gardner, K.E., Gardner, J.M., Takahashi, Y.H., Chandrasekharan, M.B., Sun, Z.W., Osley, M.A., Strahl, B.D., Jaspersen, S.L.*, et al.* (2009). Histone H2BK123 monoubiquitination is the critical determinant for H3K4 and H3K79 trimethylation by COMPASS and Dot1. J Cell Biol *186*, 371-377.

Nalley, K., Johnston, S.A., and Kodadek, T. (2006). Proteolytic turnover of the Gal4 transcription factor is not required for function in vivo. Nature *442*, 1054-1057.

Ndoja, A., Cohen, R.E., and Yao, T. (2014). Ubiquitin signals proteolysis-independent stripping of transcription factors. Mol Cell *53*, 893-903.

Nielsen, P.R., Nietlispach, D., Mott, H.R., Callaghan, J., Bannister, A., Kouzarides, T., Murzin, A.G., Murzina, N.V., and Laue, E.D. (2002). Structure of the HP1 chromodomain bound to histone H3 methylated at lysine 9. Nature *416*, 103-107.

Obri, A., Ouararhni, K., Papin, C., Diebold, M.L., Padmanabhan, K., Marek, M., Stoll, I., Roy, L., Reilly, P.T., Mak, T.W.*, et al.* (2014). ANP32E is a histone chaperone that removes H2A.Z from chromatin. Nature *505*, 648-653.

Olzmann, J.A., Richter, C.M., and Kopito, R.R. (2013). Spatial regulation of UBXD8 and p97/VCP controls ATGL-mediated lipid droplet turnover. Proc Natl Acad Sci U S A *110*, 1345-1350.

Osley, M.A., Fleming, A.B., and Kao, C.F. (2006). Histone ubiquitylation and the regulation of transcription. Results Probl Cell Differ *41*, 47-75.

Papamichos-Chronakis, M., Watanabe, S., Rando, O.J., and Peterson, C.L. (2011). Global regulation of H2A.Z localization by the INO80 chromatin-remodeling enzyme is essential for genome integrity. Cell *144*, 200-213.

Park, E.J., Hur, S.K., and Kwon, J. (2010). Human INO80 chromatin-remodelling complex contributes to DNA double-strand break repair via the expression of Rad54B and XRCC3 genes. The Biochemical journal *431*, 179-187.

Park, Y.J., and Luger, K. (2008). Histone chaperones in nucleosome eviction and histone exchange. Current opinion in structural biology *18*, 282-289.

Pavri, R., Zhu, B., Li, G., Trojer, P., Mandal, S., Shilatifard, A., and Reinberg, D. (2006). Histone H2B monoubiquitination functions cooperatively with FACT to regulate elongation by RNA polymerase II. Cell *125*, 703-717.

Pchelintsev, N.A., McBryan, T., Rai, T.S., van Tuyn, J., Ray-Gallet, D., Almouzni, G., and Adams, P.D. (2013). Placing the HIRA histone chaperone complex in the chromatin landscape. Cell reports *3*, 1012-1019.

Peng, J., Schwartz, D., Elias, J.E., Thoreen, C.C., Cheng, D., Marsischky, G., Roelofs, J., Finley, D., and Gygi, S.P. (2003). A proteomics approach to understanding protein ubiquitination. Nature biotechnology *21*, 921-926.

Peters, J.M., Franke, W.W., and Kleinschmidt, J.A. (1994). Distinct 19 S and 20 S subcomplexes of the 26 S proteasome and their distribution in the nucleus and the cytoplasm. J Biol Chem *269*, 7709-7718.

Pickart, C.M. (2001). Ubiquitin enters the new millennium. Mol Cell *8*, 499-504.

Pickart, C.M., and Cohen, R.E. (2004). Proteasomes and their kin: proteases in the machine age. Nat Rev Mol Cell Biol *5*, 177-187.

Pickart, C.M., and Fushman, D. (2004). Polyubiquitin chains: polymeric protein signals. Curr Opin Chem Biol *8*, 610-616.

Prest, S.J., May, F.E., and Westley, B.R. (2002). The estrogen-regulated protein, TFF1, stimulates migration of human breast cancer cells. FASEB journal : official publication of the Federation of American Societies for Experimental Biology *16*, 592-594.

Raisner, R.M., Hartley, P.D., Meneghini, M.D., Bao, M.Z., Liu, C.L., Schreiber, S.L., Rando, O.J., and Madhani, H.D. (2005). Histone variant H2A.Z marks the 5' ends of both active and inactive genes in euchromatin. Cell *123*, 233-248.

Ramadan, K., Bruderer, R., Spiga, F.M., Popp, O., Baur, T., Gotta, M., and Meyer, H.H. (2007). Cdc48/p97 promotes reformation of the nucleus by extracting the kinase Aurora B from chromatin. Nature *450*, 1258-1262.

Raman, M., Havens, C.G., Walter, J.C., and Harper, J.W. (2011). A genome-wide screen identifies p97 as an essential regulator of DNA damage-dependent CDT1 destruction. Mol Cell *44*, 72-84.

Rangasamy, D. (2010). Histone variant H2A.Z can serve as a new target for breast cancer therapy. Current medicinal chemistry *17*, 3155-3161.

Rape, M., Hoppe, T., Gorr, I., Kalocay, M., Richly, H., and Jentsch, S. (2001). Mobilization of processed, membrane-tethered SPT23 transcription factor by CDC48(UFD1/NPL4), a ubiquitin-selective chaperone. Cell *107*, 667-677.

Reid, G., Hubner, M.R., Metivier, R., Brand, H., Denger, S., Manu, D., Beaudouin, J., Ellenberg, J., and Gannon, F. (2003). Cyclic, proteasome-mediated turnover of unliganded and liganded ERalpha on responsive promoters is an integral feature of estrogen signaling. Mol Cell *11*, 695-707.

Rhee, H.S., Bataille, A.R., Zhang, L., and Pugh, B.F. (2014). Subnucleosomal structures and nucleosome asymmetry across a genome. Cell *159*, 1377-1388.

Richly, H., Rape, M., Braun, S., Rumpf, S., Hoege, C., and Jentsch, S. (2005). A series of ubiquitin binding factors connects CDC48/p97 to substrate multiubiquitylation and proteasomal targeting. Cell *120*, 73-84.

Robzyk, K., Recht, J., and Osley, M.A. (2000). Rad6-dependent ubiquitination of histone H2B in yeast. Science *287*, 501-504.

Rouiller, I., DeLaBarre, B., May, A.P., Weis, W.I., Brunger, A.T., Milligan, R.A., and Wilson-Kubalek, E.M. (2002). Conformational changes of the multifunction p97 AAA ATPase during its ATPase cycle. Nature structural biology *9*, 950-957.

Rouillon, A., Barbey, R., Patton, E.E., Tyers, M., and Thomas, D. (2000). Feedback-regulated degradation of the transcriptional activator Met4 is triggered by the SCF(Met30)complex. EMBO J *19*, 282-294.

Rufiange, A., Jacques, P.E., Bhat, W., Robert, F., and Nourani, A. (2007). Genome-wide replication-independent histone H3 exchange occurs predominantly at promoters and implicates H3 K56 acetylation and Asf1. Mol Cell *27*, 393-405.

Rumpf, S., and Jentsch, S. (2006). Functional division of substrate processing cofactors of the ubiquitin-selective Cdc48 chaperone. Mol Cell *21*, 261-269.

Saeki, Y., Tayama, Y., Toh-e, A., and Yokosawa, H. (2004). Definitive evidence for Ufd2-catalyzed elongation of the ubiquitin chain through Lys48 linkage. Biochemical and biophysical research communications *320*, 840-845.

Sahtoe, D.D., van Dijk, W.J., El Oualid, F., Ekkebus, R., Ovaa, H., and Sixma, T.K. (2015). Mechanism of UCH-L5 Activation and Inhibition by DEUBAD Domains in RPN13 and INO80G. Mol Cell *57*, 887-900.

Salghetti, S.E., Caudy, A.A., Chenoweth, J.G., and Tansey, W.P. (2001). Regulation of transcriptional activation domain function by ubiquitin. Science *293*, 1651-1653.

Salghetti, S.E., Muratani, M., Wijnen, H., Futcher, B., and Tansey, W.P. (2000). Functional overlap of sequences that activate transcription and signal ubiquitin-mediated proteolysis. Proc Natl Acad Sci U S A *97*, 3118-3123.

Schones, D.E., Cui, K., Cuddapah, S., Roh, T.Y., Barski, A., Wang, Z., Wei, G., and Zhao, K. (2008). Dynamic regulation of nucleosome positioning in the human genome. Cell *132*, 887-898.

Schreiner, P., Chen, X., Husnjak, K., Randles, L., Zhang, N., Elsasser, S., Finley, D., Dikic, I., Walters, K.J., and Groll, M. (2008). Ubiquitin docking at the proteasome through a novel pleckstrin-homology domain interaction. Nature *453*, 548-552.

Schuberth, C., and Buchberger, A. (2005). Membrane-bound Ubx2 recruits Cdc48 to ubiquitin ligases and their substrates to ensure efficient ER-associated protein degradation. Nat Cell Biol *7*, 999-1006.

Sevenet, N., Sheridan, E., Amram, D., Schneider, P., Handgretinger, R., and Delattre, O. (1999). Constitutional mutations of the hSNF5/INI1 gene predispose to a variety of cancers. American journal of human genetics *65*, 1342-1348.

Sevilla, A., and Binda, O. (2014). Post-translational modifications of the histone variant H2AZ. Stem cell research *12*, 289-295.

Shaw, P.A., Sahasrabuddhe, C.G., Hodo, H.G., 3rd, and Saunders, G.F. (1978). Transcription of nucleosomes from human chromatin. Nucleic Acids Res *5*, 2999-3012.

Shema, E., Kim, J., Roeder, R.G., and Oren, M. (2011). RNF20 inhibits TFIIS-facilitated transcriptional elongation to suppress pro-oncogenic gene expression. Mol Cell *42*, 477-488.

Shen, X., Mizuguchi, G., Hamiche, A., and Wu, C. (2000). A chromatin remodelling complex involved in transcription and DNA processing. Nature *406*, 541-544.

Shen, X., Ranallo, R., Choi, E., and Wu, C. (2003). Involvement of actin-related proteins in ATP-dependent chromatin remodeling. Mol Cell *12*, 147-155.

Sikder, D., Johnston, S.A., and Kodadek, T. (2006). Widespread, but non-identical, association of proteasomal 19 and 20 S proteins with yeast chromatin. J Biol Chem *281*, 27346-27355.

Singh, J., and Padgett, R.A. (2009). Rates of in situ transcription and splicing in large human genes. Nat Struct Mol Biol *16*, 1128-1133.

Smolle, M., Venkatesh, S., Gogol, M.M., Li, H., Zhang, Y., Florens, L., Washburn, M.P., and Workman, J.L. (2012). Chromatin remodelers Isw1 and Chd1 maintain chromatin structure during transcription by preventing histone exchange. Nat Struct Mol Biol *19*, 884-892.

Smolle, M., Workman, J.L., and Venkatesh, S. (2013). reSETting chromatin during transcription elongation. Epigenetics : official journal of the DNA Methylation Society *8*, 10-15.

Stapf, C., Cartwright, E., Bycroft, M., Hofmann, K., and Buchberger, A. (2011). The general definition of the p97/valosin-containing protein (VCP)-interacting motif (VIM) delineates a new family of p97 cofactors. J Biol Chem *286*, 38670-38678.

Sun, L., and Chen, Z.J. (2004). The novel functions of ubiquitination in signaling. Curr Opin Cell Biol *16*, 119-126.

Sun, Z.W., and Allis, C.D. (2002). Ubiquitination of histone H2B regulates H3 methylation and gene silencing in yeast. Nature *418*, 104-108.

Suto, R.K., Clarkson, M.J., Tremethick, D.J., and Luger, K. (2000). Crystal structure of a nucleosome core particle containing the variant histone H2A.Z. Nature structural biology *7*, 1121-1124.

Svaren, J., and Horz, W. (1997). Transcription factors vs nucleosomes: regulation of the PHO5 promoter in yeast. Trends Biochem Sci *22*, 93-97.

Teves, S.S., Weber, C.M., and Henikoff, S. (2014). Transcribing through the nucleosome. Trends Biochem Sci *39*, 577-586.

Thatcher, T.H., and Gorovsky, M.A. (1994). Phylogenetic analysis of the core histones H2A, H2B, H3, and H4. Nucleic Acids Res *22*, 174-179.

Tosi, A., Haas, C., Herzog, F., Gilmozzi, A., Berninghausen, O., Ungewickell, C., Gerhold, C.B., Lakomek, K., Aebersold, R., Beckmann, R*., et al.* (2013). Structure and subunit topology of the INO80 chromatin remodeler and its nucleosome complex. Cell *154*, 1207-1219.

Tyrrell, A., Flick, K., Kleiger, G., Zhang, H., Deshaies, R.J., and Kaiser, P. (2010). Physiologically relevant and portable tandem ubiquitin-binding domain stabilizes polyubiquitylated proteins. Proc Natl Acad Sci U S A *107*, 19796-19801.

Udugama, M., Sabri, A., and Bartholomew, B. (2011). The INO80 ATP-dependent chromatin remodeling complex is a nucleosome spacing factor. Mol Cell Biol *31*, 662-673.

van Attikum, H., Fritsch, O., Hohn, B., and Gasser, S.M. (2004). Recruitment of the INO80 complex by H2A phosphorylation links ATP-dependent chromatin remodeling with DNA double-strand break repair. Cell *119*, 777-788.

van Daal, A., and Elgin, S.C. (1992). A histone variant, H2AvD, is essential in Drosophila melanogaster. Mol Biol Cell *3*, 593-602.

VanderLinden, R.T., Hemmis, C.W., Schmitt, B., Ndoja, A., Whitby, F.G., Robinson, H., Cohen, R.E., Yao, T., and Hill, C.P. (2015). Structural Basis for the Activation and Inhibition of the UCH37 Deubiquitylase. Mol Cell *57*, 901-911.

Varshavsky, A. (2005). Regulated protein degradation. Trends Biochem Sci *30*, 283-286.

Venkatesh, S., and Workman, J.L. (2015). Histone exchange, chromatin structure and the regulation of transcription. Nat Rev Mol Cell Biol *16*, 178-189.

Verma, R., Oania, R., Fang, R., Smith, G.T., and Deshaies, R.J. (2011). Cdc48/p97 mediates UV-dependent turnover of RNA Pol II. Mol Cell *41*, 82-92.

von der Lehr, N., Johansson, S., Wu, S., Bahram, F., Castell, A., Cetinkaya, C., Hydbring, P., Weidung, I., Nakayama, K., Nakayama, K.I.*, et al.* (2003). The F-box protein Skp2 participates in c-Myc proteosomal degradation and acts as a cofactor for c-Myc-regulated transcription. Mol Cell *11*, 1189-1200.

Wang, H., Wang, L., Erdjument-Bromage, H., Vidal, M., Tempst, P., Jones, R.S., and Zhang, Y. (2004). Role of histone H2A ubiquitination in Polycomb silencing. Nature *431*, 873-878.

Wang, L., Du, Y., Ward, J.M., Shimbo, T., Lackford, B., Zheng, X., Miao, Y.L., Zhou, B., Han, L., Fargo, D.C.*, et al.* (2014). INO80 facilitates pluripotency gene activation in embryonic stem cell self-renewal, reprogramming, and blastocyst development. Cell stem cell *14*, 575-591.

Wang, X., Muratani, M., Tansey, W.P., and Ptashne, M. (2010). Proteolytic instability and the action of nonclassical transcriptional activators. Curr Biol *20*, 868-871.

Watanabe, S., Radman-Livaja, M., Rando, O.J., and Peterson, C.L. (2013). A histone acetylation switch regulates H2A.Z deposition by the SWR-C remodeling enzyme. Science *340*, 195-199.

Weake, V.M., and Workman, J.L. (2008). Histone ubiquitination: triggering gene activity. Mol Cell *29*, 653-663.

Weber, C.M., Henikoff, J.G., and Henikoff, S. (2010). H2A.Z nucleosomes enriched over active genes are homotypic. Nat Struct Mol Biol *17*, 1500-1507.

Weber, C.M., and Henikoff, S. (2014). Histone variants: dynamic punctuation in transcription. Genes Dev *28*, 672-682.

Weber, C.M., Ramachandran, S., and Henikoff, S. (2014). Nucleosomes are context-specific, H2A.Z-modulated barriers to RNA polymerase. Mol Cell *53*, 819-830.

Welcker, M., Orian, A., Jin, J., Grim, J.E., Harper, J.W., Eisenman, R.N., and Clurman, B.E. (2004). The Fbw7 tumor suppressor regulates glycogen synthase kinase 3 phosphorylation-dependent c-Myc protein degradation. Proc Natl Acad Sci U S A *101*, 9085-9090.

Wilcox, A.J., and Laney, J.D. (2009). A ubiquitin-selective AAA-ATPase mediates transcriptional switching by remodelling a repressor-promoter DNA complex. Nat Cell Biol *11*, 1481-1486.

Wolf, D.H., and Stolz, A. (2012). The Cdc48 machine in endoplasmic reticulum associated protein degradation. Biochim Biophys Acta *1823*, 117-124.

Wu, R.S., Kohn, K.W., and Bonner, W.M. (1981). Metabolism of ubiquitinated histones. J Biol Chem *256*, 5916-5920.

Wu, S., Shi, Y., Mulligan, P., Gay, F., Landry, J., Liu, H., Lu, J., Qi, H.H., Wang, W., Nickoloff, J.A.*, et al.* (2007). A YY1-INO80 complex regulates genomic stability through homologous recombination-based repair. Nat Struct Mol Biol *14*, 1165-1172.

Wu, W.H., Alami, S., Luk, E., Wu, C.H., Sen, S., Mizuguchi, G., Wei, D., and Wu, C. (2005). Swc2 is a widely conserved H2AZ-binding module essential for ATP-dependent histone exchange. Nat Struct Mol Biol *12*, 1064-1071.

Wunsch, A.M., Haas, A.L., and Lough, J. (1987). Synthesis and ubiquitination of histones during myogenesis. Developmental biology *119*, 85-93.

Wyce, A., Xiao, T., Whelan, K.A., Kosman, C., Walter, W., Eick, D., Hughes, T.R., Krogan, N.J., Strahl, B.D., and Berger, S.L. (2007). H2B ubiquitylation acts as a barrier to Ctk1 nucleosomal recruitment prior to removal by Ubp8 within a SAGA-related complex. Mol Cell *27*, 275-288.

Xie, W., Song, C., Young, N.L., Sperling, A.S., Xu, F., Sridharan, R., Conway, A.E., Garcia, B.A., Plath, K., Clark, A.T.*, et al.* (2009). Histone h3 lysine 56 acetylation is linked to the core transcriptional network in human embryonic stem cells. Mol Cell *33*, 417-427.

Yada, M., Hatakeyama, S., Kamura, T., Nishiyama, M., Tsunematsu, R., Imaki, H., Ishida, N., Okumura, F., Nakayama, K., and Nakayama, K.I. (2004). Phosphorylation-dependent degradation of c-Myc is mediated by the F-box protein Fbw7. EMBO J *23*, 2116-2125.

Yamada, K., Frouws, T.D., Angst, B., Fitzgerald, D.J., DeLuca, C., Schimmele, K., Sargent, D.F., and Richmond, T.J. (2011). Structure and mechanism of the chromatin remodelling factor ISW1a. Nature *472*, 448-453.

Yamanaka, K., Okubo, Y., Suzaki, T., and Ogura, T. (2004). Analysis of the two p97/VCP/Cdc48p proteins of Caenorhabditis elegans and their suppression of polyglutamine-induced protein aggregation. Journal of structural biology *146*, 242-250.

Yao, T., and Ndoja, A. (2012). Regulation of gene expression by the ubiquitin-proteasome system. Semin Cell Dev Biol *23*, 523-529.

Yao, T., Song, L., Jin, J., Cai, Y., Takahashi, H., Swanson, S.K., Washburn, M.P., Florens, L., Conaway, R.C., Cohen, R.E.*, et al.* (2008). Distinct modes of regulation of the Uch37 deubiquitinating enzyme in the proteasome and in the Ino80 chromatin-remodeling complex. Mol Cell *31*, 909-917.

Ye, Y. (2006). Diverse functions with a common regulator: ubiquitin takes command of an AAA ATPase. Journal of structural biology *156*, 29-40.

Yen, K., Vinayachandran, V., Batta, K., Koerber, R.T., and Pugh, B.F. (2012). Genome-wide nucleosome specificity and directionality of chromatin remodelers. Cell *149*, 1461-1473.

Yen, K., Vinayachandran, V., and Pugh, B.F. (2013). SWR-C and INO80 chromatin remodelers recognize nucleosome-free regions near +1 nucleosomes. Cell *154*, 1246-1256.

Yuan, G.C., Liu, Y.J., Dion, M.F., Slack, M.D., Wu, L.F., Altschuler, S.J., and Rando, O.J. (2005). Genome-scale identification of nucleosome positions in S. cerevisiae. Science *309*, 626-630.

Zhang, H., Roberts, D.N., and Cairns, B.R. (2005). Genome-wide dynamics of Htz1, a histone H2A variant that poises repressed/basal promoters for activation through histone loss. Cell *123*, 219-231.

Zhang, X.Y., Varthi, M., Sykes, S.M., Phillips, C., Warzecha, C., Zhu, W., Wyce, A., Thorne, A.W., Berger, S.L., and McMahon, S.B. (2008). The putative cancer stem cell marker USP22 is a subunit of the human SAGA complex required for activated transcription and cell-cycle progression. Mol Cell *29*, 102-111.

Zhao, Y., Lang, G., Ito, S., Bonnet, J., Metzger, E., Sawatsubashi, S., Suzuki, E., Le Guezennec, X., Stunnenberg, H.G., Krasnov, A.*, et al.* (2008). A TFTC/STAGA module mediates histone H2A and H2B deubiquitination, coactivates nuclear receptors, and counteracts heterochromatin silencing. Mol Cell *29*, 92-101.

Zhu, P., Zhou, W., Wang, J., Puc, J., Ohgi, K.A., Erdjument-Bromage, H., Tempst, P., Glass, C.K., and Rosenfeld, M.G. (2007). A histone H2A deubiquitinase complex coordinating histone acetylation and H1 dissociation in transcriptional regulation. Mol Cell *27*, 609-621.

Zilberman, D., Coleman-Derr, D., Ballinger, T., and Henikoff, S. (2008). Histone H2A.Z and DNA methylation are mutually antagonistic chromatin marks. Nature *456*, 125-129.

Zou, W., Chen, X., Shim, J.H., Huang, Z., Brady, N., Hu, D., Drapp, R., Sigrist, K., Glimcher, L.H., and Jones, D. (2011). The E3 ubiquitin ligase Wwp2 regulates craniofacial development through mono-ubiquitylation of Goosecoid. Nat Cell Biol *13*, 59-65.

Table A1.1. Yeast strains used in experiments detailed in Chapter 2.

Strain	Genotype	Parent strain	Source
MTY1803	*MATa ade2 his3 leu2 ura3 trp1 met4::TRP1*		M. Tyers
CC807-1C	*MATa ade2 his3 leu2 ura3 trp1 met4::TRP1 met30::LEU2*		M. Tyers
YYH1	*MATa ura3-52 leu2Δ1 trp1Δ63 npl4-1*		Y. Ye
YYH2	*MATa ura3-52 leu2Δ1 trp1Δ63 npl4-2*		Y. Ye
YYH3	*MATa his4-519 ura3-52 ade1-00 leu2-3, -112*		Y. Ye
YYH4	*MATa his4-519 ura3-52 ade1-00 leu2-3, -112 ufd1-1*		Y. Ye
YYH6	*MATa his3-11 trp1-1 ura3-1 ade2-1 leu2-3, -112 can1-100*		Y. Ye
YYH75	*MATa ura3-52 leu2-3 cdc48-3 (3 times backcrossed with YYH6)*		Y. Ye
DY61	*MATa his3-Δ200 lys2-801 leu2-3, -112 trp1-1 ura3-52 Δrpt5::HIS3 pDP41[RPT5::LEU2]*		D. Finley
DY85	*MATa his3-Δ200 lys2-801 leu2-3, -112 trp1-1 ura3-52 Δrpt1::HIS3 pDP73[RPT1::LEU2]CEN*		D. Finley
DY92	*MATa his3-Δ200 lys2-801 leu2-3, -112 trp1-1 ura3-52 Δrpt3::HIS3 pDP74[RPT3::LEU2]CEN*		D. Finley
DY93	*MATa his3-Δ200 lys2-801 leu2-3, -112 trp1-1 ura3-52 Δrpt3::HIS3 pDP75[rpt3R::LEU2]CEN*		D. Finley
DY98	*MATa his3-Δ200 lys2-801 leu2-3, -112 trp1-1 ura3-52 Δrpt1::HIS3 pDP87[rpt1R::LEU2]CEN*		D. Finley
DY100	*MATa his3-Δ200 lys2-801 leu2-3, -112 trp1-1 ura3-52 Δrpt6::HIS3 pDP89[rpt6R::LEU2]CEN*		D. Finley
DY104	*MATa his3-Δ200 lys2-801 leu2-3, -112 trp1-1 ura3-52 Δrpt6::HIS3 pDP80[RPT6::LEU2]CEN*		D. Finley
DY155	*MATa his3-Δ200 lys2-801 leu2-3, -112 trp1-1 ura3-52 Δrpt5::HIS3 pDP41[rpt5R::LEU2]*		D. Finley
DY218	*MATa his3-Δ200 lys2-801 leu2-3, -112 trp1-1 ura3-52 Δrpt4::HIS3 pUB328[RPT4::LEU2]CEN*		D. Finley
DY219	*MATa his3-Δ200 lys2-801 leu2-3, -112 trp1-1 ura3-52 Δrpt4::HIS3 pUB326[rpt4R::LEU2]CEN*		D. Finley
SBY214	*MATa ura3-1 leu2-3, -112 lys2 bar1 can1-100 ade2-1 his3-11 [pCUP1-GFP12-LacI12::HIS] trp1-1 [256LacO::TRP]*		S. Biggins
SBY331	*MATa ura3-1 leu2-3, -112 lys2 bar1 can1-100 ade2-1 his3-11 [pCUP1-GFP12-LacI12::HIS] trp1-1 [256LacO::TRP] smt3-331*		S. Biggins

YTY076	*MATa his3Δ1 leu2Δ0 met15Δ0 ura3Δ0 pM4366[HO-4XLexAOP-LacZ URA3-HO integrative]*	BY4741	This study
YTY224	*MATa ade2 his3 leu2 ura3 trp1 met4::TRP1 met30::LEU2 pM4366[HO-4XLexAOP-LacZ URA3-HO integrative]*	CC807-1C	This study
YTY358	*MATa ade2 his3 leu2 ura3 trp1 met4::TRP1 pM4366[HO-4XLexAOP-LacZ URA3-HO integrative]*	MTY1803	This study
YTY375	*MATa his3-11 trp1-1 ura3-1 ade2-1 leu2-3, -112 can1-100 pM4297[HO-4XLexAOP-LacZ KAN-HO integrative]*	YYH6	This study
YTY376	*MATa his4-519 ura3-52 ade1-00 leu2-3, -112 pM4297[HO-4XLexAOP-LacZ KAN-HO integrative]*	YYH3	This study
YTY377	*MATa his4-519 ura3-52 ade1-00 leu2-3, -112 ufd1-1 pM4297[HO-4XLexAOP-LacZ KAN-HO integrative]*	YYH4	This study
YTY378	*MATa ura3-52 leu2Δ1 trp1Δ63 npl4-1 pM4297[HO-4XLexAOP-LacZ KAN-HO integrative]*	YYH1	This study
YTY379	*MATa ura 3-52 leu2Δ1 trp1Δ63 npl4-2 pM4297[HO-4XLexAOP-LacZ KAN-HO integrative]*	YYH2	This study
YTY380	*MATa ura3-52 leu2-3 cdc48-3 pM4297[HO-4XLexAOP-LacZ KAN-HO integrative]*	YYH75	This study
YTY482	*MATa his4-519 ura3-52 ade1-00 leu2-3, -112 met4::CloNAT*	YYH3	This study
YTY487	*MATa his4-519 ura3-52 ade1-00 leu2-3, -112 ufd1-1 met4::CloNAT*	YYH4	This study
YTY511	*MATa his3Δ1 leu2Δ0 met15Δ0 ura3Δ0 pM4366[HO-4XLexAOP-LacZ-URA3-HO integrative] CDC48-13xMyc::KANMX6*	YTY076	This study
YTY531	*MATa ura3-52 leu2-3 cdc48-3 met4::CloNAT*	YYH75	This study
YTY548	*MATa ade2 his3 leu2 ura3 trp1 met4::TRP1 pM4366[HO-1XLexAOP^{hybrid}-LacZ URA3-HO integrative]*	MTY1803	This study
YTY610	*MATa ura3-52 leu2-3 CDC48-13xMyc::KANMX6*	YYH75	This study
YTY611	*MATa ura3-52 leu2-3 CDC48-13xMyc::KANMX6 met32::HIS3*	YTY610	This study
YTY612	*MATa ura3-52 leu2-3 CDC48-13xMyc::KANMX6 met32::HIS3 met30::LEU2*	YTY611	This study
YTY613	*MATa ura3-52 leu2-3 cdc48-3 met4::CloNAT met32::HIS3*	YTY531	This study
YTY614	*MATa ura3-52 leu2-3 cdc48-3 met4::CloNAT met32::HIS3 met30::LEU2*	YTY613	This study
YTY615	*MATa ade2 his3 leu2 ura3 trp1 met4::TRP1 pM4297[HO-1XLexAOP KAN-HO integrative]*	MTY1803	This study
YTY616	*MATa his3Δ1 leu2Δ0 met15Δ0 ura3Δ0 pM4366[HO-4XLexAOP-LacZ-URA3-HO integrative] UFD1$^{\Delta SIM}$::CloNAT*	YTY076	This study

Table A1.2. Sequences of oligos used in experiments detailed in Chapter 2.

Name	Sequence (5' to 3')
LacZ Promoter-F	TTTGCGCTAGAATTGAACTCAGGTACAA
LacZ Promoter-R	TCGAGGGATGATAATGCGATTAGTTTTT
LexA operator-F	GGCGGAACTTCTCTTGTTTTGTGACC
LexA operator-R	AAAAACTAATCGCATTATCATCCCTCGA
LacZ-3P-F	GCCGCTACAGTCAACAGCAA
LacZ-3P-R	ATATTCAGCCATGTGCCTTCTTC
MET17 mid-F	GCTCACAAACACGGTATTCCAGTTGTC
MET17 mid-R	GGCAGGTTGAGAGAATTGAGGGAACT
MET3 mid-F	ACGTTGCCGGTGATTATTACGTCG
MET3 mid-R	AGCTTCTCTGGCGGCTCTCACA
CYS3 mid-F	CTAATAACAAGCCATTGTACGAGCGTCTG
CYS3 mid-R	CGTCGTAGTTAGGGTGTGTCTTCAAAC
ACT1-F	CCAAGAGAGGTATCTTGACTTTAC
ACT1-R	AGAAGGTATGATGCCAGATCTTTT
GAL1 mid-F	TGCGTATTACGGTCGTTGCA
GAL1 mid-R	AACAGAGGCAGCCTGATCCA
MET17 Promoter-F	GAGGTCACATGATCGCAAAATGG
MET17 Promoter-R	CATCGAGCGTGTTCAATTGGAC
IL-11 mid-F	ACTGCTGCTGCTGAAGACTC
IL-11 mid-R	CCACCCCTGCTCCTGAAATA
CTGF mid-F	GCTACCACATTTCCTACCTAGAAATCA
CTGF mid-R	GACAGTCCGTCAAAACAGATTGTT
CTGF Promoter-F	CTATTTGGTGCTGGAAATACTGCGC
CTGF Promoter-R	GACATTCCTCGCATTCCTCCCC

LexA hybrid operator-F	TACCGTATGTACATACAGTACTCGAGGG
LexA hybrid operator-R	CTGTTAATAGATCAAAAATCATCGCTTCGCT
RPL11-F	TCACATCCACGTGACCAGTTT
RPL11-R	AACTTTCGCATAGCTGAGTGG